

***Prediction of PDZ interactions and classifications
using Structures and Machine Learning Methods***

by

Tayfun TÜMKAYA

A Thesis Submitted to the

Graduate School of Science and Engineering

in Partial Fulfillment of the Requirements for

the Degree of

Master of Science

in

Computational Sciences and Engineering

Koc University

July 2014

Abstract

PDZ domains (PSD-95/Discs-large/ZO-1 homology) are one of the most abundant and evolutionary conserved domain families through uni- and multi-cellular organisms. As its abundance and high evolutionary conservation indicates, PDZ domains mediate a number of distinct functions in the cell including vesicular sorting, neuronal synaptic plasticity, development and neural guidance. Therefore, malfunction of the PDZ domain causes several crucial diseases such as Usher's syndrome, epilepsy, schizophrenia and types of cancer.

PDZ domains are 80-100 residues long and consist of two α -helices (α A- α B) and six β -sheets (β A to β F). The canonical interaction is the most common interaction type of PDZ domain where the PDZ domain binds the C-terminal of the target protein via the binding cavity. PDZ domains are categorized into three classes according to the motif of their binding partners as Class I, Class II and Class III. Although, PDZ domains prefer to bind a particular class of peptides there are cases where the PDZ domain can interact with both Class I and Class II peptides, classified as Class I-II.

This study focuses on building prediction models for PDZ domain mediated interactions and PDZ domain classification by using their structural features. By utilizing the properties of the PDZ domains and their ligands, those have the available interaction experimental data, an interaction prediction and classification model was built via machine learning approaches. One of the most robust machine learning approach, support vector machine (SVM) algorithm, was selected to train the models. The interaction prediction and the classification models performances were evaluated by cross-fold validation test and validation of human proteome scanning results on experimentally known interactions data. The interaction prediction model and the classification model have area under ROC curve with a number of 0.99 and 0.91, respectively. Moreover, the human proteome scanning results showed that the interaction prediction model was able to predict the known PDZ domain mediated interactions correctly with a TP rate of 17 %. Additionally, the general knowledge of classification of PDZ domains were supported by our results. These models could be utilized by future experimental studies to narrow the search space of the novel binding partners of PDZ domains as well as drug discovery studies that target PDZ domain containing proteins.

Özet

PDZ domain'i (PSD-95/Discs-large/ZO-1 homology) tek ve çok hücreli organizmalarda evrimsel süreç boyunca oldukça korunmuş ve en bol miktarda bulunan domain ailelerinden biridir. Evrimsel korunmuşluğun ve birçok organizmada yaygın olarak bulunuyor olmasının işaret ettiği gibi PDZ domain'inin önemli sayıda hücresel fonksiyonun yerine getirilmesinde rolü büyüktür. Bu fonksiyonlar arasında vesiküler taşıma, nöronal sinaptik bağlantılar, nöron gelişim ve dağılım örnek gösterilebilir. Dolayısıyla, PDZ domain işlevinde meydana gelecek bir aksama, Usher's sendromu, epilepsi, şizofreni ve bazı kanser türleri gibi oldukça ciddi hastalıklara sebebiyet verebilir.

PDZ domainleri 80-100 amino asit uzunluğunda, iki α -helix (αA - αB) ve six β -sheet (βA to βF) ten meydana gelir. PDZ domaininin en yaygın bağlanma şekli olarak bilinen 'canonical' etkileşimi, domain üzerinde bulunan bir bağlanma oluğu ile hedef proteinin C-terminal ucundaki 5 amino asitlik peptidler ile gerçekleşir. PDZ domainleri etkileşimlerinden ligand seçimlerindeki özelleşmeye dayanarak Tip I, Tip II ve Tip III olmak üzere 3 sınıfa ayrılırlar. Genel olarak PDZ domainleri belirli bir sınıf peptide bağlansalar da, aralarında hem Tip I hem de Tip II ile etkileşebilen domainler olduğu bilinmektedir ve bunlar Tip I-II olarak sınıflandırılmaktadır.

Bu çalışma, PDZ domainlerinin yapısal özelliklerinden faydalanarak, onlara yeni ligandlar bulunması ve sınıflandırılması üzerine yoğunlaşmaktadır. Deneysel olarak etkileşim bilgileri bulunan domainlerin ve ligandlarının özelliklerinden faydalanarak, yapay öğrenme ile etkileşim tahmini ve sınıflandırma için modeller geliştirilmiştir. Bu modelleri geliştirmek için en güvenilir yapay öğrenme algoritmalarından biri olan 'support vector machine (SVM)' kullanılmıştır. Bu modellerin performans analizleri çapraz validasyon ('cross-validation') testlerinin yanı sıra insan proteomunun taranıp, doğru tahmin edilen etkileşimlerin istatistikleri kullanılarak yapılmıştır. Sonuç olarak, sırasıyla 0.99 ve 0.91 AUC değerlerine sahip etkileşim tahmin eden model ve sınıflandırma modeli geliştirilmiştir. İnsan proteomu tarama sonuçlarına göre de etkileşim tahmin eden model, PDZ domainleri aracılığıyla gerçekleşen etkileşimleri 17 % lik doğruluk oranı ile tahmin etmiştir. Ayrıca, PDZ domaini genel-geçer sınıflandırma sisteminin doğruluğunu da güçlendirmiştir. Bu modeller ileride PDZ domaini barındıran proteinlerin yeni ligandlarını bulmak ya da bu proteinleri hedefleyen ilaç molekülleri tasarlamak amacıyla yapılacak olan çalışmalarda, aday olacak peptidlerin sayıca aza indirgenmesinde kullanılabilir.

Acknowledgements

I would like to thank my advisors Prof. Dr. Özlem Keskin and Prof. Dr. Attila Gürsoy for their guidance and support.

I would like to express my gratitude to all my friends who have shared the past two years or more with me, Kerem Fidan, Alper Başpınar, Engin Çukuroğlu, Güray Kuzu, Serena Muratçıoğlu, Emine Güven Mayorov, Yusuf D. Doğru, Deniz Demircioğlu, Emel Şen, Nilay Karahan, Derya Cavga and all of my past office mates.

Finally, no word exist to express the greatness of my gratitude to my family for their endless support and love. I am deeply pleased to dedicate this work to my dearest nephew Kaya 一男 Zeng Tüm kaya.

Table of Contents

Abstract	ii
Özet	iii
Acknowledgements	iv
LIST OF TABLES	vi
LIST OF FIGURES	vii
Chapter 1	1
INTRODUCTION	1
Chapter 2	3
LITERATURE REVIEW	3
2.1 PDZ Domain (PSD-95, Discs large, Zona occludens 1)	3
2.2 Previous prediction models	5
Chapter 3	8
MATERIALS AND METHODS	8
3.1 Dataset	8
3.2 Feature Encoding	9
3.3 Relative Solvent Accessible Surface Area (rASA)	10
3.4 Hydrophobicity and Electrostatic Potential	10
3.5 Possible Phosphorylation Sites (PPS)	11
3.6 Peptide Feature Encoding	11
3.7 Model Training and Performance Measures	11
Chapter 4	13
RESULTS	13
4.1 PDZ domain interaction prediction model	13
4.2 PDZ domain class prediction model	18
4.3 Human proteome scanning	27
Chapter 5	32
CONCLUSION	32
APPENDIX	34
BIBLIOGRAPHY	83

LIST OF TABLES

Table 4-1 Interaction prediction model's detailed accuracy and confusion matrix results.....	18
Table 4-2 Multi-classification model's detailed accuracy and confusion matrix results.....	20
Table 4-3 Class I/Class II binary classification model's detailed accuracy and confusion matrix results.....	24
Table 4-4 Class I/Class I-II binary classification model's detailed accuracy and confusion matrix results.....	25
Table 4-5 Class II/Class I-II binary classification model's detailed accuracy and confusion matrix results.....	26
Table 4-6 Prediction results for multi-class learning and binary learning for pair wise combinations of three classes.....	27
Table 4-7 Multi-classification and binary classification weighted average results were shown for Kalyoncu et al.'s study [11].....	27
Table 4-8 Human proteome scanning results.....	31
Table S1.a PDZ domain interaction dataset	25
Table S1.b PDZ Domain sequences.....	55
Table S1.c Peptide sequences.....	58
Table S2 Class data of PDZ domains.....	65
Table S3 Data table of 218 PDZ Domains used to scan human proteome.....	67

LIST OF FIGURES

Figure 2-1 Representative structure of a PDZ domain as free and bound form.....	4
Figure 4-1.a ROC curve for interaction prediction model.....	12
Figure 4-1.b Precision vs Recall curve for interaction prediction model.....	12
Figure 4-2 Precision vs Recall curve for interaction prediction model.....	15
Figure 4-3.a ROC curve for multi-classification model.....	20
Figure 4-3.b Precision vs Recall curve for multi-classification model.....	20
Figure 4-4 Structural comparison of Class I but predicted as Class I-II (a-d-g), Class I and predicted as Class I (b-e-h) and Class I-II and predicted Class I-II domains (c-f-i).....	22
Figure 4-5 Multiple-sequence alignment results.....	23

Chapter 1

INTRODUCTION

Protein-protein interactions are critical processes that are responsible for proper maintenance of cell functions. These interactions are mediated by conserved, specific interaction modules called domains [1]. The PDZ domain is one of the most abundant domains in the family among all other recognition domains from yeast to human. Their importance in a human cell is emphasized by their distinct functions such as epithelial polarity, phototransduction, vesicular sorting, and neuronal synaptic communication. Their malfunction causes several Mendelian human diseases such as Usher syndrome, Dejerine-Sottas neuropathy, some types of cancer and neurodegenerative diseases [2].

The inducement of such diseases in the case of PDZ domain malfunction and their role in several crucial cell processes make PDZ domain of great interest. The revelation of the interactions that are mediated by PDZ domain may shed light on several serious diseases mechanism and cellular processes, as well. The most common interaction type of PDZ domain is called ‘canonical interaction’ which occurs between the domain and the five-residue long C-terminal of the protein [4,5]. PDZ domain mediated interactions depend on several properties of the domain such as hydrophobicity, electrostatic potential, amino acid content and tertiary structure of the domain. Moreover, post-translational modifications are important modulators of these interactions. Furthermore, the classification (Class I, Class II, and Class III) of the domains is done based on C-terminal peptide’s motif [6]. Although the PDZ domains interact with a particular class of peptide, some PDZ domains may show promiscuous behavior and interact with distinct classes of peptide.

Currently, sequence-based and structure-based prediction models exist in the literature. For PDZ domain interaction prediction, sequence-based models were built by utilizing statistical approach [8,9,10] or machine learning approach [11]. These models made use of the primary sequence of the PDZ domains and generated features based on their amino acid types. A structure-based model was built by utilizing the support vector machine (SVM) algorithm, as well [12]. In this study, accessible surface area and hydrophobicity-electrostatic potential of the domains was used as features. For PDZ domain classification, Kalyoncu et al. [11] constructed a model based on general classification knowledge of PDZ domains by using primary sequence information.

In this study, we present a PDZ domain-peptide interaction prediction and classification model that is trained by using a both structural information of PDZ domains and sequential information of peptide ligands. Our model uses a combination of features that are known to mediate the PDZ domain-peptide interactions. To construct the interaction and classification models, a collection of known PDZ domain mediated interactions that available in the literature was used. SVM (support vector machine) algorithm was utilized to train models on the dataset. By testing the model with cross validation, we showed that a combination of features is more effective than using only one type of information. Moreover, we performed a human proteome scanning with the result of a high rate of true predicted interactions which proved the power of prediction model. Finally, the classification model was tested with 10-fold cross-validation for both multiple-classification (Class I / Class II / Class I-II) and binary classification of combinations of three classes (Class I / Class II , Class I / Class I-II, Class II / Class I-II). The results proved that classification model has a great differentiation ability on Class I, Class II and Class I-II PDZ domains.

Literature review related to the subject is provided in Chapter 2. In this section, background information including the structure and function of PDZ domains are given. Furthermore, previous studies of constructing machine learning models for prediction and classification of PDZ domain are reviewed as well as the support vector machine (SVM) algorithm.

In Chapter 3, the training dataset retrieving processes for both interaction and classification models are explained. The encoding steps and description of the features that are used in the study are given along with the performance measures definitions and training optimizations.

Chapter 4 represents the results for the interaction prediction and classification models, seperately. For classification part, both multi-classification and binary classification 10-fold cross-valdiation performance evaluation is achieved as the comparison of binary classification results. The performance evaluation for interaction prediction model is also showed. Moreover, the human proteome scanning process and the assesment are given in this chapter.

Finally, a brief summary of the study can be found in Chapter 5.

Chapter 2

LITERATURE REVIEW

In this chapter, background information of PDZ domain was given. The secondary structure data of PDZ domains and their interaction mechanism and the classification system were explained in detail. Moreover, the prediction models that exist in the literature also were discussed.

2.1 PDZ Domain (PSD-95, Discs large, Zona occludens 1)

PDZ domain is one of the most widespread protein-protein modulating domain which are specialized for binding to five-residue long C-terminal of partner proteins. Human genome encodes over 250 PDZ domains in over 100 proteins [7]. The name is derived from the three proteins in which it was first identified, namely postsynaptic density protein-95 (PDZ-95), disks large tumor suppressor (DLG) and zonula occludens-1 (ZO-1) [33-35]. PDZ domains are fewer in unicellular organisms than multicellular organism which indicates the co-evolution of the PDZ domain along with the multi-cellularity. PDZ domains are involved in several distinct functions that in the nervous system, excitatory synapses provide fascinating PDZ domain mediated functions [36-38].

PDZ domains are 80-100 residues long and consist of two α -helices (α A- α B) and six β -sheets (β A to β F) [3] (Figure 2.1.a). In the most common interaction type of PDZ domain, which is called canonical interaction, the PDZ domain binds the C-terminal of the target protein via the binding groove formed between the α B helix and the β B sheet [4,5]. Particular residues that are in close contact with their ligand (<4.5 angstroms) are crucial for PDZ domain mediated interactions. Previous studies used 16-residue and ten-residue binding site definitions. The ten-residue binding site definition was annotated by using nine PDZ domain-peptide complexes whereas the 16-residue binding site definition was identified only using one PDZ domain-peptide complex [9,10,12] (Figure 2.1.b).

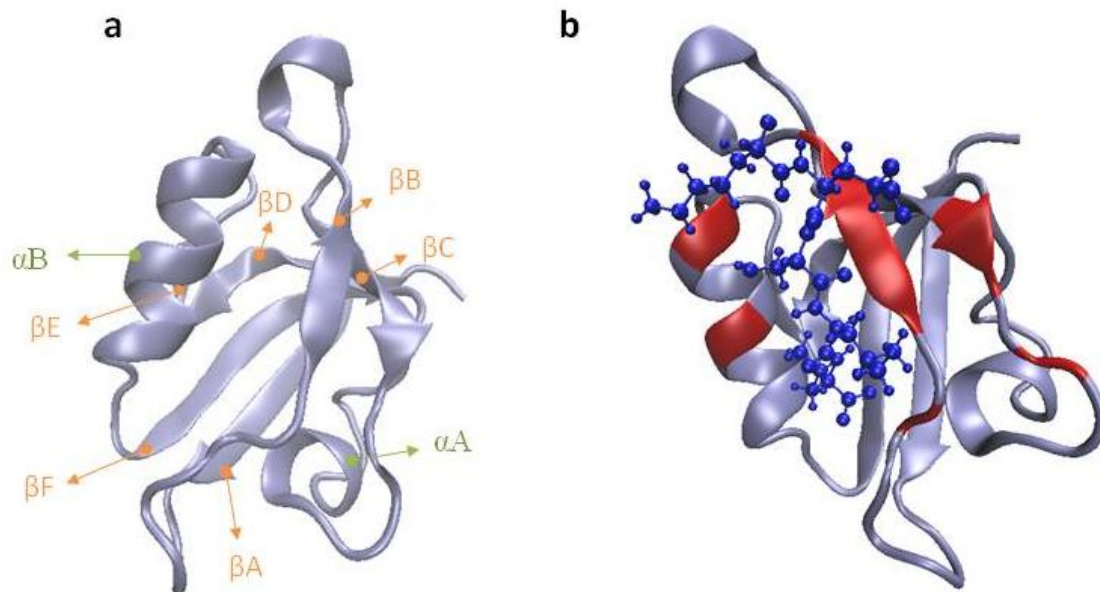


Figure 2-1 Representative structure of a PDZ domain as free and bound form. (a) The common representation of a PDZ domain (α -1 syntrophin) with labeled secondary structures (α helices and β sheets are colored as green and orange, respectively). **(b)** The canonical interaction of PDZ domain with five residues long C-terminal peptide (KESLV). The ten core binding residues of PDZ domain are highlighted in red whereas the peptide is colored blue.

The PDZ domain mediated interactions are regulated by post-translational modifications which include phosphorylation mechanism as the most common regulator. Experimental studies that have mutational approach (phospho-mimicking mutations) on binding residues of PDZ domains proved that phosphorylation has a dramatic reduction effect to the binding affinity [18, 24, 39]. Hydrophobicity, electrostatic potential, amino acid content and tertiary structure have also decisive role on PDZ domain-peptide interaction dynamics.

The specificity of PDZ domains for certain ligands led to the classification of PDZ domains into three classes according to the motif of their ligand. PDZ domain classes and their specific peptide selections are the following: Class I PDZ domains bind to the ligands with the motif of [X-S/T-X- ϕ -COOH], Class II PDZ domains bind to the ligand with the motif of [X- ϕ -X- ϕ -COOH] and the Class III PDZ domains bind to the C-terminal motifs [X-D/E-X- ϕ -COOH] [6] (X: any amino acid residue, ϕ : hydrophobic residue, S: serine, T: threonine, D: aspartate, E: glutamate). Although, PDZ domains prefer to bind a particular

class of peptides there are cases that the PDZ domain can interact with both Class I and Class II, which are classified as Class I-II.

2.2 Previous prediction models

High throughput experimental studies gave birth to a vast quantity of PDZ domain-peptide interaction information. One example for such high throughput study is from Stiffler et al. [7]. They scanned the billions of peptides to map binding specificity human and *Caenorhabditis elegans* PDZ domains, accurately. They used C-terminal peptide-phage display to conduct such a large-scale analysis of PDZ domain specificity. Moreover, both human and *Caenorhabditis elegans* PDZ domains were used in this study for comparison purposes. As a result, they mapped the binding specificity and identified partner preferences of half of the over 330 PDZ domains successfully. In another study Stiffler et al. [8] generated vast of experimental interaction information for mouse PDZ domains. This time they used 217 genome-encoded peptides instead of random peptides. Then they tested all possible interactions between 157 mouse PDZ domains and genome encoded-peptides via protein microarrays. Therefore, several computational prediction models have become possible to train by using experimental informations.

Chen et al.'s [9] study is one of the examples of computational models. In this study, it is reasoned that if the peptide ligand preferences of the PDZ domain are determined by the amino acid types at specific positions in the domain's three dimensional structure, it may be captured by integrating sequence and structural information. They constructed a multiple sequence alignment of mouse PDZ domain's primary sequences which have structural information in Protein Data Bank (PDB). After the elimination step of any residue position that has a gap in the alignment with the reference PDZ domain structure (α 1-syntrophin in contact with GVKESLV peptide), a total of 38 position pairs were identified between 16 PDZ domain residues (referred as binding-site residues) and 5 peptide residues. Afterwards, an additive model comprising 38 scoring matrices per each domain-peptide pair was formulated. These matrices (20 x 20) include scores for amino acid pairs as one residue on the PDZ domain and the other on the peptide. To fit the model, they trained it by using interaction data that included 82 PDZ domains and 93 peptide ligands. Moreover, since the number of data points were much more less than the number of model parameters, which makes the model highly underdetermined, they utilized the Bayesian approach to circumvent this problem. As a

result, they had a statistical model that predicts PDZ domain-peptide interactions by using primary sequence information with an area under curve value of 0.87.

A model for sequence-based prediction was built by Stiffler et al. [8]. First, they cloned, expressed and purified 157 PDZ domains encoded in mouse genome. As distinct from their another study [7], they focused on genome-encoded peptide ligands instead of random peptides. After synthesizing and purifying 217 fluorescently labeled peptides, they designed a strategy that combines the throughput of protein microarray and the reliability of fluorescence polarization methods to investigate the biophysical interactions between 157 PDZ domains and 217 fluorescence peptides. Furthermore, to eliminate the false positive rate of the high-throughput method, they retested and quantified every array positive with solution-phase fluorescence polarization which was utilized as ‘gold standart’ in the study. The gold standart involved 85 PDZ domains that interact at least one peptide in the training set. Since the traditional position specific scoring matrix (PSSM) did not fit in one of their purposes, which were distinguishing one domain from another, they built a variation of PSSM. The model that includes many PDZ domains reffered as multidoman selectivity model (MDSM). To avoid the overfitting problem that may happen such a high-dimensional model, they implemented smoothing techniques. The trained model performs well on the microarray dataset with a true-positive rate of 96%. By considering the high agreement of the MDSM with the training-set data, they used the model to scan mouse proteome that involves 31,302 peptides to find 74 PDZ domain’s binding partners. Finally, they provided these interaction predictions data (18,149 PDZ domain-peptide interactions) to help guide future biological investigations.

In another study a sequence-based prediction models is accomplished by Hui et al.[10]. Unlike the studies discussed above, a huge dataset from two independent high-throughput studies, which generated a vast of data by using protein microarray and phage display technologies, was utilized in this study [7,8]. Since the phage display method produces only positive data, they developed a method to generate artificial negative data. As it is referred, the commonly used random and shuffled peptides have not been resulted very well on predicted real negative inetactions in previous studies. Therefore, a position weight matrix (PWM) was trained on positive interactors and they used it to pick the negative interactors among a set of peptides those have a score below the threshold. In total, interaction data of 20 human and 82 mouse PDZ domains with over 3000 peptides were used to train the model. As primary sequence feature, the 16 binding-site residues defintion of PDZ domains from Chen et al.’s study was used. They encoded binary vectors with a length of 20 x 20 that represents

each type of amino acid for 38 residue pairs between 16 PDZ domain binding-site and 5 peptide ligand residues (in total, 38 x 400). Afterall, support vector machine (SVM) algorithm was used to train a model on the dataset with an AUC result of 0.89. Finally, the model was used to scan human, worm and fly proteomes to define 13 PDZ domain's interactors that have available validation data in PDZBase with a result of 85%, 25% and 37%, respectively.

One more computational study for building sequence-based predictor was conducted by Kalyoncu et al. [11]. They generated bigram and trigram amino acid frequencies of primary sequences of PDZ domains and peptides. For instance, a sequence of 'ABCDE' results in a trigram set of 'ABC', 'BCD', 'CDE' and a bigram dataset of 'AB', 'BC', 'CD', 'DE'. Moreover, to reduce the dimension of the features they categorized 20 amino acid types into 7 classes with respect to their physicochemical properties. Eventually, a sequence-based PDZ domain interaction prediction model was created with an accuracy of 91.4 % by using random forest classifier. Additionally, a PDZ domain classification model was established in order to differentiate both multi-classes among them and binary classes. The multi-class differentiating model was achieved 90.7 % accuracy.

Since the structural features include more accurate information about protein-ligand interactions, Hui et al. [12] constructed a structure-based predictor. They used the dataset that has 2795 interaction information (both binding and non-binding) of 83 PDZ domains that are related to human and mouse, and corresponding 871 peptides data. The electrostatic potential, hydrophobicity and accessible surface area properties were used as structural features. SVM (support vector machine) algorithm was used to train the model. The performance analysis of the model with cross validations gives an AUC value of 0.93. In addition, they used the model to scan the human proteome for 218 PDZ domains. As a result, they had true predictions for only 88 PDZ domains but not for remaining 130 domains. For 88 domains, they calculated an average TP rate with a value of over 21%.

Chapter 3

MATERIALS AND METHODS

In this chapter, the dataset that is used in the study was explained. The features description and the calculation process was given, as well. Moreover, the SVM classifier and the performance measures that we used in the study were described.

3.1 Dataset

A dataset which contains both positive (binding) and negative (non-binding) informations was needed to build the machine learning model. The PDZ domain interaction dataset, which is composed of 83 PDZ domains and 871 ligands, was retrieved from Hui et al. [12]. They collected the PDZ-peptide interactions from published high throughput phage display and protein microarray experiments for both human and mouse, respectively [7,8]. Since the phage display data contains only positive interactions, they used an established protocol and generated artificial negative interactions [10]. At the end, a PDZ domain-peptide interaction dataset with 942 binding and 1843 non-binding interactions between 83 PDZ domains and 871 ligands was generated (see Appendix: Table S1 for PDZ interaction data). The structures of the PDZ domains were collected from the web server of Bader Lab. The dataset contains one NMR and 17 X-ray structures for humans and five NMR structures for mice from the Protein Data Bank (PDB) [13]. We used only the first model was used for NMR structures as it was used in the previous study. Furthermore, 11 human and 54 mouse PDZ domain models in this dataset were modelled by SWISS-MODEL [14]. As it is referred in this study, homology models were used to increase the number of PDZ domain structures to build a robust prediction model. The quality of the homology models was estimated by template sequence ID and QMEAN score by Hui et al. [12]. Template sequence id is the measure of the identical residues between the domain and the template as a percentage where the QMEAN score is a scoring function that measures multiple geometrical aspects of protein structure, ranging from 0 to 1 with higher values indicate more qualified models.

For class prediction, PDZ domains were signed as Class I and Class II with respect to the C-terminal motif of interacting peptides, [X-S/T-X- ϕ -COOH] for Class I and [X- ϕ -X- ϕ -COOH] for Class II, respectively. The domains that both interact with Class I and Class II peptides were annotated as Class I-II. All PDZ domains in our dataset were classified,

resulted in 12 Class I, 27 Class II and 27 Class I-II. These classes were determined by using the interaction informations of the PDZ domains with different classes of peptides in our dataset. The experimentally proved interactions were retrieved from IRefIndex [25], PDZBase server [40] and literature manually. However, 17 domains could not be classified due to the non-fitting of their interaction partners into any class pattern (see Appendix: Table S2 for class data of the domains). Since the peptides were used to label the classes of PDZ domains, the peptide's features (20 amino acid type x 5 residues) were removed from the feature vector space to avoid biased data.

3.2 Feature Encoding

Particular protein residues that are in close contact with their ligand (<4.5 angstroms) are crucial for PDZ domain mediated interactions. Previous studies used either 16-residue or ten-residue binding site definitions. However, the ten-residue binding site definition was annotated by using nine PDZ domain-peptide complexes where the 16-residue binding site definition was identified only using one PDZ domain-peptide complex [9,10,12]. Therefore, in this study ten binding residues were identified for each of the PDZ domains. Four types of features that are responsible for protein-protein interactions and stability of proteins were computed to describe the PDZ domain. Then, the values corresponding to the ten binding residues were extracted and each PDZ domain was represented by a vector of length 301 features, in total.

The representation of the feature vector space of interaction is as following:

$$(X, Y, W) = \{(x_1, x_2, \dots, x_{200}), (Y_1, Y_2, \dots, Y_{100}), (\omega_1/\omega_2)\} \quad (3.1)$$

where X is the vector space for PDZ domain information ($x_1 - x_{90}$: electrostatic potential, $x_{91} - x_{180}$: hydrophobicity, $x_{181} - x_{190}$: relative accessible surface area, $x_{191} - x_{200}$: phosphorylation sites), Y is the vector space for peptide information ($Y_1 - Y_{100}$: binary vector

of 20 amino acid type for each of the five residues), and W is the label (ω_1 : binding or ω_2 : non-binding).

3.3 Relative Solvent Accessible Surface Area (rASA)

Relative accessible surface area is a simple measure, which is calculated by normalizing the residue's accessibility on the surface of a protein with its the standart ASA value. The rASA gives insight about the rate of the buried surface area and the accessible surface area for a residue. Furthermore, rASA can be utilized to define the magnitude of interaction-induced conformational changes of proteins. rASA of PDZ domains in our dataset were computed using the NACCESS software [16]. Each value corresponds to the ten binding sites of PDZ domains that were extracted, used to generate a feature vector with a length of 10 (1 feature x 10 binding residues).

3.4 Hydrophobicity and Electrostatic Potential

Electrostatic and hydrophobic characteristics of proteins have a major role in protein-protein interactions. Therefore, these properties were selected as the second and third features of the PDZ domains in the dataset. These features were generated by the VASCo software [17] and nine values were sampled for each of the ten binding residues as they were used and resulted well in one of the previous studies [12]. Sampling was done by extracting the hydrophobic and electrostatic potentials of the ten residues from the VASCo output which contains atom-based data. Afterwards, the atoms corresponded to the ten binding residues was ordered according to their x,y,z coordinates, and ninety values sampled that are equally far away from each other. By doing this calculation, we had a normalized sampling value for the ten binding domains that has different numbers of atoms. In the end, in a vector of length 90 (9 features x 10 binding residues) were generated for hydrophobic and electrostatic features, separately (18 features x 10 binding residue, in total).

3.5 Possible Phosphorylation Sites (PPS)

Post-translational modifications are known as the regulator of the protein-protein interactions [18]. In particular, phosphorylation of Ser, Thr, or Tyr residues within the PDZ domains have been proposed to modulate PDZ-mediated interactions and a recent study proves that the phosphorylation of PDZ domain binding site residue effected its binding ability dramatically [19,24,39]. Since the experimental phosphorylation data for all the PDZ domains in training dataset were not available, we used possible phosphorylation sites, the Ser, Thr and Tyr residues, in ten binding residues are marked as ‘1’ in a binary vector of length 10 (1 feature x 10 binding residues).

3.6 Peptide Feature Encoding

We followed the literature and restricted the peptide length to five C-terminal residues. Since the primary sequence of the peptide is one of the decisive determinants of interaction, amino acid content of the peptides were converted to feature. As a sequential feature, each residue of the C-terminal of ligand was mapped into a binary vector with a length of 20 where each bit represents an aminoacid, resulting in a vector of length 100, in total (20 features x 5 C-terminal residues).

3.7 Model Training and Performance Measures

We preferred to train our model with the SVM (Support Vector Machine) algorithm among several machine learning approaches. The SVM algorithm maps the feature vector to a high-dimensional space and constructs a set of hyperplanes which can be used for classification or regression [20]. The LibSVM library was used for the application of SVM [21].

The support vector machine (SVM) algorithm is a supervised binary classification learning algorithm [20]. It is well suited on discriminative classification which is learning by utilizing example data and predicting on unseen data before. The algorithm needs three components to perform: a training set, corresponding class labels to training set and a test set.

SVM generates a hyper-plane that is maximally distant (known as ‘the maximal margin hyper-plane’) from each classes on training set. In the case of linear separation is not possible, ‘kernels’ technique steps in and realizes the non-linear function to feature space [41].

The algorithm has been applied on various fields, including text categorization, image recognition and hand-written digit recognition [42]. Furthermore, SVM algorithm have been used in bioinformatics studies, including recognition of translation start sites, protein remote homology detection, protein folding issue, microarray gene expression analysis and prediction protein-protein interaction [43-47]. The popularity of the SVM stands on its flexibility and robustness as well as its accuracy even on relatively large datasets as evidenced by the listed studies. In this study, after optimization was done in a systematic manner, cost parameter, C , was choosed as 2.0, where 0.15 was picked as the Gamma parameter for interaction prediction model. Additionally, the Gamma and the cost parameter was selected as 0.05 and 2.0, respectively, for classification models.

The following statistical measurements were calculated to assess the model:

- *Sensitivity or Recall(TPR) = $TP/(TP+FN)$*
- *Precision = $TP/(TP+FP)$*
- *False Positive Rate(FPR) = $FP/(FP+TN)$*
- *Specificity = $TN/(FP+TN)$* (3.2)

where TP denotes true positive, FP denotes false positive, TN denotes true negative and FN represents false negative. We measure the performance of the model by using the receiver operating characteristics (ROC) curve which is obtained by plotting sensitivity (TPR) versus FPR and the area under the ROC curve (AUC).

Chapter 4

RESULTS

The results of this study were presented in two parts. First, the interaction prediction model's results were explained. Afterwards, the human proteome scanning test results were presented. Second, the classification model's results were presented. Then, the case study, which is based on the classification results, were discussed.

4.1 PDZ domain interaction prediction model

Significant differences in sample quantity of different classes cause imbalance problem and degenerate the performance of classifier [22]. Since the dataset we used have two times more non-binding information than binding information, we resampled our dataset before the SVM classifier was trained and optimized. Resampling is a supervised pre-process which generates samples by taking the class distribution into account. SVM classifier was optimized by altering the parameters of LibSVM systematically. To test the performance of the model we ran 10-fold cross-validation test and plotted ROC and PR curves to visualize the performance (Figure 4-1a and Figure 4-1b, respectively). The model achieved very high ROC and accuracy, namely 0.99 and 96.9 %, respectively. These results showed the model's performance is better than the previous sequence-based and structure-based models [8-12].

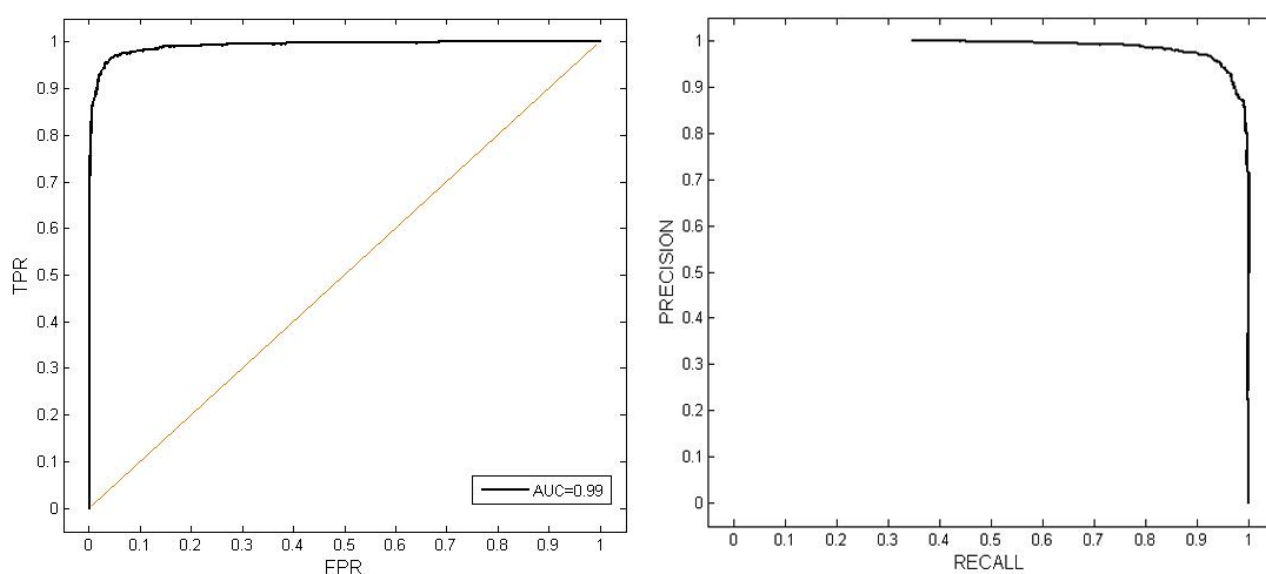


Figure 4-1 (a) ROC curve for interaction prediction model **(b)** Precision vs recall curve for interaction prediction model

ROC graphs are two-dimensional plots in which true positive rate (TPR) is plotted on the Y axis and false positive rate (FPR) is plotted on X axis. It is used to visualize the performance of a classifier. Basically, the ROC curve depicts the relative tradeoffs between benefits (TPR) and costs (FPR) of a classifier for distinct decision thresholds. Moreover, the area under the curve (AUC) is the measure of classifier performance. Since the AUC value is a portion of an unit square area, its value is always be between 0 and 1. Additionally, higher AUC value indicates a better classifier performance. Our model's ROC curve has an AUC value is 0.99. The previous structure-based interaction prediction model has an AUC value of 0.96 [12]. Even though the same dataset was used in both studies, the better performance of our model shows that the features we used are more descriptive on PDZ domain-peptide interaction. The contrubution of each feature to the model performance can be seen in Figure 4-2.

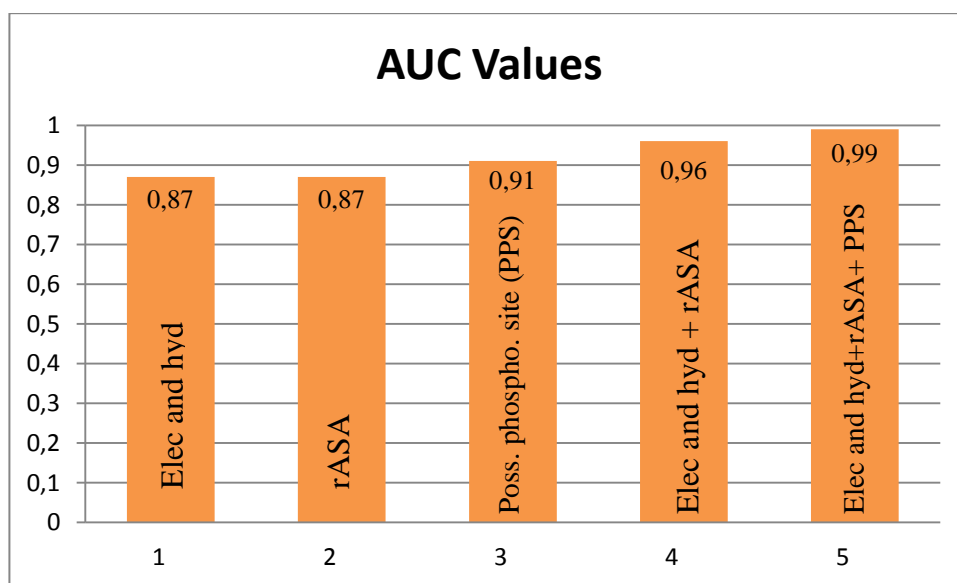


Figure 4-2 Area under ROC curve (AUC) comparison chart. AUC values for each of the features and combination of the features is showed (column number: 1- electrostatic potential and hydrophobicity, 2- relative accessible surface area, 3- possible phosphorylation sites, 4- electrostatic potential and hydrophobicity + relative accessible surface area, 5- electrostatic potential and hydrophobicity + relative accessible surface area + possible phosphorylation site)

Features has high AUC values when individually. However, even small improvements on the prediction model, with an AUC value in a certain interval (0.8-1.0), is a challenging task. By considering this fact, it is reasonable not to have dramatic AUC value differences between a single feature and a combination of them. Both the electrostatic potential-hydrophobicity and relative accessible surface area (rASA) features resulted 0.87 AUC value when they were used separately. However, when we integrate these two features, the model resulted with an AUC value of 0.96. Furthermore, when we added the possible phosphorylation sites (PPS) feature into our model, the AUC value increased from 0.96 to 0.99. Such an increase, while the model has already reached to 0.96, suggests that the PPS feature is highly informative on PDZ domain-peptide interactions.

In the study of Hui et al. [12], the electrostatic potential-hydrophobicity feature and accessible surface area were used to construct a structure-based model that resulted the AUC value of 0.96. By comparing Hui et al.'s prediction model with our model, that is represented in Figure 4-2 with a column number of 4, it can be seen that the AUC values of two are the same, namely 0.96. As we investigated the different features for these two models, it is noticed that the electrostatic potential-hydrophobicity feature is the same whereas we used relative accessible surface area (rASA) instead of accessible surface area (ASA). By considering that the two different models were utilized the same dataset, it can be said that rASA did not perform better than ASA, in this case.

Furthermore, when we compared the Hui et al.'s prediction model with our model, that is represented in Figure 4-2 with a column number of 5, the better performance of our model can be seen. In this model, we used an additional feature, possible phosphorylation sites (PPS), as a difference from the previous model (in Figure 4-2 with a column number of 4). The PPS feature carried our prediction model's performance ahead of Hui et al.'s model, where the AUC value of our's is 0.99 as the other model's is 0.96. As this results indicated, the feature of PPS had a great improvement effect on our model and increased its AUC value over previous prediction model. It is reasonable to had such an improvement for this feature, by looking at previous experimental studies that have proved the phosphorylation role in PDZ domain mediated interactions [19,24,39].

In another study that is achieved by Chen et al. [9], an interaction prediction model was constructed by using primary sequence and structure information in a different manner resulted with an AUC value of 0.87. In this study, they conducted multiple-alignment for all

PDZ domains that have available three-dimensional structural data, and identified the conserved positions among all these domains and peptides. As a result, they defined 38 pairs of residues that include 16 domain and 5 peptide residues and the amino acid type of these specific positions were used as features. However, even if they were in specific aligned positions, it is not much likely to capture PDZ domain-peptide interactions just by looking at the residue's amino acid type, as the study's results indicate, as well. Moreover, they had to use a reference structure for the alignment purposes which made generalizing the model harder. Our model has superiorities including investigation of domains from distinct aspects and utilization of 2786 interaction data between 83 PDZ domains and 217 peptide ligands. As a result of the superiorities of our model, we achieved higher performance.

One another study of Hui et al. [10], they used Chen et al.'s [9] 16-binding residue site definition to generate sequence-based features for building an interaction prediction model which resulted with an AUC value of 0.89. In this study, they generated feature vectors that represents the amino acid types of each residue in the binding site. This study differs from Chen et al.'s due in usage of broader interaction dataset which helps the generalize the model. However, still the AUC value is much lower than our interaction prediction model, namely 0.89 and 0.99, respectively. The advantages of our model which are using structural and using more condensed 10-binding residue site definition, is showed much better than primary sequence-based information.

One more example of sequence-based interaction predictor construction is achieved by Kalyoncu et al. [11] which resulted with an AUC value of 0.97. In this study, novel sequence-based features, that is called bigram and trigram, were presented. Basically, bigram and trigram features represent the frequencies of the of two and three consecutive amino acids, respectively, in the primary sequence. As it is in most of the other studies, using only sequence-based information resulted a lower AUC value than our model's. Moreover, the classifier that was used in this study, which is random forest, has less robustness than SVM classifier which we used to construct the model.

Additionally, the confusion matrix and the detailed accuracy results of interaction prediction model can be seen in Table 4-1. As it represents, our interaction prediction model has quite high true positive rate (TPR), namely 0.969 and low false positive rate (FPR) with a value of 0.043. This values indicate the power of the model on predicting positive interactions. The model were able to predict 928 positive interactions out of 984 positives.

Moreover, it was able to predict 1771 negative interactions out of 1801 negatives which gives us an insight on the high specificity of the model.

Table 4-1 Interaction prediction model’s detailed accuracy and confusion matrix results

		TP Rate	FP Rate	Precision	Recall	F-Measure	ROC Area
<i>Detailed Accuracy Results</i>	Binding	0.943	0.017	0.969	0.943	0.956	0.993
	Non-binding	0.983	0.057	0.969	0.983	0.976	0.993
	Weighted Avg.	0.969	0.043	0.969	0.969	0.969	0.993
<i>Confusion Matrix</i>			Binding		Non-binding		
	Binding		928		56		
	Non-binding		30		1771		

Here we present a stable PDZ domain mediated interaction prediction model that is constructed by utilizing the structural and possible phosphorylation features of the domains with higher accuracy than previous models [8-12]. Moreover, it is concluded that using the combination of different types of features results better than using only one type information as it has been done so far [8-12]. Our model can be used to narrow the putative partner space of PDZ domains for experimental studies. The powerful predictions of our model on both experimentally determined (X-Ray, NMR) and homology modeled domains points that its ability to predict interactions even if the domain's crystal structure is not available.

Since the experimental information of phosphorylation for the most of PDZ domains is not available, only possible site phosphorylation site definition could be used in this study. However, the model may be improved by the addition of new interaction data of PDZ mediated interactions to our dataset and by using experimental phosphorylation information instead of possible phosphorylation sites.

4.2 PDZ domain class prediction model

Promiscuousity of PDZ domains cause a multi-classification problem for class prediction, because a number of PDZ domains bind to both Class I and Class II peptides which are labeled as Class I-II. Therefore, we trained our class prediction model on these classification dataset and used to discriminate both multi-classes (Class I/ Class II/ Class I-II) and binary classes (Class I/Class II, Class I/Class I-II, Class II/Class I-II) to have an insight on their pair wise classifications. ROC and PR curves were plotted to visualize class predictors' performance (Figure 4-3 and Figure 4-4, respectively). As the ROC plot represents, the area under ROC curve (AUC) is quite high, namely 0.91. The high AUC value shows the performance of the classification model, higher AUC value indicates more qualified model.

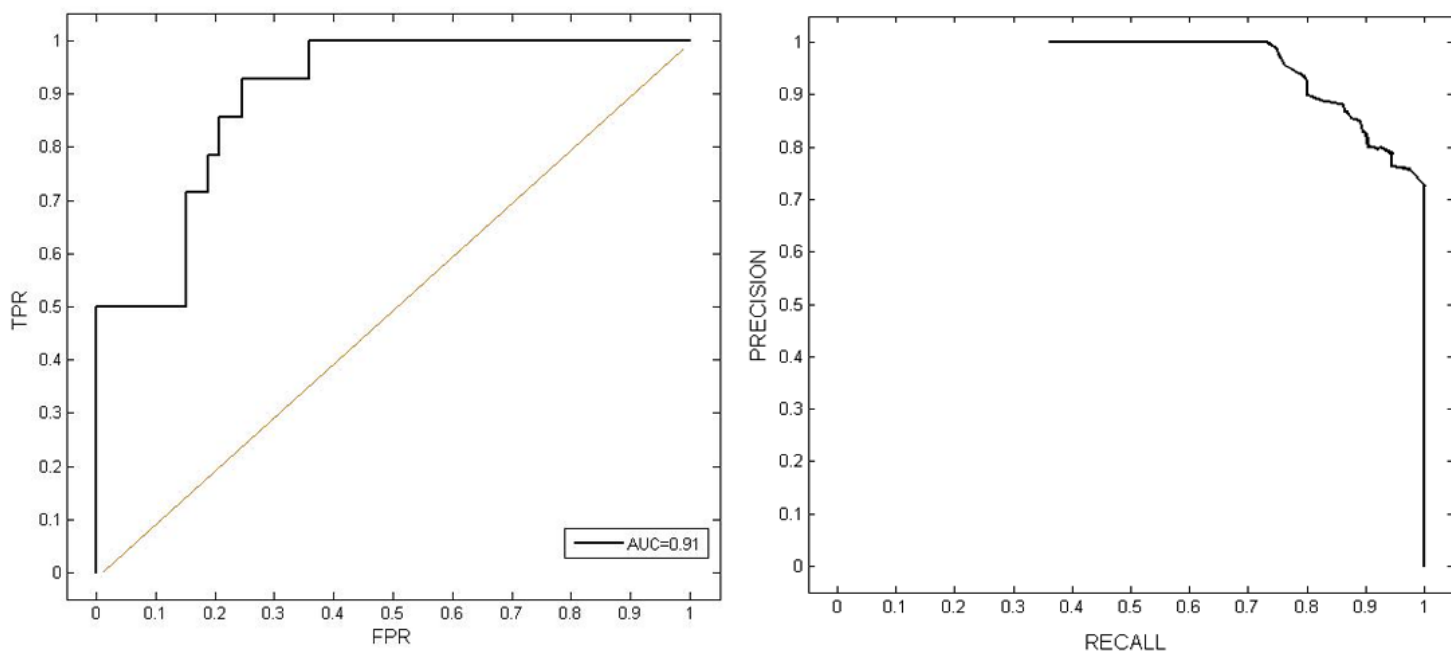


Figure 4-3 (a) ROC curve for multi-classification model **(b)** Precision vs recall curve for multi-classification model

The multi-classification model correctly classifies 7 of 13 Class I, 19 of 27 Class II and 25 of 27 Class I-II PDZ domains as it is represented in Table 4-2.

Table 4-2 Multi-classification model’s detailed accuracy and confusion matrix results

		TP Rate	FP Rate	Precision	Recall	F-Measure	ROC Area
<i>Detailed Accuracy Results</i>	Class I	0.5	0.038	0.778	0.5	0.609	0.896
	Class II	0.792	0.163	0.731	0.792	0.76	0.907
	Class I-II	0.897	0.158	0.813	0.897	0.852	0.938
	Weighted Avg.	0.776	0.135	0.776	0.776	0.768	0.918
<i>Confusion Matrix</i>		Class I		Class II		Class I-II	
	Class I	7		1		5	
	Class II	2		19		6	
	Class I-II	1		1		25	

One case of the multi-classification, that is the one between Class I and Class I-II, has the highest number of wrong classified Class I PDZ domains. Therefore, it was selected as a case study. A set of three-dimensional structures including: an originally Class I PDZ domain but predicted as Class I-II, an originally Class I PDZ domain and predicted as Class I, an originally Class I-II PDZ domain and classified as Class I-II, three structures per each category, in total 9 structures were examined (Figure 4-4). Originally Class I but predicted as Class I-II domains are LRRC7-1, SAP102-2 and SAP102-3 (Figure 4-4-a.d.g) and originally Class I and predicted as Class I domains are MAGI3-5, MASL2-1, PDZK1-1 (Figure 4-4-b.e.h), lastly, known as Class I-II and predicted as Class I-II domains are PSD95-2, PSD95-3, SAP97-3 (Figure 4-4-c.f.i) (see Appendix Table S3 for more details of PDZ domain structures). The structures investigated according to their hydrophobicity properties per residue. As the hydrophobic residues were highlighted in blue, a pattern recognized on the α B-helix of the domains (circled with dashed line in Figure 4-4). The hydrophobic residue content of α B-helix, which includes binding site of PDZ domain, is found more dense in the case of originally Class I domains that were classified as Class I-II (Figure 4-4-a.d.g). However, in the case of Class I domain predicted as Class I, the residue in the same position were hydrophilic for all three examples (Figure 4-4-b.e.h). Therefore, we conclude that if the residue in this exact position is hydrophobic in Class I PDZ domain, our multi-classification model predicted it as Class I-II. As a next step, we looked into three Class I-II domains that were predicted as Class I-II by our model. Interestingly, Class I-II domains had the same hydrophobic residue content with the wrong predicted Class I domains. Thus, these hydrophobic residues caused the wrong prediction of Class I PDZ domains which had this hydrophobic pattern.

The multiple-sequence alignment was conducted to identify the position of this hydrophobic residue (Figure 4-5). According to the alignment results, this particular residue position is detected as the 65th residue of the PDZ domain which corresponds to the 5th residue of α B-helix (marked on Figure 4-4). Furthermore, the 5th residue of α B-helix is one of the binding residues in ten-binding site definition (see Figure 2-1.b for correspondence).

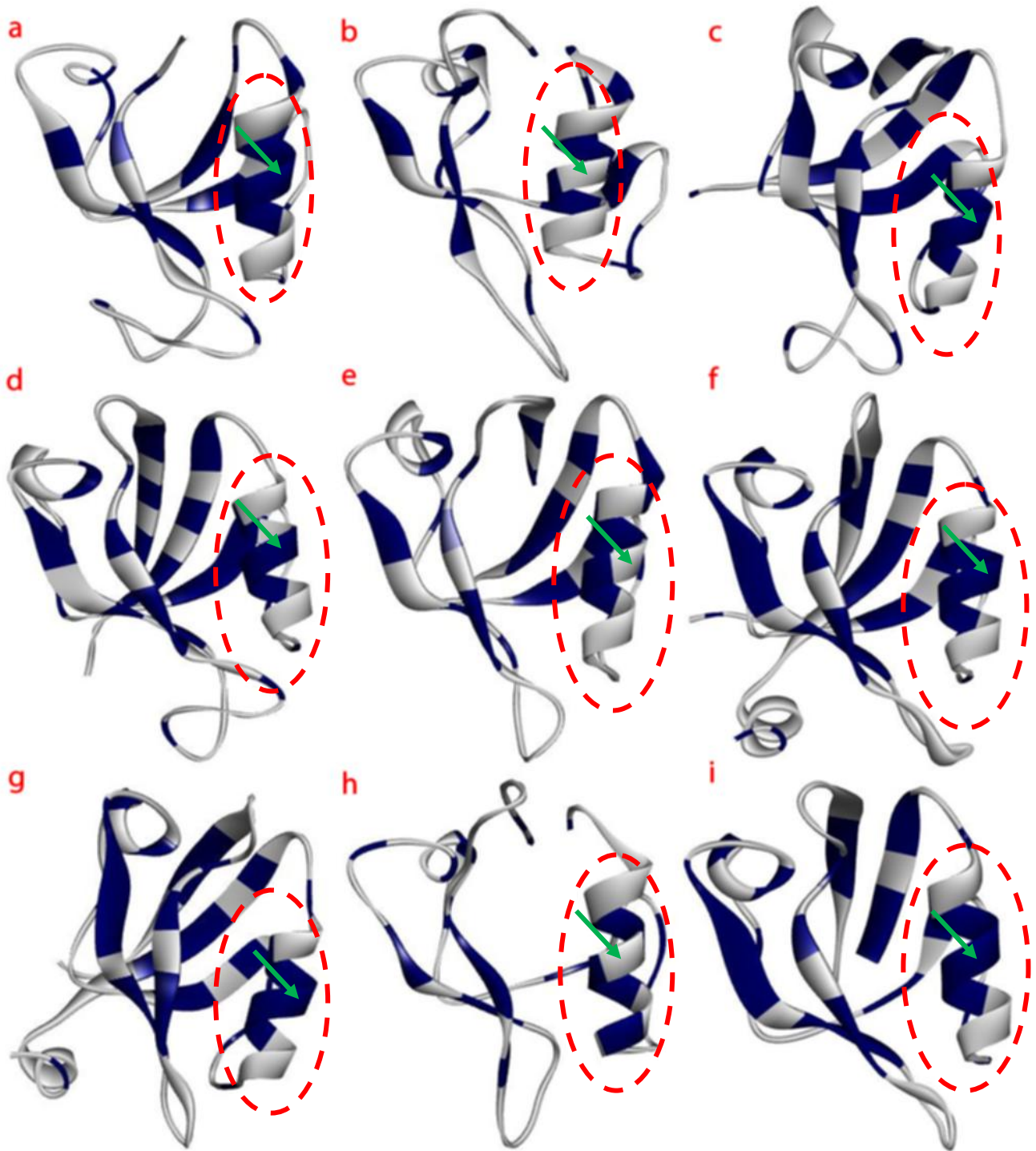


Figure 4-4 Structural comparison of Class I but predicted as Class I-II (a-d-g), Class I and predicted as Class I (b-e-h) and Class I-II and predicted Class I-II domains (c-f-i) Hydrophobic residues are highlighted in blue, α B-helices are circled with dashed line, 5th residue of the α B-helices marked with a green pointer. (a: LRRC7-1, b: MAGI3-5, c: PSD95-2, d: SAP102-2, e: MASL2-1, f: PSD95-3, g: SAP102-3, h: PDZK1-1, i: SAP9703)

We concluded that the hydrophobicity properties of particular residues on PDZ domain structure has more important role than others on its binding preferences. As it is explained in *3.4 Hydrophobicity and Electrostatic Potential* section, we generated hydrophobicity value by considering PDZ domain as a whole. Instead, by using hydrophobicity feature per residue may contribute to the classification model's performance according to the case study.

```

LRRC7-1  1  -----NP--GLGFSISGGISGQGNPFKPSDKGIFVTRVQPDGPA--SNLLQPGDKILQANGHSFVHMEHEKAVLLLKSFQNTVDLVIQRE-----
SAP102-2 1  ----TIMEVNLLKGP-KGLGFSIAGGI---GNQHIPGDNSIYITKIEGGAAQKDGRLQIGDRLLAVNNTNLQDVRHEEAVASLKNTSDMVYLKVA-KPGS-----
SAP102-3 1  --TREPRKIILHKGS-TGLGFNIVGG----ED----GEGIFVSFILAGGPADLSGELRRGDRILSVNGVNLRNATHEQAAAALKRAGQSVTIIVAQYRPEEYSRFES
MAGI3-5  1  -----LQRKEN-EGFGFVILTSK---NKPPPVGVIPHKIGRVIEGSPADRCGKLVGDHISAVNGQSIVELSHDNIVQLIKDAGVTVILTVI-----
PDZK1-1  1  -----CKLSKQEGQNYGFFLRIEK-----DTEGHLVRVVEKCSPAEKAG-LQDGDRVLRINGVVFVDKEEHMQVVDLVRKSGNSV-----
MALS2-1  1  -----VVELPKTD-EGLGFNIMGGK---EQ----NSPIYISRVIPGGVADRHGGLKRGDQLLSVNGVSVVEGEHHEKAVELLKAAQGSVKLVVRYTP-----
PSD95-2  1  -----EIKLIKGP-KGLGFSIAGGV---GNQHIPGDNSIYVTKIEGGAAHKDGRLQIGDKILAVNSVGLEDVMHEDAVAALKNTYDVVYLKVA-KPSNA-----
PSD95-3  1  DIPREPRRIVIHRGS-TGLGFNIVGG---ED----GEGIFISFILAGGPADLSGELRKGQILSVNGVDLRNASHEQAAAIALKNAGQTVTIIIAQYKPEEYSRFEA
SAP97-3  1  ---EPRKVVLHRGS-TGLGFNIVGG---ED----GEGIFISFILAGGPADLSGELRKGDRIISVNSVDLRAASHEQAAAALKNAGQAVTIVA-----

```

Figure 4-5 Multiple-sequence alignment results (the specific position of 65th residue of the domain is marked with a red box.)

As it can be seen in more detail in Table 4-3, Table 4-4 and Table 4-5, the binary classification models were able to differentiate most of the classes correctly. Differentiating Class I from Class II was achieved with an AUC value of 0.91 (Table 4-3).

Table 4-3 Class I/Class II binary classification model’s detailed accuracy and confusion matrix results

		TP Rate	FP Rate	Precision	Recall	F-Measure	ROC Area
<i>Detailed Accuracy Results</i>	Class I	0.538	0.037	0.875	0.538	0.667	0.915
	Class II	0.963	0.462	0.813	0.963	0.881	0.915
	Weighted Avg.	0.825	0.324	0.833	0.825	0.812	0.915
<i>Confusion Matrix</i>		Class I			Class II		
	Class I	7			6		
	Class II	1			26		

Another binary classification model, that discriminates Class I from Class I-II, has the lowest accuracy among all binary classifiers with an AUC value of 0.75 (Table 4-4). This results suggest that Class I is more similar to Class I-II than Class II. Surprisingly, in this binary classification model, Class I TP rate is lower than Class I-II TP rate. By considering the results of the case study for multi-classification model, it can be explained that if Class I domains had a hydrophobic residue at the aB-helix, the classifier TP rate for Class I decreased. This results are consistent with the case study very well.

Table 4-4 Class I/Class I-II binary classification model's detailed accuracy and confusion matrix results

		TP Rate	FP Rate	Precision	Recall	F-Measure	ROC Area
<i>Detailed Accuracy Results</i>	Class I	0.308	0.037	0.8	0.308	0.444	0.752
	Class I-II	0.963	0.692	0.743	0.963	0.839	0.752
	Weighted Avg.	0.75	0.479	0.761	0.75	0.711	0.752
<i>Confusion Matrix</i>		Class I			Class I-II		
	Class I	4			9		
	Class I-II	1			26		

The last binary classification model, which is Class II/Class I-II classifier, has the highest accuracy among all binary classification models with an AUC value of 0.97 (Table 4-5). The success on differentiating Class II from Class I-II suggests that Class II binding preferences and structural properties are quite different from Class I-II.

Table 4-5 Class II/Class I-II binary classification model's detailed accuracy and confusion matrix results

		TP Rate	FP Rate	Precision	Recall	F-Measure	ROC Area
<i>Detailed Accuracy Results</i>	Class II	0.889	0.074	0.923	0.889	0.906	0.977
	Class I-II	0.926	0.111	0.893	0.926	0.909	0.977
	Weighted Avg.	0.907	0.093	0.908	0.907	0.907	0.977
<i>Confusion Matrix</i>		Class II			Class I-II		
	Class II	24			3		
	Class I-II	2			25		

To sum up with, the comparison of performances of binary classifications in Table 4-3 shows that Class II / Class I-II classification has the highest accuracy whereas Class I / Class I-II differentiation has the lowest accuracy. These results suggest that the peptide selections of Class II and Class I-II is more similar than any others and Class I-II may have its unique binding preferences. Moreover, the binary classification results are highly consistent with the multi-classification and the case study results.

Table 4-6: Prediction results for multi-class learning and binary learning for pair wise combinations of three classes (Weighted average results were shown.)

	TP Rate	FP Rate	Precision	ROC Area	Accuracy(%)
Class I, Class II, Class I-II	0.791	0.135	0.798	0.918	79.1
Class I, Class II	0.825	0.324	0.833	0.915	82.5
Class I, Class I-II	0.75	0.479	0.761	0.752	75
Class II, Class I-II	0.907	0.093	0.908	0.977	90.7

In the study of Kalyoncu et al.'s [11], the same classification definition, which includes Class I, Class II and Class I-II as a promiscuous class, was used to construct classification models. As it can be seen in Table 4-7, they had quite high accuracy for both multi-classification and binary classification models. In this study, a novel primary sequence based feature was used which are named as bigram and trigram. Additionally, the results of all classifier were shown separately for bigram and trigram features. As a difference from our classification models, they utilized Random Forest classifier to construct models. The lower accuracy of our model may be explained as the sequence-based features give more information about the classification of the PDZ domains. However, since we used different classifiers to construct the models, testing these models on the same dataset would be more informative on the comparison of the model performances.

Table 4-7 Multi-classification and binary classification weighted average results were shown for Kalyoncu et al.'s study [11]

	TP Rate		FP Rate		Precision		Accuracy(%)	
	<i>Bigram - Trigram</i>							
Class I, Class II, Class I-II	0.895	0.907	0.093	0.081	0.902	0.911	89.5	90.7
Class I, Class II	0.956	0.918	0.200	0	0.915	1	90.8	93.8
Class I, Class I-II	0.955	0.900	0.227	0	0.894	1	89.4	92.4
Class II, Class I-II	0.813	1	0	0.107	1	0.812	92.7	92.7

The classification model that we have proposed in this study is based on the general knowledge of PDZ domain's classification issue. Although the PDZ domains show high interaction selectivity, there are PDZ domains that can interact both Class I and Class II which are named as Class I-II [11]. The high performance of discriminating this promiscuous class of PDZ domain among other classes suggest that there may be a pattern for Class I-II PDZ domains. This result supports the general classification knowledge of PDZ domains.

4.3 Human proteome scanning

To interrogate the reliability of the interaction prediction model, we scanned the human proteome for 218 PDZ domain interactions and compared them with the known interactions of these PDZ domains. For comparison purpose of the model with previous structure-based prediction model [12], we used the same human proteome C-terminals and human PDZ domains (defined by genome assembly Ensembl:GRCh37.64). In total, 61 XRAY and nine NMR structures were retrieved from PDB whereas 148 PDZ domains were modeled via SWISS-MODEL (see Appendix: Table S3 for more details, the same data was used with the Bader et. al study [12]). All models had a similarity above 22% (average 72%) with template sequence and QMEAN score of at least 0.36 (average 0.78). All of PDZ domain containing protein's interactions were obtained from IRefIndex [25] database that collects interactions from various databases including BioGRID [26], BIND [27], IntAct[28], CORUM [29], DIP [30], HPRD [31] and MINT [32].

As a result, the model had positive interaction predictions for 101 domains out of 218, where the model could not predict any positive interactions for remaining 117 PDZ domains. Then, we validated these positive predicted interactions of 101 domains with their experimentally known interactions. To be consistent with the previous structure-based model's human proteome scanning results, an average value of TP rate's of 101 PDZ domains was calculated. The average of 101 PDZ domain TP rates was over 17%. Previous structure-based interaction model's human proteome scanning resulted with positive predictions for 88 domains out of the same 218 PDZ domains that we used, and could not have positive interaction predictions for remaining 130 domains. Moreover, the same average calculation for 88 domain TP rates was ended up with a value of 21%. To be able to compare these two results, that are an average TP rate value of 17% for 101 PDZ domains and an average TP rate

value of 21% for 88 PDZ domains, we calculated the total averages for the same 218 domains that we both used. The total averages concluded with the value of 8% for both models. However, since our model had true positive predictions for 101 domains where the previous one had for 88 domains, these results show that our model has more generalized rules than the previous one.

Afterwards, we investigated the common PDZ domains between 101 domains and 88 domains, that have true positive interaction predictions from our and the previous model, respectively. It is found for 69 common PDZ domains both models had true positive predictions. Our model has a TP rate with a number of over 23% for 69 common PDZ domains.

There were some issues that might affect proteome scanning ability dramatically. First of all, known PPIs information is not specific to PDZ domains but to the protein as a whole that means the interaction might occur via other domains. Second, almost all the proteins that are scanned for PPIs have multiple PDZ domains, therefore, assigning an interaction to particular PDZ domain was not possible. In spite of the handicaps that affect the scanning results, correct predictions for 101 PDZ domains out of 218 with an average of greater than 17% shows the achievement of the predictor model.

Table 4-8 Human proteome scanning results (Number of experimentally proved interactions and number of the model predicted correctly for each domain. The first 69 domains are the mutual domains with the previous study [12])

Row indices	PDZ Domain name	# of known interactions	# of correctly predicted interactions
1	APBA3-1	4	0
2	APBA3-2	4	0
3	CASK-1	54	4
4	DLG1-1	77	25
5	DLG1-2	77	25
6	DLG1-3	77	25
7	DLG2-1	43	19
8	DLG2-2	43	24
9	DLG2-3	43	27
10	DLG3-1	50	13
11	DLG3-2	50	19
12	DLG3-3	50	12
13	DLG4-1	119	36
14	DLG4-2	119	33
15	DLG4-3	119	41
16	ERBB2IP-1	31	6
17	IL16-1	24	4
18	LIN7A-1	15	3
19	LIN7B-1	14	3
20	LIN7C-1	14	1
21	LRRC7-1	12	2
22	MAGI1-2	32	1
23	MAGI1-4	32	1
24	MAGI1-5	32	2
25	MAGI1-6	32	4
26	MAGI2-2	18	1
27	MAGI2-4	18	0
28	MAGI2-5	18	1
29	MAGI2-6	18	3
30	MAGI3-2	20	7
31	MAGI3-4	20	0
32	MAGI3-5	20	1
33	MAGI3-6	20	6
34	MAST2-1	13	0
35	MPDZ-1	22	0

36	MPDZ-2	22	0
37	MPDZ-3	22	1
38	MPDZ-4	22	0
39	MPDZ-5	22	1
40	MPDZ-7	22	1
41	MPDZ-10	22	7
42	MPDZ-12	22	2
43	MPDZ-13	22	1
44	MPP6-1	26	1
45	PDZD3-1	13	0
46	PDZK1-1	30	5
47	PTPN3-1	13	0
48	SCRIB-1	20	5
49	SCRIB-2	20	6
50	SCRIB-4	20	1
51	SHANK2-1	21	5
52	SLC9A3R2-2	41	22
53	SNTA1-1	29	6
54	SNTB1-1	11	6
55	SNTB2-1	16	5
56	SNTG2-1	4	1
57	SYNJ2BP-1	9	1
58	TJP1-1	62	10
59	TJP2-1	20	1
60	PDZD2-3	6	1
61	PDZD2-5	6	0
62	INADL-8	39	1
63	INADL-9	39	0
64	INADL-2	39	7
65	INADL-3	39	1
66	INADL-6	39	14
67	PTPN4-1	16	0
68	SCRIB-3	20	4
69	PTPN13-1	26	0
70	MAGI3-3	20	0
71	PTPN13-2	26	0
72	NOS1-1	31	0
73	APBA2-2	12	0
74	APBA2-1	12	0
75	APBA1-2	24	0
76	DVL1-1	32	0

77	GRIP1-2	28	0
78	LDB3-1	4	0
79	PSCDBP-1	3	0
80	PDZRN3-1	4	0
81	PARD3B-2	10	1
82	PDZD4-1	1	0
83	INADL-5	39	6
84	DVL1L1-1	2	0
85	DVL2-1	63	0
86	RGS3-1	20	0
87	SHANK3-1	8	1
88	ARHGEF12-1	11	0
89	WHRN-1	1	0
90	SHROOM3-1	2	0
91	MAGI2-3	18	0
92	PICK1-1	51	0
93	PDLIM7-1	29	0
94	MPP4-1	3	0
95	PDLIM4-1	5	0
96	PDZD11-1	3	1
97	RADIL-1	10	0
98	PTPN13-4	26	0
99	IL16-3	24	3
100	MPDZ-11	22	0
101	DVL3-1	31	0
	TOTAL	2729	477

Chapter 5

CONCLUSION

PDZ domain's binding specificity preferences becomes more and more clear with the computational and high-throughput experimental studies. Since the PDZ domains are involved several cell processes, revealing PDZ domain mediated interactions and finding out its binding behaviour will contribute to many of the studies including PDZ related disease mechanisms and novel drug development.

This study aims to construct a powerful and robust model for prediction PDZ domain – peptide interactions and classification of PDZ domains. A model was trained on interaction dataset of PDZ domains which contains 83 PDZ domains with 871 ligands. To train such a model hydrophobicity, electrostatic potential and relatively accessible surface area were used as structural features whereas possible phosphorylation sites were used as post-translational feature of the PDZ domains. Peptides were converted into sequential information according to the amino acid types as a binary vector with a length of 20 per residue.

For interaction prediction, the model performance was tested on cross-validation set resulted a high area under ROC curve, namely, 0.99. Such high performance proved that utilizing structural and sequential features in the same model is more advantageous than using only one type of feature. Additionally, using the number of threonine, tyrosine and serine residues in the binding site of PDZ domain as possible phosphorylation sites feature, had a great contribution on the interaction prediction model performance which shows the important role of post-translational modifications on binding preferences of PDZ domains.

Both the multi-classification and the binary classification models achieved high performance on categorizing the PDZ domains. The multi-classification of the PDZ domains was one of the challenges because we did not want to discriminate only Class I and Class II PDZ domains, but also the promiscuous PDZ domain class, namely Class I-II. Nevertheless, our model achieved very well performance on multi-classification issue with an area under ROC curve of 0.88. Since the model was constructed based on the general pattern of PDZ domain classification, these results encourages the current knowledge. Moreover, the comparison of the binary classifications of the pair wise combinations of three classes gave

insight about the diversity of the PDZ domain classes. As the results indicated, the most diverse classes were Class II/Class I-II where the most alike ones were Class I/Class I-II. Moreover, a case study that examines the differences between Class I and Class I-II in terms of the surface properties was accomplished. As the results indicated, Class I-II has a hydrophobic residue in the 5th position of α B-helix secondary structure. Additionally, it is also concluded that if Class I domains have a hydrophobic residue in this position, the classification models may classify the Class I PDZ domain as Class I-II.

Furthermore, we scanned the human proteome for 218 PDZ domains to be able to compare our model with the previous one that we used the same dataset and have an insight of the predictor's performance. All the PDZ domains that were possible to generate structural features, with a total number of 218 were used to scan the human proteome with a number of peptides of over 43000. After the scanning process, only the 101 domains that have positive predicted interactions were validated by using their experimentally known interactions. As a result of validation, the model predicted several human known PPIs successfully with an average of TP rate of 101 domains greater than 17%.

Concerning the future directions, current study might have implications on finding novel binding partners of PDZ domains as well as drug discovery. The robustness and performance of the models may be improved by using experimental phosphorylation information for PDZ domain. The quality of the model may be increased by integrating the recent experimental data to the training set, as well. Lastly, a web server of the model may be developed to make it easier to use by others.

APPENDIX

Table S1.a PDZ domain interaction dataset (PDZ domain name, Experiment(PM = Protein microarray, PD = Phage display), Organism(M = Mouse, H = Human), Domain ID(see Table S1.b), Peptide ID(see Table S1.c), Interaction).

PDZ domain name	Experiment	Organism	Domain ID	Peptide ID	Interaction	PDZ domain name	Experiment	Organism	Domain ID	Peptide ID	Interaction
A1-SYNTROPHIN-1	PM	M	0	0	Y	MAGI-3-1	PM	M	21	523	N
A1-SYNTROPHIN-1	PM	M	0	1	Y	MAGI-3-1	PM	M	21	564	N
A1-SYNTROPHIN-1	PM	M	0	2	Y	MAGI-3-1	PM	M	21	7	N
A1-SYNTROPHIN-1	PM	M	0	3	Y	MAGI-3-1	PM	M	21	565	N
A1-SYNTROPHIN-1	PM	M	0	4	Y	MAGI-3-1	PM	M	21	566	N
A1-SYNTROPHIN-1	PM	M	0	5	Y	MAGI-3-1	PM	M	21	567	N
B1-SYNTROPHIN-1	PM	M	1	5	Y	MAGI-3-1	PM	M	21	454	N
B1-SYNTROPHIN-1	PM	M	1	6	Y	MAGI-3-1	PM	M	21	496	N
B1-SYNTROPHIN-1	PM	M	1	7	Y	MAGI-3-1	PM	M	21	568	N
B1-SYNTROPHIN-1	PM	M	1	3	Y	MAGI-3-1	PM	M	21	569	N
B1-SYNTROPHIN-1	PM	M	1	5	Y	MAGI-3-1	PM	M	21	570	N
B1-SYNTROPHIN-1	PM	M	1	8	Y	MAGI-3-1	PM	M	21	571	N
B1-SYNTROPHIN-1	PM	M	1	9	Y	MAGI-3-2	PM	M	22	25	N
B1-SYNTROPHIN-1	PM	M	1	10	Y	MAGI-3-2	PM	M	22	21	N
B1-SYNTROPHIN-1	PM	M	1	2	Y	MAGI-3-2	PM	M	22	1	N
B1-SYNTROPHIN-1	PM	M	1	4	Y	MAGI-3-2	PM	M	22	519	N
B1-SYNTROPHIN-1	PM	M	1	11	Y	MAGI-3-2	PM	M	22	508	N
B1-SYNTROPHIN-1	PM	M	1	12	Y	MAGI-3-2	PM	M	22	23	N
B1-SYNTROPHIN-1	PM	M	1	0	Y	MAGI-3-2	PM	M	22	6	N
B1-SYNTROPHIN-1	PM	M	1	13	Y	MAGI-3-5	PM	M	23	572	N
B1-SYNTROPHIN-1	PM	M	1	14	Y	MAGI-3-5	PM	M	23	573	N
CHAPSYN-110-2	PM	M	2	15	Y	MAGI-3-5	PM	M	23	7	N
CHAPSYN-110-2	PM	M	2	0	Y	MAGI-3-5	PM	M	23	574	N
CHAPSYN-110-2	PM	M	2	4	Y	MAGI-3-5	PM	M	23	575	N
CHAPSYN-110-2	PM	M	2	16	Y	MAGI-3-5	PM	M	23	2	N
CHAPSYN-110-2	PM	M	2	17	Y	MAGI-3-5	PM	M	23	20	N
CHAPSYN-110-2	PM	M	2	9	Y	MAGI-3-5	PM	M	23	62	N
CHAPSYN-110-2	PM	M	2	5	Y	MAGI-3-5	PM	M	23	560	N
CHAPSYN-110-2	PM	M	2	18	Y	MAGI-3-5	PM	M	23	576	N
CHAPSYN-110-2	PM	M	2	19	Y	MAGI-3-5	PM	M	23	65	N
CHAPSYN-110-2	PM	M	2	20	Y	MAGI-3-5	PM	M	23	472	N
CHAPSYN-110-2	PM	M	2	2	Y	MAGI-3-5	PM	M	23	559	N
CHAPSYN-110-2	PM	M	2	17	Y	MAGI-3-5	PM	M	23	68	N
CHAPSYN-110-2	PM	M	2	21	Y	MAGI-3-5	PM	M	23	554	N
CHAPSYN-110-2	PM	M	2	8	Y	MAGI-3-5	PM	M	23	561	N

CHAPSYN-110-2	PM	M	2	6	Y	MAGI-3-5	PM	M	23	577	N
CHAPSYN-110-2	PM	M	2	5	Y	MAGI-3-5	PM	M	23	578	N
CHAPSYN-110-2	PM	M	2	1	Y	MAGI-3-5	PM	M	23	67	N
CHAPSYN-110-2	PM	M	2	11	Y	MAGI-3-5	PM	M	23	579	N
CHAPSYN-110-3	PM	M	3	22	Y	MAGI-3-5	PM	M	23	534	N
CHAPSYN-110-3	PM	M	3	0	Y	MAGI-3-5	PM	M	23	445	N
CHAPSYN-110-3	PM	M	3	16	Y	MAGI-3-5	PM	M	23	580	N
CHAPSYN-110-3	PM	M	3	14	Y	MAGI-3-5	PM	M	23	581	N
CHAPSYN-110-3	PM	M	3	5	Y	MAGI-3-5	PM	M	23	555	N
CHAPSYN-110-3	PM	M	3	5	Y	MAGI-3-5	PM	M	23	582	N
CHAPSYN-110-3	PM	M	3	6	Y	MALS2-1	PM	M	24	583	N
CHAPSYN-110-3	PM	M	3	20	Y	MALS2-1	PM	M	24	584	N
CHAPSYN-110-3	PM	M	3	23	Y	MALS2-1	PM	M	24	506	N
CHAPSYN-110-3	PM	M	3	24	Y	MALS2-1	PM	M	24	585	N
CHAPSYN-110-3	PM	M	3	2	Y	MALS2-1	PM	M	24	586	N
CHAPSYN-110-3	PM	M	3	8	Y	MALS2-1	PM	M	24	587	N
CHAPSYN-110-3	PM	M	3	25	Y	MALS2-1	PM	M	24	567	N
CHAPSYN-110-3	PM	M	3	15	Y	MALS2-1	PM	M	24	37	N
CHAPSYN-110-3	PM	M	3	1	Y	MALS2-1	PM	M	24	588	N
CHAPSYN-110-3	PM	M	3	9	Y	MALS2-1	PM	M	24	589	N
CIPP-10	PM	M	4	26	Y	MALS2-1	PM	M	24	502	N
CIPP-10	PM	M	4	22	Y	MALS2-1	PM	M	24	566	N
CIPP-10	PM	M	4	27	Y	MPP7-1	PM	M	25	474	N
CIPP-3	PM	M	5	26	Y	MPP7-1	PM	M	25	473	N
CIPP-3	PM	M	5	28	Y	MPP7-1	PM	M	25	475	N
CIPP-5	PM	M	6	29	Y	MPP7-1	PM	M	25	64	N
CIPP-5	PM	M	6	30	Y	MPP7-1	PM	M	25	472	N
CIPP-5	PM	M	6	31	Y	MPP7-1	PM	M	25	35	N
CIPP-5	PM	M	6	32	Y	MPP7-1	PM	M	25	15	N
CIPP-5	PM	M	6	32	Y	MPP7-1	PM	M	25	57	N
CIPP-8	PM	M	7	26	Y	MPP7-1	PM	M	25	463	N
CIPP-8	PM	M	7	21	Y	MPP7-1	PM	M	25	3	N
CIPP-8	PM	M	7	20	Y	MPP7-1	PM	M	25	73	N
CIPP-8	PM	M	7	23	Y	MPP7-1	PM	M	25	17	N
CIPP-8	PM	M	7	9	Y	MPP7-1	PM	M	25	23	N
CIPP-8	PM	M	7	33	Y	MPP7-1	PM	M	25	467	N
CIPP-8	PM	M	7	34	Y	MPP7-1	PM	M	25	465	N
CIPP-8	PM	M	7	35	Y	MPP7-1	PM	M	25	466	N
CIPP-8	PM	M	7	36	Y	MPP7-1	PM	M	25	45	N
CIPP-8	PM	M	7	25	Y	MPP7-1	PM	M	25	43	N
CIPP-9	PM	M	8	29	Y	MPP7-1	PM	M	25	26	N
CIPP-9	PM	M	8	37	Y	MPP7-1	PM	M	25	29	N
CIPP-9	PM	M	8	26	Y	MPP7-1	PM	M	25	16	N
CIPP-9	PM	M	8	38	Y	MPP7-1	PM	M	25	470	N
CIPP-9	PM	M	8	39	Y	MPP7-1	PM	M	25	476	N
CIPP-9	PM	M	8	40	Y	MPP7-1	PM	M	25	22	N

CIPP-9	PM	M	8	41	Y	MPP7-1	PM	M	25	13	N
CIPP-9	PM	M	8	42	Y	MPP7-1	PM	M	25	41	N
DVL1-1	PM	M	9	26	Y	MPP7-1	PM	M	25	65	N
DVL1-1	PM	M	9	30	Y	MPP7-1	PM	M	25	468	N
DVL1-1	PM	M	9	27	Y	MPP7-1	PM	M	25	469	N
DVL3-1	PM	M	10	30	Y	MPP7-1	PM	M	25	454	N
DVL3-1	PM	M	10	43	Y	MPP7-1	PM	M	25	63	N
DVL3-1	PM	M	10	26	Y	MUPP1-1	PM	M	26	64	N
DVL3-1	PM	M	10	27	Y	MUPP1-1	PM	M	26	473	N
ERBIN-1	PM	M	11	17	Y	MUPP1-1	PM	M	26	474	N
ERBIN-1	PM	M	11	9	Y	MUPP1-1	PM	M	26	65	N
GRIP1-6	PM	M	12	44	Y	MUPP1-1	PM	M	26	41	N
HARMONIN-2	PM	M	13	26	Y	MUPP1-1	PM	M	26	472	N
HARMONIN-2	PM	M	13	45	Y	MUPP1-1	PM	M	26	15	N
LARG-1	PM	M	14	8	Y	MUPP1-1	PM	M	26	57	N
LARG-1	PM	M	14	0	Y	MUPP1-1	PM	M	26	463	N
LARG-1	PM	M	14	20	Y	MUPP1-1	PM	M	26	23	N
LIN-7C-1	PM	M	15	15	Y	MUPP1-1	PM	M	26	465	N
LIN-7C-1	PM	M	15	1	Y	MUPP1-1	PM	M	26	13	N
LIN-7C-1	PM	M	15	2	Y	MUPP1-1	PM	M	26	2	N
LIN-7C-1	PM	M	15	7	Y	MUPP1-1	PM	M	26	467	N
LIN-7C-1	PM	M	15	14	Y	MUPP1-1	PM	M	26	468	N
LIN-7C-1	PM	M	15	9	Y	MUPP1-1	PM	M	26	17	N
LIN-7C-1	PM	M	15	5	Y	MUPP1-1	PM	M	26	475	N
LIN-7C-1	PM	M	15	0	Y	MUPP1-1	PM	M	26	43	N
LIN-7C-1	PM	M	15	46	Y	MUPP1-1	PM	M	26	3	N
LIN-7C-1	PM	M	15	47	Y	MUPP1-1	PM	M	26	29	N
LIN-7C-1	PM	M	15	12	Y	MUPP1-1	PM	M	26	454	N
LIN-7C-1	PM	M	15	13	Y	MUPP1-1	PM	M	26	45	N
LIN-7C-1	PM	M	15	24	Y	MUPP1-1	PM	M	26	73	N
LIN-7C-1	PM	M	15	10	Y	MUPP1-1	PM	M	26	470	N
LIN-7C-1	PM	M	15	19	Y	MUPP1-1	PM	M	26	16	N
LIN-7C-1	PM	M	15	5	Y	MUPP1-1	PM	M	26	469	N
LIN-7C-1	PM	M	15	4	Y	MUPP1-1	PM	M	26	466	N
LIN-7C-1	PM	M	15	8	Y	MUPP1-1	PM	M	26	476	N
LIN-7C-1	PM	M	15	6	Y	MUPP1-1	PM	M	26	22	N
LRRC7-1	PM	M	16	0	Y	MUPP1-1	PM	M	26	63	N
LRRC7-1	PM	M	16	14	Y	MUPP1-1	PM	M	26	35	N
LRRC7-1	PM	M	16	9	Y	MUPP1-1	PM	M	26	30	N
MAGI-1-6	PM	M	17	17	Y	MUPP1-10	PM	M	27	470	N
MAGI-1-6	PM	M	17	11	Y	MUPP1-10	PM	M	27	467	N
MAGI-1-6	PM	M	17	39	Y	MUPP1-10	PM	M	27	475	N
MAGI-1-6	PM	M	17	14	Y	MUPP1-10	PM	M	27	472	N
MAGI-1-6	PM	M	17	17	Y	MUPP1-10	PM	M	27	16	N
MAGI-1-6	PM	M	17	3	Y	MUPP1-10	PM	M	27	63	N
MAGI-1-6	PM	M	17	0	Y	MUPP1-10	PM	M	27	29	N

MAGI-1-6	PM	M	17	9	Y	MUPP1-10	PM	M	27	30	N
MAGI-1-6	PM	M	17	18	Y	MUPP1-10	PM	M	27	454	N
MAGI-1-6	PM	M	17	8	Y	MUPP1-10	PM	M	27	65	N
MAGI-1-6	PM	M	17	48	Y	MUPP1-10	PM	M	27	83	N
MAGI-1-6	PM	M	17	49	Y	MUPP1-10	PM	M	27	3	N
MAGI-2-2	PM	M	18	20	Y	MUPP1-10	PM	M	27	463	N
MAGI-2-2	PM	M	18	6	Y	MUPP1-10	PM	M	27	476	N
MAGI-2-2	PM	M	18	15	Y	MUPP1-10	PM	M	27	466	N
MAGI-2-2	PM	M	18	16	Y	MUPP1-10	PM	M	27	469	N
MAGI-2-2	PM	M	18	16	Y	MUPP1-10	PM	M	27	22	N
MAGI-2-2	PM	M	18	1	Y	MUPP1-10	PM	M	27	473	N
MAGI-2-2	PM	M	18	21	Y	MUPP1-10	PM	M	27	508	N
MAGI-2-2	PM	M	18	0	Y	MUPP1-10	PM	M	27	64	N
MAGI-2-2	PM	M	18	17	Y	MUPP1-10	PM	M	27	465	N
MAGI-2-2	PM	M	18	4	Y	MUPP1-10	PM	M	27	17	N
MAGI-2-2	PM	M	18	9	Y	MUPP1-10	PM	M	27	41	N
MAGI-2-2	PM	M	18	2	Y	MUPP1-10	PM	M	27	474	N
MAGI-2-2	PM	M	18	5	Y	MUPP1-10	PM	M	27	73	N
MAGI-2-2	PM	M	18	50	Y	MUPP1-10	PM	M	27	11	N
MAGI-2-2	PM	M	18	51	Y	MUPP1-10	PM	M	27	468	N
MAGI-2-5	PM	M	19	15	Y	MUPP1-10	PM	M	27	13	N
MAGI-2-5	PM	M	19	5	Y	MUPP1-11	PM	M	28	40	N
MAGI-2-6	PM	M	20	18	Y	MUPP1-11	PM	M	28	473	N
MAGI-2-6	PM	M	20	17	Y	MUPP1-11	PM	M	28	476	N
MAGI-2-6	PM	M	20	20	Y	MUPP1-11	PM	M	28	73	N
MAGI-2-6	PM	M	20	49	Y	MUPP1-11	PM	M	28	23	N
MAGI-2-6	PM	M	20	11	Y	MUPP1-11	PM	M	28	3	N
MAGI-2-6	PM	M	20	48	Y	MUPP1-11	PM	M	28	45	N
MAGI-2-6	PM	M	20	52	Y	MUPP1-11	PM	M	28	15	N
MAGI-2-6	PM	M	20	26	Y	MUPP1-11	PM	M	28	57	N
MAGI-2-6	PM	M	20	9	Y	MUPP1-11	PM	M	28	463	N
MAGI-2-6	PM	M	20	3	Y	MUPP1-11	PM	M	28	472	N
MAGI-2-6	PM	M	20	0	Y	MUPP1-11	PM	M	28	7	N
MAGI-2-6	PM	M	20	27	Y	MUPP1-11	PM	M	28	470	N
MAGI-2-6	PM	M	20	17	Y	MUPP1-11	PM	M	28	474	N
MAGI-3-1	PM	M	21	15	Y	MUPP1-11	PM	M	28	13	N
MAGI-3-1	PM	M	21	0	Y	MUPP1-11	PM	M	28	32	N
MAGI-3-1	PM	M	21	4	Y	MUPP1-11	PM	M	28	467	N
MAGI-3-1	PM	M	21	16	Y	MUPP1-11	PM	M	28	468	N
MAGI-3-1	PM	M	21	17	Y	MUPP1-11	PM	M	28	17	N
MAGI-3-1	PM	M	21	2	Y	MUPP1-11	PM	M	28	475	N
MAGI-3-1	PM	M	21	5	Y	MUPP1-11	PM	M	28	19	N
MAGI-3-1	PM	M	21	53	Y	MUPP1-11	PM	M	28	43	N
MAGI-3-1	PM	M	21	6	Y	MUPP1-11	PM	M	28	35	N
MAGI-3-1	PM	M	21	5	Y	MUPP1-11	PM	M	28	42	N
MAGI-3-1	PM	M	21	51	Y	MUPP1-11	PM	M	28	454	N

MAGI-3-1	PM	M	21	21	Y	MUPP1-11	PM	M	28	65	N
MAGI-3-1	PM	M	21	23	Y	MUPP1-11	PM	M	28	508	N
MAGI-3-1	PM	M	21	19	Y	MUPP1-11	PM	M	28	64	N
MAGI-3-1	PM	M	21	9	Y	MUPP1-11	PM	M	28	16	N
MAGI-3-1	PM	M	21	20	Y	MUPP1-11	PM	M	28	469	N
MAGI-3-1	PM	M	21	1	Y	MUPP1-11	PM	M	28	14	N
MAGI-3-1	PM	M	21	12	Y	MUPP1-11	PM	M	28	466	N
MAGI-3-2	PM	M	22	20	Y	MUPP1-11	PM	M	28	465	N
MAGI-3-5	PM	M	23	47	Y	MUPP1-11	PM	M	28	22	N
MAGI-3-5	PM	M	23	17	Y	MUPP1-11	PM	M	28	63	N
MAGI-3-5	PM	M	23	54	Y	MUPP1-11	PM	M	28	26	N
MAGI-3-5	PM	M	23	8	Y	MUPP1-11	PM	M	28	30	N
MAGI-3-5	PM	M	23	49	Y	MUPP1-12	PM	M	29	476	N
MAGI-3-5	PM	M	23	10	Y	MUPP1-12	PM	M	29	29	N
MAGI-3-5	PM	M	23	26	Y	MUPP1-12	PM	M	29	65	N
MAGI-3-5	PM	M	23	36	Y	MUPP1-12	PM	M	29	73	N
MAGI-3-5	PM	M	23	9	Y	MUPP1-12	PM	M	29	17	N
MAGI-3-5	PM	M	23	4	Y	MUPP1-12	PM	M	29	23	N
MAGI-3-5	PM	M	23	0	Y	MUPP1-12	PM	M	29	463	N
MAGI-3-5	PM	M	23	48	Y	MUPP1-12	PM	M	29	57	N
MAGI-3-5	PM	M	23	34	Y	MUPP1-12	PM	M	29	467	N
MAGI-3-5	PM	M	23	13	Y	MUPP1-12	PM	M	29	41	N
MAGI-3-5	PM	M	23	18	Y	MUPP1-12	PM	M	29	22	N
MAGI-3-5	PM	M	23	55	Y	MUPP1-12	PM	M	29	45	N
MAGI-3-5	PM	M	23	25	Y	MUPP1-12	PM	M	29	63	N
MAGI-3-5	PM	M	23	14	Y	MUPP1-12	PM	M	29	466	N
MAGI-3-5	PM	M	23	27	Y	MUPP1-12	PM	M	29	473	N
MAGI-3-5	PM	M	23	17	Y	MUPP1-12	PM	M	29	16	N
MAGI-3-5	PM	M	23	3	Y	MUPP1-12	PM	M	29	469	N
MAGI-3-5	PM	M	23	56	Y	MUPP1-12	PM	M	29	470	N
MAGI-3-5	PM	M	23	11	Y	MUPP1-12	PM	M	29	64	N
MAGI-3-5	PM	M	23	46	Y	MUPP1-12	PM	M	29	15	N
MAGI-3-5	PM	M	23	52	Y	MUPP1-12	PM	M	29	472	N
MALS2-1	PM	M	24	16	Y	MUPP1-12	PM	M	29	5	N
MALS2-1	PM	M	24	9	Y	MUPP1-12	PM	M	29	35	N
MALS2-1	PM	M	24	15	Y	MUPP1-12	PM	M	29	474	N
MALS2-1	PM	M	24	0	Y	MUPP1-12	PM	M	29	468	N
MALS2-1	PM	M	24	16	Y	MUPP1-12	PM	M	29	475	N
MALS2-1	PM	M	24	19	Y	MUPP1-12	PM	M	29	26	N
MALS2-1	PM	M	24	8	Y	MUPP1-12	PM	M	29	30	N
MALS2-1	PM	M	24	7	Y	MUPP1-12	PM	M	29	13	N
MALS2-1	PM	M	24	1	Y	MUPP1-12	PM	M	29	465	N
MALS2-1	PM	M	24	46	Y	MUPP1-12	PM	M	29	454	N
MALS2-1	PM	M	24	2	Y	MUPP1-12	PM	M	29	43	N
MALS2-1	PM	M	24	6	Y	MUPP1-12	PM	M	29	3	N
MPP7-1	PM	M	25	30	Y	MUPP1-12	PM	M	29	436	N

MPP7-1	PM	M	25	28	Y	MUPP1-13	PM	M	30	445	N
MUPP1-1	PM	M	26	26	Y	MUPP1-13	PM	M	30	446	N
MUPP1-10	PM	M	27	23	Y	MUPP1-13	PM	M	30	0	N
MUPP1-10	PM	M	27	45	Y	MUPP1-13	PM	M	30	23	N
MUPP1-10	PM	M	27	43	Y	MUPP1-13	PM	M	30	20	N
MUPP1-10	PM	M	27	15	Y	MUPP1-13	PM	M	30	52	N
MUPP1-10	PM	M	27	35	Y	MUPP1-13	PM	M	30	68	N
MUPP1-10	PM	M	27	26	Y	MUPP1-13	PM	M	30	67	N
MUPP1-10	PM	M	27	33	Y	MUPP1-13	PM	M	30	48	N
MUPP1-10	PM	M	27	57	Y	MUPP1-13	PM	M	30	26	N
MUPP1-11	PM	M	28	41	Y	MUPP1-13	PM	M	30	25	N
MUPP1-11	PM	M	28	29	Y	MUPP1-13	PM	M	30	449	N
MUPP1-12	PM	M	29	27	Y	MUPP1-13	PM	M	30	19	N
MUPP1-13	PM	M	30	9	Y	MUPP1-13	PM	M	30	27	N
MUPP1-13	PM	M	30	8	Y	MUPP1-13	PM	M	30	21	N
MUPP1-13	PM	M	30	13	Y	MUPP1-5	PM	M	31	590	N
MUPP1-13	PM	M	30	1	Y	MUPP1-5	PM	M	31	591	N
MUPP1-13	PM	M	30	6	Y	MUPP1-5	PM	M	31	592	N
MUPP1-5	PM	M	31	29	Y	MUPP1-5	PM	M	31	593	N
MUPP1-5	PM	M	31	42	Y	MUPP1-5	PM	M	31	14	N
MUPP1-5	PM	M	31	32	Y	MUPP1-5	PM	M	31	37	N
MUPP1-5	PM	M	31	32	Y	MUPP1-5	PM	M	31	594	N
NHERF-2-2	PM	M	32	8	Y	MUPP1-5	PM	M	31	595	N
NHERF-2-2	PM	M	32	55	Y	MUPP1-5	PM	M	31	596	N
NHERF-2-2	PM	M	32	58	Y	MUPP1-5	PM	M	31	508	N
NHERF-2-2	PM	M	32	59	Y	MUPP1-5	PM	M	31	597	N
NNOS-1	PM	M	33	43	Y	MUPP1-5	PM	M	31	598	N
NNOS-1	PM	M	33	45	Y	MUPP1-5	PM	M	31	447	N
NNOS-1	PM	M	33	15	Y	MUPP1-5	PM	M	31	599	N
OMP25-1	PM	M	34	6	Y	MUPP1-5	PM	M	31	600	N
OMP25-1	PM	M	34	5	Y	NHERF-2-2	PM	M	32	61	N
OMP25-1	PM	M	34	25	Y	NHERF-2-2	PM	M	32	601	N
OMP25-1	PM	M	34	19	Y	NHERF-2-2	PM	M	32	17	N
OMP25-1	PM	M	34	21	Y	NHERF-2-2	PM	M	32	574	N
OMP25-1	PM	M	34	23	Y	NHERF-2-2	PM	M	32	602	N
OMP25-1	PM	M	34	47	Y	NHERF-2-2	PM	M	32	603	N
OMP25-1	PM	M	34	60	Y	NHERF-2-2	PM	M	32	604	N
OMP25-1	PM	M	34	20	Y	NHERF-2-2	PM	M	32	605	N
OMP25-1	PM	M	34	2	Y	NHERF-2-2	PM	M	32	606	N
OMP25-1	PM	M	34	5	Y	NHERF-2-2	PM	M	32	5	N
OMP25-1	PM	M	34	48	Y	NHERF-2-2	PM	M	32	607	N
OMP25-1	PM	M	34	17	Y	NHERF-2-2	PM	M	32	19	N
OMP25-1	PM	M	34	34	Y	NHERF-2-2	PM	M	32	608	N
OMP25-1	PM	M	34	15	Y	NHERF-2-2	PM	M	32	609	N
OMP25-1	PM	M	34	7	Y	NNOS-1	PM	M	33	16	N
OMP25-1	PM	M	34	9	Y	NNOS-1	PM	M	33	473	N

OMP25-1	PM	M	34	14	Y	NNOS-1	PM	M	33	22	N
OMP25-1	PM	M	34	50	Y	NNOS-1	PM	M	33	468	N
OMP25-1	PM	M	34	0	Y	NNOS-1	PM	M	33	13	N
OMP25-1	PM	M	34	17	Y	NNOS-1	PM	M	33	41	N
OMP25-1	PM	M	34	57	Y	NNOS-1	PM	M	33	470	N
OMP25-1	PM	M	34	4	Y	NNOS-1	PM	M	33	474	N
OMP25-1	PM	M	34	61	Y	NNOS-1	PM	M	33	463	N
OMP25-1	PM	M	34	1	Y	NNOS-1	PM	M	33	57	N
OMP25-1	PM	M	34	24	Y	NNOS-1	PM	M	33	464	N
OMP25-1	PM	M	34	62	Y	NNOS-1	PM	M	33	466	N
OMP25-1	PM	M	34	11	Y	NNOS-1	PM	M	33	26	N
OMP25-1	PM	M	34	12	Y	NNOS-1	PM	M	33	475	N
OMP25-1	PM	M	34	46	Y	NNOS-1	PM	M	33	452	N
OMP25-1	PM	M	34	16	Y	NNOS-1	PM	M	33	63	N
OMP25-1	PM	M	34	63	Y	NNOS-1	PM	M	33	17	N
OMP25-1	PM	M	34	16	Y	NNOS-1	PM	M	33	467	N
OMP25-1	PM	M	34	8	Y	NNOS-1	PM	M	33	448	N
PAR6B-1	PM	M	35	64	Y	NNOS-1	PM	M	33	469	N
PAR6B-1	PM	M	35	65	Y	NNOS-1	PM	M	33	65	N
PDZK1-1	PM	M	36	8	Y	NNOS-1	PM	M	33	465	N
PDZK1-1	PM	M	36	27	Y	NNOS-1	PM	M	33	546	N
PDZK1-1	PM	M	36	58	Y	NNOS-1	PM	M	33	462	N
PDZK1-1	PM	M	36	23	Y	NNOS-1	PM	M	33	551	N
PDZK1-1	PM	M	36	13	Y	NNOS-1	PM	M	33	29	N
PDZK1-1	PM	M	36	58	Y	NNOS-1	PM	M	33	472	N
PDZK1-1	PM	M	36	66	Y	NNOS-1	PM	M	33	73	N
PDZK1-1	PM	M	36	64	Y	NNOS-1	PM	M	33	72	N
PDZK1-1	PM	M	36	0	Y	NNOS-1	PM	M	33	476	N
PDZK1-1	PM	M	36	9	Y	NNOS-1	PM	M	33	3	N
PDZK1-1	PM	M	36	67	Y	NNOS-1	PM	M	33	30	N
PDZK1-3	PM	M	37	64	Y	NNOS-1	PM	M	33	64	N
PDZK1-3	PM	M	37	68	Y	NNOS-1	PM	M	33	553	N
PDZK1-3	PM	M	37	58	Y	NNOS-1	PM	M	33	454	N
PDZK1-3	PM	M	37	13	Y	NNOS-1	PM	M	33	35	N
PDZK1-3	PM	M	37	58	Y	NNOS-1	PM	M	33	436	N
PDZK1-3	PM	M	37	66	Y	NNOS-1	PM	M	33	23	N
PDZK1-3	PM	M	37	67	Y	NNOS-1	PM	M	33	471	N
PDZK11-1	PM	M	38	7	Y	OMP25-1	PM	M	34	529	N
PSD95-2	PM	M	39	17	Y	OMP25-1	PM	M	34	610	N
PSD95-2	PM	M	39	17	Y	OMP25-1	PM	M	34	436	N
PSD95-2	PM	M	39	9	Y	OMP25-1	PM	M	34	457	N
PSD95-2	PM	M	39	5	Y	OMP25-1	PM	M	34	446	N
PSD95-2	PM	M	39	5	Y	OMP25-1	PM	M	34	37	N
PSD95-2	PM	M	39	1	Y	OMP25-1	PM	M	34	611	N
PSD95-2	PM	M	39	2	Y	OMP25-1	PM	M	34	53	N
PSD95-2	PM	M	39	11	Y	OMP25-1	PM	M	34	612	N

PSD95-2	PM	M	39	20	Y	OMP25-1	PM	M	34	613	N
PSD95-2	PM	M	39	4	Y	OMP25-1	PM	M	34	454	N
PSD95-2	PM	M	39	15	Y	OMP25-1	PM	M	34	476	N
PSD95-2	PM	M	39	6	Y	OMP25-1	PM	M	34	614	N
PSD95-3	PM	M	40	15	Y	OMP25-1	PM	M	34	615	N
PSD95-3	PM	M	40	0	Y	OMP25-1	PM	M	34	3	N
PSD95-3	PM	M	40	16	Y	OMP25-1	PM	M	34	445	N
PSD95-3	PM	M	40	5	Y	OMP25-1	PM	M	34	26	N
PSD95-3	PM	M	40	1	Y	OMP25-1	PM	M	34	28	N
PSD95-3	PM	M	40	9	Y	OMP25-1	PM	M	34	35	N
PSD95-3	PM	M	40	5	Y	OMP25-1	PM	M	34	515	N
PSD95-3	PM	M	40	23	Y	OMP25-1	PM	M	34	524	N
PSD95-3	PM	M	40	6	Y	OMP25-1	PM	M	34	544	N
PSD95-3	PM	M	40	2	Y	OMP25-1	PM	M	34	442	N
PSD95-3	PM	M	40	20	Y	PAR6B-1	PM	M	35	26	N
PSD95-3	PM	M	40	8	Y	PAR6B-1	PM	M	35	29	N
PSD95-3	PM	M	40	14	Y	PAR6B-1	PM	M	35	474	N
PTP-BL-2	PM	M	41	5	Y	PAR6B-1	PM	M	35	454	N
PTP-BL-2	PM	M	41	47	Y	PAR6B-1	PM	M	35	3	N
PTP-BL-2	PM	M	41	33	Y	PAR6B-1	PM	M	35	52	N
PTP-BL-2	PM	M	41	57	Y	PAR6B-1	PM	M	35	17	N
PTP-BL-2	PM	M	41	4	Y	PAR6B-1	PM	M	35	27	N
PTP-BL-2	PM	M	41	17	Y	PAR6B-1	PM	M	35	476	N
PTP-BL-2	PM	M	41	9	Y	PAR6B-1	PM	M	35	15	N
PTP-BL-2	PM	M	41	60	Y	PAR6B-1	PM	M	35	57	N
PTP-BL-2	PM	M	41	20	Y	PAR6B-1	PM	M	35	463	N
PTP-BL-2	PM	M	41	13	Y	PAR6B-1	PM	M	35	446	N
PTP-BL-2	PM	M	41	5	Y	PAR6B-1	PM	M	35	23	N
PTP-BL-2	PM	M	41	14	Y	PAR6B-1	PM	M	35	6	N
PTP-BL-2	PM	M	41	25	Y	PAR6B-1	PM	M	35	465	N
PTP-BL-2	PM	M	41	34	Y	PAR6B-1	PM	M	35	445	N
PTP-BL-2	PM	M	41	19	Y	PAR6B-1	PM	M	35	13	N
PTP-BL-2	PM	M	41	11	Y	PAR6B-1	PM	M	35	25	N
PTP-BL-2	PM	M	41	15	Y	PAR6B-1	PM	M	35	467	N
PTP-BL-2	PM	M	41	26	Y	PAR6B-1	PM	M	35	41	N
PTP-BL-2	PM	M	41	8	Y	PAR6B-1	PM	M	35	63	N
PTP-BL-2	PM	M	41	17	Y	PAR6B-1	PM	M	35	470	N
SAP102-2	PM	M	42	15	Y	PAR6B-1	PM	M	35	73	N
SAP102-2	PM	M	42	0	Y	PAR6B-1	PM	M	35	468	N
SAP102-2	PM	M	42	23	Y	PAR6B-1	PM	M	35	0	N
SAP102-2	PM	M	42	16	Y	PAR6B-1	PM	M	35	9	N
SAP102-2	PM	M	42	16	Y	PAR6B-1	PM	M	35	67	N
SAP102-2	PM	M	42	2	Y	PAR6B-1	PM	M	35	473	N
SAP102-2	PM	M	42	25	Y	PAR6B-1	PM	M	35	449	N
SAP102-2	PM	M	42	5	Y	PAR6B-1	PM	M	35	475	N
SAP102-2	PM	M	42	18	Y	PAR6B-1	PM	M	35	16	N

SAP102-2	PM	M	42	4	Y	PAR6B-1	PM	M	35	472	N
SAP102-2	PM	M	42	19	Y	PAR6B-1	PM	M	35	22	N
SAP102-2	PM	M	42	20	Y	PAR6B-1	PM	M	35	48	N
SAP102-2	PM	M	42	21	Y	PAR6B-1	PM	M	35	466	N
SAP102-2	PM	M	42	11	Y	PAR6B-1	PM	M	35	30	N
SAP102-2	PM	M	42	9	Y	PAR6B-1	PM	M	35	19	N
SAP102-2	PM	M	42	8	Y	PAR6B-1	PM	M	35	469	N
SAP102-2	PM	M	42	6	Y	PAR6B-1	PM	M	35	35	N
SAP102-2	PM	M	42	5	Y	PAR6B-1	PM	M	35	21	N
SAP102-2	PM	M	42	17	Y	PAR6B-1	PM	M	35	45	N
SAP102-2	PM	M	42	1	Y	PAR6B-1	PM	M	35	43	N
SAP102-2	PM	M	42	17	Y	PAR6B-1	PM	M	35	68	N
SAP102-3	PM	M	43	15	Y	PAR6B-1	PM	M	35	8	N
SAP102-3	PM	M	43	14	Y	PDZK11-1	PM	M	38	448	N
SAP102-3	PM	M	43	0	Y	PDZK11-1	PM	M	38	26	N
SAP102-3	PM	M	43	9	Y	PDZK11-1	PM	M	38	21	N
SAP102-3	PM	M	43	8	Y	PDZK11-1	PM	M	38	63	N
SAP102-3	PM	M	43	20	Y	PDZK11-1	PM	M	38	59	N
SAP102-3	PM	M	43	1	Y	PDZK11-1	PM	M	38	6	N
SAP102-3	PM	M	43	2	Y	PDZK1-1	PM	M	36	446	N
SAP102-3	PM	M	43	6	Y	PDZK1-1	PM	M	36	21	N
SAP97-1	PM	M	44	18	Y	PDZK1-1	PM	M	36	574	N
SAP97-1	PM	M	44	17	Y	PDZK1-1	PM	M	36	52	N
SAP97-1	PM	M	44	20	Y	PDZK1-1	PM	M	36	440	N
SAP97-1	PM	M	44	15	Y	PDZK1-1	PM	M	36	616	N
SAP97-1	PM	M	44	11	Y	PDZK1-1	PM	M	36	617	N
SAP97-1	PM	M	44	14	Y	PDZK1-1	PM	M	36	6	N
SAP97-1	PM	M	44	6	Y	PDZK1-1	PM	M	36	449	N
SAP97-1	PM	M	44	4	Y	PDZK1-1	PM	M	36	618	N
SAP97-1	PM	M	44	2	Y	PDZK1-1	PM	M	36	619	N
SAP97-1	PM	M	44	3	Y	PDZK1-1	PM	M	36	26	N
SAP97-1	PM	M	44	1	Y	PDZK1-1	PM	M	36	68	N
SAP97-1	PM	M	44	9	Y	PDZK1-1	PM	M	36	620	N
SAP97-1	PM	M	44	17	Y	PDZK1-1	PM	M	36	621	N
SAP97-2	PM	M	45	20	Y	PDZK1-1	PM	M	36	445	N
SAP97-2	PM	M	45	6	Y	PDZK1-1	PM	M	36	19	N
SAP97-2	PM	M	45	15	Y	PDZK1-1	PM	M	36	25	N
SAP97-2	PM	M	45	17	Y	PDZK1-1	PM	M	36	614	N
SAP97-2	PM	M	45	5	Y	PDZK1-1	PM	M	36	48	N
SAP97-2	PM	M	45	8	Y	PDZK1-1	PM	M	36	622	N
SAP97-2	PM	M	45	9	Y	PDZK1-3	PM	M	37	606	N
SAP97-2	PM	M	45	0	Y	PDZK1-3	PM	M	37	623	N
SAP97-2	PM	M	45	3	Y	PDZK1-3	PM	M	37	533	N
SAP97-2	PM	M	45	17	Y	PDZK1-3	PM	M	37	51	N
SAP97-2	PM	M	45	21	Y	PDZK1-3	PM	M	37	624	N
SAP97-2	PM	M	45	1	Y	PDZK1-3	PM	M	37	590	N

SAP97-2	PM	M	45	11	Y	PDZK1-3	PM	M	37	50	N
SAP97-2	PM	M	45	2	Y	PDZK1-3	PM	M	37	625	N
SAP97-3	PM	M	40	1	Y	PDZK1-3	PM	M	37	626	N
SAP97-3	PM	M	40	6	Y	PDZK1-3	PM	M	37	627	N
SAP97-3	PM	M	40	20	Y	PDZK1-3	PM	M	37	628	N
SAP97-3	PM	M	40	15	Y	PDZK1-3	PM	M	37	629	N
SAP97-3	PM	M	40	46	Y	PDZK1-3	PM	M	37	608	N
SAP97-3	PM	M	40	24	Y	PSD95-2	PM	M	39	630	N
SAP97-3	PM	M	40	8	Y	PSD95-2	PM	M	39	19	N
SAP97-3	PM	M	40	23	Y	PSD95-2	PM	M	39	62	N
SAP97-3	PM	M	40	9	Y	PSD95-2	PM	M	39	604	N
SAP97-3	PM	M	40	2	Y	PSD95-2	PM	M	39	454	N
SAP97-3	PM	M	40	0	Y	PSD95-2	PM	M	39	631	N
SAP97-3	PM	M	40	69	Y	PSD95-2	PM	M	39	632	N
SAP97-3	PM	M	40	14	Y	PSD95-2	PM	M	39	633	N
SCRB1-1	PM	M	46	1	Y	PSD95-2	PM	M	39	634	N
SCRB1-1	PM	M	46	10	Y	PSD95-2	PM	M	39	593	N
SCRB1-1	PM	M	46	0	Y	PSD95-2	PM	M	39	635	N
SCRB1-1	PM	M	46	8	Y	PSD95-2	PM	M	39	636	N
SCRB1-1	PM	M	46	9	Y	PSD95-2	PM	M	39	637	N
SCRB1-2	PM	M	47	0	Y	PSD95-3	PM	M	40	464	N
SCRB1-2	PM	M	47	9	Y	PSD95-3	PM	M	40	436	N
SCRB1-2	PM	M	47	11	Y	PSD95-3	PM	M	40	57	N
SCRB1-3	PM	M	48	1	Y	PSD95-3	PM	M	40	462	N
SCRB1-3	PM	M	48	46	Y	PSD95-3	PM	M	40	549	N
SCRB1-3	PM	M	48	12	Y	PSD95-3	PM	M	40	465	N
SCRB1-3	PM	M	48	0	Y	PSD95-3	PM	M	40	452	N
SCRB1-3	PM	M	48	2	Y	PSD95-3	PM	M	40	7	N
SCRB1-3	PM	M	48	61	Y	PSD95-3	PM	M	40	551	N
SCRB1-3	PM	M	48	9	Y	PSD95-3	PM	M	40	28	N
SCRB1-3	PM	M	48	7	Y	PSD95-3	PM	M	40	72	N
SCRB1-3	PM	M	48	63	Y	PSD95-3	PM	M	40	19	N
SCRB1-3	PM	M	48	3	Y	PSD95-3	PM	M	40	61	N
SCRB1-3	PM	M	48	67	Y	PSD95-3	PM	M	40	471	N
SCRB1-3	PM	M	48	10	Y	PSD95-3	PM	M	40	476	N
SCRB1-3	PM	M	48	24	Y	PSD95-3	PM	M	40	37	N
SCRB1-3	PM	M	48	27	Y	PTP-BL-2	PM	M	41	0	N
SCRB1-3	PM	M	48	56	Y	PTP-BL-2	PM	M	41	3	N
SCRB1-3	PM	M	48	52	Y	PTP-BL-2	PM	M	41	638	N
SCRB1-3	PM	M	48	13	Y	PTP-BL-2	PM	M	41	29	N
SCRB1-3	PM	M	48	8	Y	PTP-BL-2	PM	M	41	6	N
SCRB1-3	PM	M	48	14	Y	PTP-BL-2	PM	M	41	470	N
SCRB1-3	PM	M	48	6	Y	PTP-BL-2	PM	M	41	83	N
SCRB1-3	PM	M	48	11	Y	PTP-BL-2	PM	M	41	475	N
SEMCAP3-1	PM	M	49	14	Y	PTP-BL-2	PM	M	41	63	N
SEMCAP3-1	PM	M	49	0	Y	PTP-BL-2	PM	M	41	64	N

SEMCAP3-1	PM	M	49	46	Y	PTP-BL-2	PM	M	41	639	N
SEMCAP3-1	PM	M	49	16	Y	PTP-BL-2	PM	M	41	22	N
SEMCAP3-1	PM	M	49	2	Y	PTP-BL-2	PM	M	41	473	N
SEMCAP3-1	PM	M	49	8	Y	PTP-BL-2	PM	M	41	562	N
SEMCAP3-1	PM	M	49	13	Y	PTP-BL-2	PM	M	41	7	N
SHANK1-1	PM	M	50	0	Y	PTP-BL-2	PM	M	41	21	N
SHANK1-1	PM	M	50	58	Y	PTP-BL-2	PM	M	41	468	N
SHANK1-1	PM	M	50	70	Y	PTP-BL-2	PM	M	41	502	N
SHANK1-1	PM	M	50	51	Y	PTP-BL-2	PM	M	41	508	N
SHANK1-1	PM	M	50	58	Y	PTP-BL-2	PM	M	41	35	N
SHANK1-1	PM	M	50	15	Y	PTP-BL-2	PM	M	41	474	N
SHANK1-1	PM	M	50	8	Y	PTP-BL-2	PM	M	41	67	N
SHANK1-1	PM	M	50	67	Y	PTP-BL-2	PM	M	41	555	N
SHANK1-1	PM	M	50	10	Y	PTP-BL-2	PM	M	41	463	N
SHANK1-1	PM	M	50	68	Y	PTP-BL-2	PM	M	41	454	N
SHANK1-1	PM	M	50	64	Y	PTP-BL-2	PM	M	41	53	N
SHANK1-1	PM	M	50	13	Y	PTP-BL-2	PM	M	41	65	N
SHANK1-1	PM	M	50	27	Y	PTP-BL-2	PM	M	41	73	N
SHANK1-1	PM	M	50	9	Y	PTP-BL-2	PM	M	41	519	N
SHANK1-1	PM	M	50	66	Y	PTP-BL-2	PM	M	41	466	N
SHANK1-1	PM	M	50	71	Y	PTP-BL-2	PM	M	41	41	N
SHANK1-1	PM	M	50	50	Y	PTP-BL-2	PM	M	41	43	N
SHANK3-1	PM	M	51	70	Y	PTP-BL-2	PM	M	41	476	N
SHANK3-1	PM	M	51	58	Y	PTP-BL-2	PM	M	41	18	N
SHANK3-1	PM	M	51	72	Y	PTP-BL-2	PM	M	41	472	N
SHANK3-1	PM	M	51	7	Y	PTP-BL-2	PM	M	41	51	N
SHANK3-1	PM	M	51	51	Y	PTP-BL-2	PM	M	41	446	N
SHANK3-1	PM	M	51	64	Y	PTP-BL-2	PM	M	41	1	N
SHANK3-1	PM	M	51	55	Y	PTP-BL-2	PM	M	41	62	N
SHANK3-1	PM	M	51	8	Y	PTP-BL-2	PM	M	41	30	N
SHANK3-1	PM	M	51	67	Y	PTP-BL-2	PM	M	41	544	N
SHANK3-1	PM	M	51	10	Y	PTP-BL-2	PM	M	41	16	N
SHANK3-1	PM	M	51	68	Y	PTP-BL-2	PM	M	41	465	N
SHANK3-1	PM	M	51	50	Y	PTP-BL-2	PM	M	41	2	N
SHANK3-1	PM	M	51	58	Y	PTP-BL-2	PM	M	41	467	N
SHANK3-1	PM	M	51	13	Y	PTP-BL-2	PM	M	41	23	N
SHANK3-1	PM	M	51	52	Y	PTP-BL-2	PM	M	41	48	N
SHANK3-1	PM	M	51	66	Y	PTP-BL-2	PM	M	41	469	N
SHANK3-1	PM	M	51	71	Y	PTP-BL-2	PM	M	41	40	N
SHANK3-1	PM	M	51	27	Y	PTP-BL-2	PM	M	41	45	N
SHROOM-1	PM	M	52	8	Y	PTP-BL-2	PM	M	41	28	N
SHROOM-1	PM	M	52	0	Y	PTP-BL-2	PM	M	41	46	N
SHROOM-1	PM	M	52	13	Y	PTP-BL-2	PM	M	41	16	N
SLIM-1	PM	M	53	49	Y	PTP-BL-2	PM	M	41	36	N
ZO-1-1	PM	M	54	73	Y	PTP-BL-2	PM	M	41	32	N
ZO-1-1	PM	M	54	38	Y	SAP102-2	PM	M	42	640	N

ZO-1-1	PM	M	54	45	Y	SAP102-2	PM	M	42	641	N
ZO-1-1	PM	M	54	74	Y	SAP102-2	PM	M	42	642	N
ZO-1-1	PM	M	54	75	Y	SAP102-2	PM	M	42	53	N
ZO-1-1	PM	M	54	32	Y	SAP102-2	PM	M	42	643	N
ZO-1-1	PM	M	54	76	Y	SAP102-2	PM	M	42	644	N
ZO-1-1	PM	M	54	77	Y	SAP102-2	PM	M	42	62	N
ZO-1-1	PM	M	54	78	Y	SAP102-2	PM	M	42	637	N
ZO-1-1	PM	M	54	79	Y	SAP102-2	PM	M	42	454	N
ZO-1-1	PM	M	54	80	Y	SAP102-2	PM	M	42	566	N
ZO-1-1	PM	M	54	41	Y	SAP102-2	PM	M	42	645	N
ZO-1-1	PM	M	54	81	Y	SAP102-2	PM	M	42	646	N
ZO-1-1	PM	M	54	82	Y	SAP102-2	PM	M	42	40	N
ZO-1-1	PM	M	54	50	Y	SAP102-2	PM	M	42	647	N
ZO-1-1	PM	M	54	83	Y	SAP102-3	PM	M	43	47	N
ZO-1-1	PM	M	54	43	Y	SAP102-3	PM	M	43	19	N
ZO-1-1	PM	M	54	26	Y	SAP102-3	PM	M	43	7	N
ZO-1-1	PM	M	54	27	Y	SAP102-3	PM	M	43	23	N
ZO-1-1	PM	M	54	83	Y	SAP102-3	PM	M	43	22	N
ZO-2-1	PM	M	55	15	Y	SAP102-3	PM	M	43	476	N
ZO-2-1	PM	M	55	83	Y	SAP102-3	PM	M	43	11	N
ZO-2-1	PM	M	55	74	Y	SAP102-3	PM	M	43	46	N
ZO-2-1	PM	M	55	77	Y	SAP102-3	PM	M	43	648	N
ZO-2-1	PM	M	55	78	Y	SAP102-3	PM	M	43	3	N
ZO-2-1	PM	M	55	76	Y	SAP102-3	PM	M	43	69	N
ZO-2-1	PM	M	55	43	Y	SAP102-3	PM	M	43	12	N
ZO-2-1	PM	M	55	45	Y	SAP102-3	PM	M	43	555	N
ZO-2-1	PM	M	55	83	Y	SAP102-3	PM	M	43	13	N
ZO-2-1	PM	M	55	82	Y	SAP102-3	PM	M	43	472	N
ZO-2-1	PM	M	55	73	Y	SAP97-1	PM	M	44	7	N
ZO-2-1	PM	M	55	79	Y	SAP97-1	PM	M	44	65	N
ZO-2-1	PM	M	55	41	Y	SAP97-1	PM	M	44	546	N
ZO-3-1	PM	M	56	41	Y	SAP97-1	PM	M	44	545	N
CASK-1	PD	H	57	84	Y	SAP97-1	PM	M	44	22	N
CASK-1	PD	H	57	85	Y	SAP97-1	PM	M	44	19	N
CASK-1	PD	H	57	86	Y	SAP97-1	PM	M	44	462	N
CASK-1	PD	H	57	87	Y	SAP97-1	PM	M	44	555	N
CASK-1	PD	H	57	88	Y	SAP97-1	PM	M	44	23	N
CASK-1	PD	H	57	89	Y	SAP97-1	PM	M	44	551	N
CASK-1	PD	H	57	90	Y	SAP97-1	PM	M	44	12	N
CASK-1	PD	H	57	91	Y	SAP97-1	PM	M	44	472	N
CASK-1	PD	H	57	92	Y	SAP97-1	PM	M	44	436	N
CASK-1	PD	H	57	93	Y	SAP97-1	PM	M	44	639	N
CASK-1	PD	H	57	94	Y	SAP97-1	PM	M	44	648	N
CASK-1	PD	H	57	95	Y	SAP97-2	PM	M	45	649	N
CASK-1	PD	H	57	96	Y	SAP97-2	PM	M	45	19	N
CASK-1	PD	H	57	97	Y	SAP97-2	PM	M	45	64	N

CASK-1	PD	H	57	98	Y	SAP97-2	PM	M	45	4	N
CASK-1	PD	H	57	99	Y	SAP97-2	PM	M	45	454	N
CASK-1	PD	H	57	100	Y	SAP97-3	PM	M	40	3	N
CASK-1	PD	H	57	101	Y	SAP97-3	PM	M	40	11	N
CASK-1	PD	H	57	102	Y	SAP97-3	PM	M	40	7	N
CASK-1	PD	H	57	103	Y	SAP97-3	PM	M	40	555	N
DLG3-2	PD	H	58	104	Y	SAP97-3	PM	M	40	65	N
DLG3-2	PD	H	58	105	Y	SAP97-3	PM	M	40	10	N
DLG3-2	PD	H	58	106	Y	SAP97-3	PM	M	40	472	N
DLG3-2	PD	H	58	107	Y	SAP97-3	PM	M	40	22	N
DLG3-2	PD	H	58	108	Y	SAP97-3	PM	M	40	436	N
DLG3-2	PD	H	58	109	Y	SAP97-3	PM	M	40	650	N
DLG3-2	PD	H	58	110	Y	SAP97-3	PM	M	40	12	N
DLG3-2	PD	H	58	111	Y	SAP97-3	PM	M	40	13	N
DLG3-2	PD	H	58	112	Y	SCRB1-1	PM	M	46	464	N
DLG3-2	PD	H	58	113	Y	SCRB1-1	PM	M	46	465	N
DLG3-2	PD	H	58	114	Y	SCRB1-1	PM	M	46	473	N
DLG3-2	PD	H	58	115	Y	SCRB1-1	PM	M	46	551	N
DLG3-2	PD	H	58	116	Y	SCRB1-1	PM	M	46	462	N
DLG3-2	PD	H	58	117	Y	SCRB1-1	PM	M	46	488	N
DLG3-2	PD	H	58	118	Y	SCRB1-1	PM	M	46	7	N
DLG3-2	PD	H	58	119	Y	SCRB1-1	PM	M	46	553	N
DLG3-2	PD	H	58	120	Y	SCRB1-1	PM	M	46	471	N
DLG3-2	PD	H	58	121	Y	SCRB1-1	PM	M	46	59	N
DLG3-2	PD	H	58	122	Y	SCRB1-1	PM	M	46	547	N
DLG3-2	PD	H	58	123	Y	SCRB1-1	PM	M	46	515	N
DLG3-2	PD	H	58	124	Y	SCRB1-1	PM	M	46	552	N
DLG3-2	PD	H	58	125	Y	SCRB1-1	PM	M	46	72	N
DLG3-2	PD	H	58	126	Y	SCRB1-1	PM	M	46	546	N
DLG3-2	PD	H	58	127	Y	SCRB1-1	PM	M	46	436	N
DLG3-2	PD	H	58	128	Y	SCRB1-1	PM	M	46	452	N
DLG3-2	PD	H	58	129	Y	SCRB1-2	PM	M	47	15	N
DLG3-2	PD	H	58	130	Y	SCRB1-2	PM	M	47	436	N
DLG3-2	PD	H	58	131	Y	SCRB1-2	PM	M	47	8	N
ERBB2IP-1	PD	H	59	132	Y	SCRB1-2	PM	M	47	7	N
ERBB2IP-1	PD	H	59	133	Y	SCRB1-2	PM	M	47	2	N
ERBB2IP-1	PD	H	59	134	Y	SCRB1-2	PM	M	47	63	N
ERBB2IP-1	PD	H	59	135	Y	SCRB1-2	PM	M	47	17	N
ERBB2IP-1	PD	H	59	136	Y	SCRB1-2	PM	M	47	534	N
ERBB2IP-1	PD	H	59	137	Y	SCRB1-3	PM	M	48	651	N
ERBB2IP-1	PD	H	59	138	Y	SCRB1-3	PM	M	48	69	N
ERBB2IP-1	PD	H	59	139	Y	SCRB1-3	PM	M	48	436	N
ERBB2IP-1	PD	H	59	140	Y	SCRB1-3	PM	M	48	54	N
ERBB2IP-1	PD	H	59	141	Y	SCRB1-3	PM	M	48	509	N
ERBB2IP-1	PD	H	59	142	Y	SCRB1-3	PM	M	48	652	N
ERBB2IP-1	PD	H	59	143	Y	SCRB1-3	PM	M	48	579	N

ERBB2IP-1	PD	H	59	144	Y	SCRB1-3	PM	M	48	653	N
ERBB2IP-1	PD	H	59	145	Y	SCRB1-3	PM	M	48	65	N
ERBB2IP-1	PD	H	59	146	Y	SCRB1-3	PM	M	48	68	N
ERBB2IP-1	PD	H	59	147	Y	SCRB1-3	PM	M	48	654	N
ERBB2IP-1	PD	H	59	148	Y	SCRB1-3	PM	M	48	655	N
ERBB2IP-1	PD	H	59	149	Y	SCRB1-3	PM	M	48	66	N
ERBB2IP-1	PD	H	59	150	Y	SCRB1-3	PM	M	48	656	N
ERBB2IP-1	PD	H	59	151	Y	SCRB1-3	PM	M	48	58	N
ERBB2IP-1	PD	H	59	152	Y	SCRB1-3	PM	M	48	657	N
ERBB2IP-1	PD	H	59	153	Y	SCRB1-3	PM	M	48	658	N
ERBB2IP-1	PD	H	59	154	Y	SCRB1-3	PM	M	48	35	N
ERBB2IP-1	PD	H	59	155	Y	SCRB1-3	PM	M	48	58	N
ERBB2IP-1	PD	H	59	156	Y	SCRB1-3	PM	M	48	64	N
ERBB2IP-1	PD	H	59	157	Y	SCRB1-3	PM	M	48	472	N
ERBB2IP-1	PD	H	59	158	Y	SCRB1-3	PM	M	48	71	N
ERBB2IP-1	PD	H	59	159	Y	SEMCAP3-1	PM	M	49	7	N
ERBB2IP-1	PD	H	59	160	Y	SEMCAP3-1	PM	M	49	28	N
ERBB2IP-1	PD	H	59	161	Y	SEMCAP3-1	PM	M	49	3	N
ERBB2IP-1	PD	H	59	162	Y	SEMCAP3-1	PM	M	49	9	N
ERBB2IP-1	PD	H	59	163	Y	SEMCAP3-1	PM	M	49	476	N
ERBB2IP-1	PD	H	59	164	Y	SEMCAP3-1	PM	M	49	61	N
MPDZ-1	PD	H	60	165	Y	SEMCAP3-1	PM	M	49	19	N
MPDZ-1	PD	H	60	166	Y	SEMCAP3-1	PM	M	49	47	N
MPDZ-1	PD	H	60	167	Y	SEMCAP3-1	PM	M	49	5	N
MPDZ-1	PD	H	60	168	Y	SHANK1-1	PM	M	50	659	N
MPDZ-1	PD	H	60	169	Y	SHANK1-1	PM	M	50	465	N
MPDZ-1	PD	H	60	170	Y	SHANK1-1	PM	M	50	660	N
MPDZ-1	PD	H	60	171	Y	SHANK1-1	PM	M	50	661	N
MPDZ-1	PD	H	60	172	Y	SHANK1-1	PM	M	50	475	N
MPDZ-1	PD	H	60	173	Y	SHANK1-1	PM	M	50	662	N
MPDZ-1	PD	H	60	174	Y	SHANK1-1	PM	M	50	454	N
MPDZ-1	PD	H	60	175	Y	SHANK1-1	PM	M	50	663	N
MPDZ-1	PD	H	60	176	Y	SHANK1-1	PM	M	50	26	N
MPDZ-1	PD	H	60	177	Y	SHANK1-1	PM	M	50	638	N
MPDZ-10	PD	H	61	178	Y	SHANK1-1	PM	M	50	664	N
MPDZ-10	PD	H	61	179	Y	SHANK1-1	PM	M	50	2	N
MPDZ-10	PD	H	61	180	Y	SHANK1-1	PM	M	50	472	N
MPDZ-10	PD	H	61	181	Y	SHANK1-1	PM	M	50	533	N
MPDZ-10	PD	H	61	182	Y	SHANK1-1	PM	M	50	665	N
MPDZ-10	PD	H	61	183	Y	SHANK1-1	PM	M	50	468	N
MPDZ-10	PD	H	61	184	Y	SHANK1-1	PM	M	50	476	N
MPDZ-10	PD	H	61	185	Y	SHANK1-1	PM	M	50	470	N
MPDZ-10	PD	H	61	186	Y	SHANK1-1	PM	M	50	6	N
MPDZ-10	PD	H	61	187	Y	SHANK1-1	PM	M	50	17	N
MPDZ-10	PD	H	61	188	Y	SHANK1-1	PM	M	50	16	N
MPDZ-10	PD	H	61	189	Y	SHANK1-1	PM	M	50	30	N

MPDZ-10	PD	H	61	190	Y	SHANK1-1	PM	M	50	23	N
MPDZ-10	PD	H	61	191	Y	SHANK1-1	PM	M	50	666	N
MPDZ-10	PD	H	61	192	Y	SHANK1-1	PM	M	50	7	N
MPDZ-10	PD	H	61	193	Y	SHANK1-1	PM	M	50	473	N
MPDZ-12	PD	H	62	194	Y	SHANK1-1	PM	M	50	45	N
MPDZ-12	PD	H	62	195	Y	SHANK1-1	PM	M	50	628	N
MPDZ-12	PD	H	62	196	Y	SHANK1-1	PM	M	50	22	N
MPDZ-12	PD	H	62	197	Y	SHANK1-1	PM	M	50	41	N
MPDZ-12	PD	H	62	198	Y	SHANK1-1	PM	M	50	11	N
MPDZ-12	PD	H	62	199	Y	SHANK1-1	PM	M	50	57	N
MPDZ-12	PD	H	62	200	Y	SHANK1-1	PM	M	50	463	N
MPDZ-12	PD	H	62	201	Y	SHANK1-1	PM	M	50	65	N
MPDZ-12	PD	H	62	202	Y	SHANK1-1	PM	M	50	667	N
MPDZ-12	PD	H	62	203	Y	SHANK1-1	PM	M	50	467	N
MPDZ-12	PD	H	62	204	Y	SHANK1-1	PM	M	50	12	N
SCRIB-1	PD	H	63	205	Y	SHANK1-1	PM	M	50	668	N
SCRIB-1	PD	H	63	206	Y	SHANK1-1	PM	M	50	46	N
SCRIB-1	PD	H	63	3	Y	SHANK1-1	PM	M	50	466	N
SCRIB-1	PD	H	63	207	Y	SHANK1-1	PM	M	50	469	N
SCRIB-1	PD	H	63	208	Y	SHANK1-1	PM	M	50	55	N
SCRIB-1	PD	H	63	209	Y	SHANK1-1	PM	M	50	669	N
SCRIB-1	PD	H	63	210	Y	SHANK1-1	PM	M	50	52	N
SCRIB-1	PD	H	63	211	Y	SHANK1-1	PM	M	50	560	N
SCRIB-1	PD	H	63	212	Y	SHANK1-1	PM	M	50	29	N
SCRIB-1	PD	H	63	213	Y	SHANK1-1	PM	M	50	474	N
SCRIB-1	PD	H	63	214	Y	SHANK1-1	PM	M	50	73	N
SCRIB-1	PD	H	63	215	Y	SHANK1-1	PM	M	50	35	N
SCRIB-1	PD	H	63	216	Y	SHANK1-1	PM	M	50	63	N
SCRIB-1	PD	H	63	217	Y	SHANK1-1	PM	M	50	670	N
SCRIB-1	PD	H	63	218	Y	SHANK1-1	PM	M	50	3	N
SCRIB-1	PD	H	63	219	Y	SHANK1-1	PM	M	50	43	N
SCRIB-1	PD	H	63	220	Y	SHANK3-1	PM	M	51	560	N
SCRIB-1	PD	H	63	221	Y	SHANK3-1	PM	M	51	671	N
SCRIB-1	PD	H	63	152	Y	SHANK3-1	PM	M	51	3	N
SCRIB-1	PD	H	63	222	Y	SHANK3-1	PM	M	51	0	N
SCRIB-1	PD	H	63	223	Y	SHANK3-1	PM	M	51	672	N
SCRIB-1	PD	H	63	224	Y	SHANK3-1	PM	M	51	673	N
SCRIB-1	PD	H	63	8	Y	SHANK3-1	PM	M	51	674	N
SCRIB-1	PD	H	63	137	Y	SHANK3-1	PM	M	51	675	N
SCRIB-1	PD	H	63	225	Y	SHANK3-1	PM	M	51	664	N
SCRIB-1	PD	H	63	226	Y	SHANK3-1	PM	M	51	26	N
SCRIB-1	PD	H	63	227	Y	SHANK3-1	PM	M	51	676	N
DLG1-2	PD	H	64	228	Y	SHANK3-1	PM	M	51	21	N
DLG1-2	PD	H	64	229	Y	SHANK3-1	PM	M	51	533	N
DLG1-2	PD	H	64	230	Y	SHANK3-1	PM	M	51	677	N
DLG1-2	PD	H	64	231	Y	SHANK3-1	PM	M	51	534	N

DLG1-2	PD	H	64	232	Y	SHANK3-1	PM	M	51	678	N
DLG1-2	PD	H	64	233	Y	SHANK3-1	PM	M	51	638	N
DLG1-2	PD	H	64	124	Y	SHANK3-1	PM	M	51	679	N
DLG1-2	PD	H	64	234	Y	SHANK3-1	PM	M	51	680	N
DLG1-2	PD	H	64	235	Y	SHANK3-1	PM	M	51	681	N
DLG1-2	PD	H	64	236	Y	SHANK3-1	PM	M	51	682	N
DLG1-2	PD	H	64	237	Y	SHANK3-1	PM	M	51	683	N
DLG1-2	PD	H	64	238	Y	SHANK3-1	PM	M	51	684	N
DLG1-2	PD	H	64	239	Y	SHANK3-1	PM	M	51	669	N
DLG1-2	PD	H	64	240	Y	SHANK3-1	PM	M	51	668	N
DLG1-2	PD	H	64	241	Y	SHANK3-1	PM	M	51	6	N
DLG1-2	PD	H	64	136	Y	SHROOM-1	PM	M	52	6	N
DLG1-2	PD	H	64	242	Y	SHROOM-1	PM	M	52	27	N
DLG1-2	PD	H	64	243	Y	SHROOM-1	PM	M	52	19	N
DLG1-2	PD	H	64	168	Y	SHROOM-1	PM	M	52	23	N
DLG1-2	PD	H	64	244	Y	SHROOM-1	PM	M	52	445	N
DLG1-2	PD	H	64	245	Y	SHROOM-1	PM	M	52	446	N
DLG1-2	PD	H	64	246	Y	SHROOM-1	PM	M	52	68	N
DLG1-2	PD	H	64	127	Y	SHROOM-1	PM	M	52	52	N
DLG1-2	PD	H	64	123	Y	SHROOM-1	PM	M	52	48	N
DLG1-2	PD	H	64	247	Y	SHROOM-1	PM	M	52	26	N
DLG1-2	PD	H	64	248	Y	SHROOM-1	PM	M	52	9	N
DLG1-2	PD	H	64	249	Y	SHROOM-1	PM	M	52	449	N
DLG1-2	PD	H	64	250	Y	SHROOM-1	PM	M	52	67	N
DLG1-2	PD	H	64	251	Y	SHROOM-1	PM	M	52	25	N
DLG1-2	PD	H	64	252	Y	SHROOM-1	PM	M	52	21	N
DLG1-2	PD	H	64	253	Y	SLIM-1	PM	M	53	448	N
DLG1-2	PD	H	64	254	Y	SLIM-1	PM	M	53	470	N
DLG1-2	PD	H	64	255	Y	SLIM-1	PM	M	53	447	N
DLG1-2	PD	H	64	256	Y	SLIM-1	PM	M	53	16	N
DLG1-2	PD	H	64	257	Y	SLIM-1	PM	M	53	61	N
DLG1-2	PD	H	64	258	Y	ZO-1-1	PM	M	54	16	N
DLG1-2	PD	H	64	259	Y	ZO-1-1	PM	M	54	603	N
DLG1-2	PD	H	64	260	Y	ZO-1-1	PM	M	54	685	N
DLG1-2	PD	H	64	261	Y	ZO-1-1	PM	M	54	649	N
DLG1-2	PD	H	64	116	Y	ZO-1-1	PM	M	54	686	N
DLG1-2	PD	H	64	262	Y	ZO-1-1	PM	M	54	664	N
DLG1-2	PD	H	64	263	Y	ZO-1-1	PM	M	54	32	N
DLG1-2	PD	H	64	264	Y	ZO-1-1	PM	M	54	687	N
DLG1-2	PD	H	64	265	Y	ZO-1-1	PM	M	54	508	N
DLG1-2	PD	H	64	266	Y	ZO-1-1	PM	M	54	545	N
DLG1-2	PD	H	64	267	Y	ZO-1-1	PM	M	54	688	N
DLG1-2	PD	H	64	268	Y	ZO-1-1	PM	M	54	689	N
DLG4-3	PD	H	65	208	Y	ZO-1-1	PM	M	54	35	N
DLG4-3	PD	H	65	269	Y	ZO-1-1	PM	M	54	561	N
DLG4-3	PD	H	65	270	Y	ZO-1-1	PM	M	54	449	N

DLG4-3	PD	H	65	108	Y	ZO-1-1	PM	M	54	690	N
DLG4-3	PD	H	65	271	Y	ZO-1-1	PM	M	54	691	N
DLG4-3	PD	H	65	272	Y	ZO-1-1	PM	M	54	436	N
DLG4-3	PD	H	65	273	Y	ZO-1-1	PM	M	54	448	N
DLG4-3	PD	H	65	274	Y	ZO-1-1	PM	M	54	521	N
DLG4-3	PD	H	65	275	Y	ZO-1-1	PM	M	54	692	N
DLG4-3	PD	H	65	261	Y	ZO-1-1	PM	M	54	693	N
DLG4-3	PD	H	65	241	Y	ZO-1-1	PM	M	54	11	N
DLG4-3	PD	H	65	276	Y	ZO-1-1	PM	M	54	694	N
DLG4-3	PD	H	65	277	Y	ZO-1-1	PM	M	54	522	N
DLG4-3	PD	H	65	205	Y	ZO-1-1	PM	M	54	562	N
DLG4-3	PD	H	65	278	Y	ZO-1-1	PM	M	54	4	N
DLG4-3	PD	H	65	279	Y	ZO-1-1	PM	M	54	649	N
SCRIB-2	PD	H	66	139	Y	ZO-1-1	PM	M	54	695	N
SCRIB-2	PD	H	66	135	Y	ZO-2-1	PM	M	55	454	N
SCRIB-2	PD	H	66	156	Y	ZO-2-1	PM	M	55	29	N
SCRIB-2	PD	H	66	140	Y	ZO-2-1	PM	M	55	475	N
SCRIB-2	PD	H	66	149	Y	ZO-2-1	PM	M	55	16	N
SCRIB-2	PD	H	66	280	Y	ZO-2-1	PM	M	55	32	N
SCRIB-2	PD	H	66	238	Y	ZO-2-1	PM	M	55	446	N
SCRIB-2	PD	H	66	281	Y	ZO-2-1	PM	M	55	696	N
SCRIB-2	PD	H	66	282	Y	ZO-2-1	PM	M	55	64	N
SCRIB-2	PD	H	66	283	Y	ZO-2-1	PM	M	55	80	N
SCRIB-2	PD	H	66	284	Y	ZO-2-1	PM	M	55	463	N
SCRIB-2	PD	H	66	163	Y	ZO-2-1	PM	M	55	57	N
SCRIB-2	PD	H	66	219	Y	ZO-2-1	PM	M	55	467	N
SCRIB-2	PD	H	66	285	Y	ZO-2-1	PM	M	55	466	N
SCRIB-2	PD	H	66	133	Y	ZO-2-1	PM	M	55	649	N
SCRIB-2	PD	H	66	203	Y	ZO-2-1	PM	M	55	452	N
INADL-2	PD	H	67	286	Y	ZO-2-1	PM	M	55	649	N
INADL-2	PD	H	67	287	Y	ZO-2-1	PM	M	55	518	N
INADL-2	PD	H	67	288	Y	ZO-2-1	PM	M	55	17	N
INADL-2	PD	H	67	289	Y	ZO-2-1	PM	M	55	474	N
INADL-2	PD	H	67	290	Y	ZO-2-1	PM	M	55	473	N
INADL-2	PD	H	67	291	Y	ZO-2-1	PM	M	55	35	N
INADL-2	PD	H	67	292	Y	ZO-2-1	PM	M	55	13	N
INADL-2	PD	H	67	293	Y	ZO-2-1	PM	M	55	470	N
INADL-2	PD	H	67	294	Y	ZO-2-1	PM	M	55	447	N
INADL-2	PD	H	67	295	Y	ZO-2-1	PM	M	55	22	N
INADL-2	PD	H	67	296	Y	ZO-2-1	PM	M	55	436	N
DLG1-3	PD	H	68	208	Y	ZO-2-1	PM	M	55	685	N
DLG1-3	PD	H	68	297	Y	ZO-2-1	PM	M	55	65	N
DLG1-3	PD	H	68	1	Y	ZO-2-1	PM	M	55	5	N
DLG1-3	PD	H	68	298	Y	ZO-2-1	PM	M	55	32	N
DLG1-3	PD	H	68	261	Y	ZO-2-1	PM	M	55	81	N
DLG1-3	PD	H	68	299	Y	ZO-2-1	PM	M	55	468	N

DLG1-3	PD	H	68	300	Y	ZO-2-1	PM	M	55	26	N
DLG1-3	PD	H	68	277	Y	ZO-2-1	PM	M	55	465	N
DLG1-3	PD	H	68	237	Y	ZO-2-1	PM	M	55	522	N
DLG1-3	PD	H	68	301	Y	ZO-2-1	PM	M	55	472	N
DLG1-3	PD	H	68	302	Y	ZO-2-1	PM	M	55	469	N
DLG1-3	PD	H	68	303	Y	ZO-2-1	PM	M	55	476	N
DLG1-3	PD	H	68	2	Y	ZO-2-1	PM	M	55	38	N
DLG1-1	PD	H	69	267	Y	ZO-2-1	PM	M	55	4	N
DLG1-1	PD	H	69	304	Y	ZO-2-1	PM	M	55	3	N
DLG1-1	PD	H	69	305	Y	ZO-2-1	PM	M	55	75	N
DLG1-1	PD	H	69	168	Y	ZO-2-1	PM	M	55	63	N
DLG1-1	PD	H	69	197	Y	ZO-2-1	PM	M	55	23	N
DLG1-1	PD	H	69	306	Y	ZO-2-1	PM	M	55	30	N
DLG1-1	PD	H	69	307	Y	ZO-3-1	PM	M	56	436	N
DLG1-1	PD	H	69	308	Y	CASK-1	PD	H	57	335	N
DLG1-1	PD	H	69	244	Y	CASK-1	PD	H	57	353	N
DLG1-1	PD	H	69	309	Y	CASK-1	PD	H	57	407	N
DLG1-1	PD	H	69	124	Y	CASK-1	PD	H	57	347	N
LRRC7-1	PD	H	70	152	Y	CASK-1	PD	H	57	363	N
LRRC7-1	PD	H	70	135	Y	CASK-1	PD	H	57	170	N
LRRC7-1	PD	H	70	163	Y	CASK-1	PD	H	57	382	N
LRRC7-1	PD	H	70	310	Y	CASK-1	PD	H	57	398	N
LRRC7-1	PD	H	70	311	Y	CASK-1	PD	H	57	313	N
LRRC7-1	PD	H	70	312	Y	CASK-1	PD	H	57	413	N
LRRC7-1	PD	H	70	137	Y	CASK-1	PD	H	57	378	N
LRRC7-1	PD	H	70	140	Y	CASK-1	PD	H	57	174	N
LRRC7-1	PD	H	70	284	Y	CASK-1	PD	H	57	328	N
LRRC7-1	PD	H	70	313	Y	CASK-1	PD	H	57	266	N
LRRC7-1	PD	H	70	280	Y	CASK-1	PD	H	57	428	N
LRRC7-1	PD	H	70	133	Y	CASK-1	PD	H	57	385	N
LRRC7-1	PD	H	70	139	Y	CASK-1	PD	H	57	421	N
LRRC7-1	PD	H	70	314	Y	CASK-1	PD	H	57	418	N
LRRC7-1	PD	H	70	315	Y	CASK-1	PD	H	57	350	N
LRRC7-1	PD	H	70	143	Y	CASK-1	PD	H	57	390	N
LRRC7-1	PD	H	70	195	Y	DLG3-2	PD	H	58	377	N
LRRC7-1	PD	H	70	161	Y	DLG3-2	PD	H	58	417	N
LRRC7-1	PD	H	70	316	Y	DLG3-2	PD	H	58	697	N
LRRC7-1	PD	H	70	149	Y	DLG3-2	PD	H	58	401	N
LRRC7-1	PD	H	70	317	Y	DLG3-2	PD	H	58	402	N
LRRC7-1	PD	H	70	132	Y	DLG3-2	PD	H	58	408	N
LRRC7-1	PD	H	70	136	Y	DLG3-2	PD	H	58	325	N
LRRC7-1	PD	H	70	281	Y	DLG3-2	PD	H	58	170	N
LRRC7-1	PD	H	70	318	Y	DLG3-2	PD	H	58	698	N
LRRC7-1	PD	H	70	319	Y	DLG3-2	PD	H	58	97	N
MPP6-1	PD	H	71	320	Y	DLG3-2	PD	H	58	174	N
MPP6-1	PD	H	71	321	Y	DLG3-2	PD	H	58	287	N

MPP6-1	PD	H	71	322	Y	DLG3-2	PD	H	58	382	N
MPP6-1	PD	H	71	323	Y	DLG3-2	PD	H	58	699	N
MPP6-1	PD	H	71	324	Y	DLG3-2	PD	H	58	399	N
MPP6-1	PD	H	71	325	Y	DLG3-2	PD	H	58	397	N
MPP6-1	PD	H	71	326	Y	DLG3-2	PD	H	58	700	N
MPP6-1	PD	H	71	327	Y	DLG3-2	PD	H	58	371	N
MPP6-1	PD	H	71	328	Y	DLG3-2	PD	H	58	294	N
MPP6-1	PD	H	71	329	Y	DLG3-2	PD	H	58	701	N
MPP6-1	PD	H	71	330	Y	DLG3-2	PD	H	58	404	N
MPP6-1	PD	H	71	331	Y	DLG3-2	PD	H	58	428	N
MPP6-1	PD	H	71	332	Y	DLG3-2	PD	H	58	369	N
MPP6-1	PD	H	71	333	Y	DLG3-2	PD	H	58	702	N
MPP6-1	PD	H	71	334	Y	DLG3-2	PD	H	58	373	N
PDZK1-1	PD	H	72	335	Y	DLG3-2	PD	H	58	378	N
PDZK1-1	PD	H	72	336	Y	DLG3-2	PD	H	58	415	N
PDZK1-1	PD	H	72	337	Y	DLG3-2	PD	H	58	703	N
PDZK1-1	PD	H	72	338	Y	DLG3-2	PD	H	58	403	N
PDZK1-1	PD	H	72	339	Y	DLG3-2	PD	H	58	407	N
PDZK1-1	PD	H	72	340	Y	DLG3-2	PD	H	58	160	N
PDZK1-1	PD	H	72	341	Y	DLG3-2	PD	H	58	419	N
PDZK1-1	PD	H	72	342	Y	DLG3-2	PD	H	58	704	N
PDZK1-1	PD	H	72	343	Y	DLG3-2	PD	H	58	705	N
PDZK1-1	PD	H	72	344	Y	DLG3-2	PD	H	58	349	N
PDZK1-1	PD	H	72	345	Y	DLG3-2	PD	H	58	425	N
PDZK1-1	PD	H	72	346	Y	DLG3-2	PD	H	58	385	N
PDZK1-1	PD	H	72	347	Y	DLG3-2	PD	H	58	706	N
PDZK1-1	PD	H	72	348	Y	ERBB2IP-1	PD	H	59	385	N
PDZK1-1	PD	H	72	349	Y	ERBB2IP-1	PD	H	59	342	N
PDZK1-1	PD	H	72	350	Y	ERBB2IP-1	PD	H	59	176	N
PDZK1-1	PD	H	72	351	Y	ERBB2IP-1	PD	H	59	348	N
PDZK1-1	PD	H	72	352	Y	ERBB2IP-1	PD	H	59	378	N
PDZK1-1	PD	H	72	353	Y	ERBB2IP-1	PD	H	59	131	N
PDZK1-1	PD	H	72	354	Y	ERBB2IP-1	PD	H	59	399	N
PDZK1-1	PD	H	72	355	Y	ERBB2IP-1	PD	H	59	415	N
PDZK1-1	PD	H	72	356	Y	ERBB2IP-1	PD	H	59	340	N
PDZK1-1	PD	H	72	357	Y	ERBB2IP-1	PD	H	59	428	N
PDZK1-1	PD	H	72	358	Y	ERBB2IP-1	PD	H	59	192	N
PDZK1-1	PD	H	72	359	Y	ERBB2IP-1	PD	H	59	371	N
PDZK1-1	PD	H	72	360	Y	ERBB2IP-1	PD	H	59	416	N
PDZK1-1	PD	H	72	361	Y	ERBB2IP-1	PD	H	59	332	N
PDZK1-1	PD	H	72	362	Y	ERBB2IP-1	PD	H	59	193	N
PDZK1-1	PD	H	72	363	Y	ERBB2IP-1	PD	H	59	291	N
PDZK1-1	PD	H	72	364	Y	ERBB2IP-1	PD	H	59	298	N
MAGI1-5	PD	H	73	365	Y	ERBB2IP-1	PD	H	59	417	N
MAGI1-5	PD	H	73	366	Y	ERBB2IP-1	PD	H	59	174	N
MAGI1-5	PD	H	73	367	Y	ERBB2IP-1	PD	H	59	374	N

MAGI1-5	PD	H	73	368	Y	ERBB2IP-1	PD	H	59	389	N
MAGI1-5	PD	H	73	369	Y	ERBB2IP-1	PD	H	59	407	N
MAGI1-5	PD	H	73	370	Y	ERBB2IP-1	PD	H	59	405	N
MAGI1-5	PD	H	73	371	Y	ERBB2IP-1	PD	H	59	382	N
MAGI1-5	PD	H	73	372	Y	ERBB2IP-1	PD	H	59	96	N
MAGI1-5	PD	H	73	373	Y	ERBB2IP-1	PD	H	59	383	N
MAGI1-5	PD	H	73	374	Y	ERBB2IP-1	PD	H	59	170	N
MAGI1-5	PD	H	73	375	Y	ERBB2IP-1	PD	H	59	103	N
MAGI1-5	PD	H	73	376	Y	ERBB2IP-1	PD	H	59	404	N
MAGI3-5	PD	H	74	376	Y	ERBB2IP-1	PD	H	59	275	N
MAGI3-5	PD	H	74	377	Y	ERBB2IP-1	PD	H	59	369	N
MAGI3-5	PD	H	74	370	Y	ERBB2IP-1	PD	H	59	87	N
PSCDBP-1	PD	H	75	173	Y	ERBB2IP-1	PD	H	59	388	N
PSCDBP-1	PD	H	75	378	Y	MPDZ-1	PD	H	60	707	N
PSCDBP-1	PD	H	75	379	Y	MPDZ-1	PD	H	60	369	N
PSCDBP-1	PD	H	75	380	Y	MPDZ-1	PD	H	60	421	N
PSCDBP-1	PD	H	75	381	Y	MPDZ-1	PD	H	60	373	N
PSCDBP-1	PD	H	75	382	Y	MPDZ-1	PD	H	60	345	N
DVL2-1	PD	H	76	383	Y	MPDZ-1	PD	H	60	708	N
DVL2-1	PD	H	76	384	Y	MPDZ-1	PD	H	60	709	N
DVL2-1	PD	H	76	385	Y	MPDZ-1	PD	H	60	327	N
DVL2-1	PD	H	76	386	Y	MPDZ-1	PD	H	60	87	N
DLG2-3	PD	H	77	108	Y	MPDZ-1	PD	H	60	371	N
DLG2-3	PD	H	77	241	Y	MPDZ-1	PD	H	60	407	N
DLG2-3	PD	H	77	261	Y	MPDZ-1	PD	H	60	710	N
DLG2-3	PD	H	77	1	Y	MPDZ-1	PD	H	60	711	N
DLG2-3	PD	H	77	387	Y	MPDZ-1	PD	H	60	266	N
DLG2-3	PD	H	77	388	Y	MPDZ-1	PD	H	60	712	N
DLG2-3	PD	H	77	270	Y	MPDZ-1	PD	H	60	385	N
DLG2-3	PD	H	77	389	Y	MPDZ-1	PD	H	60	713	N
DLG2-3	PD	H	77	390	Y	MPDZ-1	PD	H	60	714	N
DLG2-3	PD	H	77	391	Y	MPDZ-1	PD	H	60	715	N
DLG2-3	PD	H	77	392	Y	MPDZ-1	PD	H	60	298	N
DLG2-3	PD	H	77	393	Y	MPDZ-1	PD	H	60	716	N
DLG2-3	PD	H	77	394	Y	MPDZ-1	PD	H	60	270	N
DLG2-3	PD	H	77	395	Y	MPDZ-1	PD	H	60	423	N
MPDZ-3	PD	H	78	396	Y	MPDZ-10	PD	H	61	717	N
MPDZ-3	PD	H	78	397	Y	MPDZ-10	PD	H	61	399	N
MPDZ-3	PD	H	78	398	Y	MPDZ-10	PD	H	61	380	N
MPDZ-3	PD	H	78	399	Y	MPDZ-10	PD	H	61	718	N
MPDZ-3	PD	H	78	400	Y	MPDZ-10	PD	H	61	719	N
MPDZ-3	PD	H	78	401	Y	MPDZ-10	PD	H	61	378	N
MPDZ-3	PD	H	78	402	Y	MPDZ-10	PD	H	61	402	N
MPDZ-3	PD	H	78	403	Y	MPDZ-10	PD	H	61	344	N
MPDZ-3	PD	H	78	404	Y	MPDZ-10	PD	H	61	405	N
MPDZ-3	PD	H	78	405	Y	MPDZ-10	PD	H	61	412	N

MPDZ-3	PD	H	78	406	Y	MPDZ-10	PD	H	61	423	N
MPDZ-3	PD	H	78	407	Y	MPDZ-10	PD	H	61	720	N
PDLIM4-1	PD	H	79	408	Y	MPDZ-10	PD	H	61	721	N
PDLIM4-1	PD	H	79	409	Y	MPDZ-10	PD	H	61	353	N
PDLIM4-1	PD	H	79	410	Y	MPDZ-10	PD	H	61	398	N
PDLIM4-1	PD	H	79	411	Y	MPDZ-10	PD	H	61	377	N
PDLIM4-1	PD	H	79	412	Y	MPDZ-10	PD	H	61	407	N
PDLIM4-1	PD	H	79	413	Y	MPDZ-10	PD	H	61	408	N
PDLIM4-1	PD	H	79	316	Y	MPDZ-10	PD	H	61	722	N
PDLIM4-1	PD	H	79	414	Y	MPDZ-10	PD	H	61	723	N
PDLIM4-1	PD	H	79	415	Y	MPDZ-10	PD	H	61	724	N
PDLIM4-1	PD	H	79	416	Y	MPDZ-10	PD	H	61	385	N
SLC9A3R2-2	PD	H	80	417	Y	MPDZ-10	PD	H	61	404	N
SLC9A3R2-2	PD	H	80	418	Y	MPDZ-10	PD	H	61	397	N
SLC9A3R2-2	PD	H	80	419	Y	MPDZ-10	PD	H	61	725	N
SLC9A3R2-2	PD	H	80	420	Y	MPDZ-10	PD	H	61	726	N
SLC9A3R2-2	PD	H	80	421	Y	MPDZ-12	PD	H	62	384	N
SLC9A3R2-2	PD	H	80	422	Y	MPDZ-12	PD	H	62	399	N
SLC9A3R2-2	PD	H	80	423	Y	MPDZ-12	PD	H	62	386	N
SLC9A3R2-2	PD	H	80	424	Y	MPDZ-12	PD	H	62	400	N
SLC9A3R2-2	PD	H	80	425	Y	MPDZ-12	PD	H	62	385	N
SLC9A3R2-2	PD	H	80	426	Y	MPDZ-12	PD	H	62	369	N
SLC9A3R2-2	PD	H	80	427	Y	MPDZ-12	PD	H	62	287	N
SLC9A3R2-2	PD	H	80	428	Y	MPDZ-12	PD	H	62	407	N
SNTA1-1	PD	H	81	429	Y	MPDZ-12	PD	H	62	371	N
SNTA1-1	PD	H	81	430	Y	MPDZ-12	PD	H	62	170	N
SNTA1-1	PD	H	81	431	Y	MPDZ-12	PD	H	62	405	N
SNTA1-1	PD	H	81	357	Y	SCRIB-1	PD	H	63	371	N
SNTA1-1	PD	H	81	205	Y	SCRIB-1	PD	H	63	369	N
SNTA1-1	PD	H	81	432	Y	SCRIB-1	PD	H	63	170	N
SNTA1-1	PD	H	81	108	Y	SCRIB-1	PD	H	63	293	N
SNTA1-1	PD	H	81	270	Y	SCRIB-1	PD	H	63	407	N
SNTA1-1	PD	H	81	433	Y	SCRIB-1	PD	H	63	87	N
A1-SYNTROPHIN-1	PM	M	0	58	N	SCRIB-1	PD	H	63	406	N
A1-SYNTROPHIN-1	PM	M	0	434	N	SCRIB-1	PD	H	63	287	N
A1-SYNTROPHIN-1	PM	M	0	435	N	SCRIB-1	PD	H	63	187	N
A1-SYNTROPHIN-1	PM	M	0	436	N	SCRIB-1	PD	H	63	405	N
A1-SYNTROPHIN-1	PM	M	0	437	N	SCRIB-1	PD	H	63	96	N
A1-SYNTROPHIN-1	PM	M	0	56	N	SCRIB-1	PD	H	63	233	N
A1-SYNTROPHIN-1	PM	M	0	438	N	SCRIB-1	PD	H	63	377	N
A1-SYNTROPHIN-1	PM	M	0	439	N	SCRIB-1	PD	H	63	412	N
A1-SYNTROPHIN-1	PM	M	0	440	N	SCRIB-1	PD	H	63	400	N
A1-SYNTROPHIN-1	PM	M	0	441	N	SCRIB-1	PD	H	63	380	N
A1-SYNTROPHIN-1	PM	M	0	442	N	SCRIB-1	PD	H	63	385	N
A1-SYNTROPHIN-1	PM	M	0	443	N	SCRIB-1	PD	H	63	350	N
A1-SYNTROPHIN-1	PM	M	0	444	N	SCRIB-1	PD	H	63	404	N

B1-SYNTROPHIN-1	PM	M	1	445	N	SCRIB-1	PD	H	63	374	N
B1-SYNTROPHIN-1	PM	M	1	446	N	SCRIB-1	PD	H	63	155	N
B1-SYNTROPHIN-1	PM	M	1	447	N	SCRIB-1	PD	H	63	171	N
B1-SYNTROPHIN-1	PM	M	1	26	N	SCRIB-1	PD	H	63	399	N
B1-SYNTROPHIN-1	PM	M	1	48	N	SCRIB-1	PD	H	63	408	N
B1-SYNTROPHIN-1	PM	M	1	436	N	SCRIB-1	PD	H	63	381	N
B1-SYNTROPHIN-1	PM	M	1	52	N	SCRIB-1	PD	H	63	382	N
B1-SYNTROPHIN-1	PM	M	1	25	N	SCRIB-1	PD	H	63	375	N
B1-SYNTROPHIN-1	PM	M	1	67	N	DLG1-2	PD	H	64	727	N
B1-SYNTROPHIN-1	PM	M	1	448	N	DLG1-2	PD	H	64	385	N
B1-SYNTROPHIN-1	PM	M	1	21	N	DLG1-2	PD	H	64	430	N
B1-SYNTROPHIN-1	PM	M	1	27	N	DLG1-2	PD	H	64	380	N
B1-SYNTROPHIN-1	PM	M	1	68	N	DLG1-2	PD	H	64	419	N
B1-SYNTROPHIN-1	PM	M	1	23	N	DLG1-2	PD	H	64	287	N
B1-SYNTROPHIN-1	PM	M	1	19	N	DLG1-2	PD	H	64	401	N
B1-SYNTROPHIN-1	PM	M	1	69	N	DLG1-2	PD	H	64	728	N
B1-SYNTROPHIN-1	PM	M	1	449	N	DLG1-2	PD	H	64	176	N
CHAPSYN-110-2	PM	M	2	436	N	DLG1-2	PD	H	64	729	N
CHAPSYN-110-2	PM	M	2	450	N	DLG1-2	PD	H	64	416	N
CHAPSYN-110-2	PM	M	2	451	N	DLG1-2	PD	H	64	399	N
CHAPSYN-110-2	PM	M	2	452	N	DLG1-2	PD	H	64	724	N
CHAPSYN-110-2	PM	M	2	453	N	DLG1-2	PD	H	64	193	N
CHAPSYN-110-2	PM	M	2	454	N	DLG1-2	PD	H	64	218	N
CHAPSYN-110-2	PM	M	2	455	N	DLG1-2	PD	H	64	103	N
CHAPSYN-110-2	PM	M	2	456	N	DLG1-2	PD	H	64	382	N
CHAPSYN-110-2	PM	M	2	457	N	DLG1-2	PD	H	64	421	N
CHAPSYN-110-2	PM	M	2	458	N	DLG1-2	PD	H	64	730	N
CHAPSYN-110-2	PM	M	2	459	N	DLG1-2	PD	H	64	731	N
CHAPSYN-110-2	PM	M	2	460	N	DLG1-2	PD	H	64	366	N
CHAPSYN-110-2	PM	M	2	461	N	DLG1-2	PD	H	64	378	N
CHAPSYN-110-3	PM	M	3	452	N	DLG1-2	PD	H	64	423	N
CHAPSYN-110-3	PM	M	3	29	N	DLG1-2	PD	H	64	87	N
CHAPSYN-110-3	PM	M	3	65	N	DLG1-2	PD	H	64	369	N
CHAPSYN-110-3	PM	M	3	46	N	DLG1-2	PD	H	64	699	N
CHAPSYN-110-3	PM	M	3	17	N	DLG1-2	PD	H	64	170	N
CHAPSYN-110-3	PM	M	3	462	N	DLG1-2	PD	H	64	377	N
CHAPSYN-110-3	PM	M	3	463	N	DLG1-2	PD	H	64	94	N
CHAPSYN-110-3	PM	M	3	57	N	DLG1-2	PD	H	64	397	N
CHAPSYN-110-3	PM	M	3	464	N	DLG1-2	PD	H	64	732	N
CHAPSYN-110-3	PM	M	3	41	N	DLG1-2	PD	H	64	352	N
CHAPSYN-110-3	PM	M	3	465	N	DLG1-2	PD	H	64	389	N
CHAPSYN-110-3	PM	M	3	45	N	DLG1-2	PD	H	64	415	N
CHAPSYN-110-3	PM	M	3	63	N	DLG1-2	PD	H	64	325	N
CHAPSYN-110-3	PM	M	3	466	N	DLG1-2	PD	H	64	289	N
CHAPSYN-110-3	PM	M	3	467	N	DLG1-2	PD	H	64	398	N
CHAPSYN-110-3	PM	M	3	468	N	DLG1-2	PD	H	64	407	N

CHAPSYN-110-3	PM	M	3	469	N	DLG1-2	PD	H	64	275	N
CHAPSYN-110-3	PM	M	3	470	N	DLG1-2	PD	H	64	733	N
CHAPSYN-110-3	PM	M	3	64	N	DLG1-2	PD	H	64	174	N
CHAPSYN-110-3	PM	M	3	471	N	DLG1-2	PD	H	64	342	N
CHAPSYN-110-3	PM	M	3	472	N	DLG1-2	PD	H	64	294	N
CHAPSYN-110-3	PM	M	3	473	N	DLG1-2	PD	H	64	404	N
CHAPSYN-110-3	PM	M	3	35	N	DLG1-2	PD	H	64	371	N
CHAPSYN-110-3	PM	M	3	474	N	DLG1-2	PD	H	64	374	N
CHAPSYN-110-3	PM	M	3	73	N	DLG1-2	PD	H	64	396	N
CHAPSYN-110-3	PM	M	3	475	N	DLG1-2	PD	H	64	734	N
CHAPSYN-110-3	PM	M	3	26	N	DLG4-3	PD	H	65	112	N
CHAPSYN-110-3	PM	M	3	30	N	DLG4-3	PD	H	65	382	N
CHAPSYN-110-3	PM	M	3	13	N	DLG4-3	PD	H	65	170	N
CHAPSYN-110-3	PM	M	3	476	N	DLG4-3	PD	H	65	735	N
CHAPSYN-110-3	PM	M	3	454	N	DLG4-3	PD	H	65	736	N
CHAPSYN-110-3	PM	M	3	43	N	DLG4-3	PD	H	65	368	N
CHAPSYN-110-3	PM	M	3	3	N	DLG4-3	PD	H	65	737	N
CHAPSYN-110-3	PM	M	3	436	N	DLG4-3	PD	H	65	738	N
CIPP-10	PM	M	4	64	N	DLG4-3	PD	H	65	739	N
CIPP-10	PM	M	4	473	N	DLG4-3	PD	H	65	401	N
CIPP-10	PM	M	4	474	N	DLG4-3	PD	H	65	294	N
CIPP-10	PM	M	4	65	N	DLG4-3	PD	H	65	371	N
CIPP-10	PM	M	4	466	N	DLG4-3	PD	H	65	400	N
CIPP-10	PM	M	4	472	N	DLG4-3	PD	H	65	381	N
CIPP-10	PM	M	4	15	N	DLG4-3	PD	H	65	740	N
CIPP-10	PM	M	4	57	N	DLG4-3	PD	H	65	741	N
CIPP-10	PM	M	4	463	N	DLG4-3	PD	H	65	396	N
CIPP-10	PM	M	4	23	N	DLG4-3	PD	H	65	174	N
CIPP-10	PM	M	4	465	N	DLG4-3	PD	H	65	369	N
CIPP-10	PM	M	4	469	N	DLG4-3	PD	H	65	728	N
CIPP-10	PM	M	4	41	N	DLG4-3	PD	H	65	384	N
CIPP-10	PM	M	4	467	N	DLG4-3	PD	H	65	97	N
CIPP-10	PM	M	4	468	N	DLG4-3	PD	H	65	404	N
CIPP-10	PM	M	4	13	N	DLG4-3	PD	H	65	415	N
CIPP-10	PM	M	4	475	N	DLG4-3	PD	H	65	742	N
CIPP-10	PM	M	4	436	N	DLG4-3	PD	H	65	176	N
CIPP-10	PM	M	4	3	N	DLG4-3	PD	H	65	743	N
CIPP-10	PM	M	4	29	N	SCRIB-2	PD	H	66	377	N
CIPP-10	PM	M	4	448	N	SCRIB-2	PD	H	66	399	N
CIPP-10	PM	M	4	45	N	SCRIB-2	PD	H	66	402	N
CIPP-10	PM	M	4	73	N	SCRIB-2	PD	H	66	407	N
CIPP-10	PM	M	4	470	N	SCRIB-2	PD	H	66	405	N
CIPP-10	PM	M	4	454	N	SCRIB-2	PD	H	66	398	N
CIPP-10	PM	M	4	63	N	SCRIB-2	PD	H	66	345	N
CIPP-10	PM	M	4	17	N	SCRIB-2	PD	H	66	378	N
CIPP-10	PM	M	4	476	N	SCRIB-2	PD	H	66	404	N

CIPP-10	PM	M	4	16	N	SCRIB-2	PD	H	66	371	N
CIPP-10	PM	M	4	30	N	SCRIB-2	PD	H	66	170	N
CIPP-10	PM	M	4	35	N	SCRIB-2	PD	H	66	323	N
CIPP-10	PM	M	4	43	N	SCRIB-2	PD	H	66	316	N
CIPP-3	PM	M	5	477	N	SCRIB-2	PD	H	66	385	N
CIPP-3	PM	M	5	478	N	SCRIB-2	PD	H	66	369	N
CIPP-3	PM	M	5	479	N	SCRIB-2	PD	H	66	368	N
CIPP-3	PM	M	5	480	N	INADL-2	PD	H	67	342	N
CIPP-3	PM	M	5	481	N	INADL-2	PD	H	67	744	N
CIPP-3	PM	M	5	482	N	INADL-2	PD	H	67	430	N
CIPP-3	PM	M	5	483	N	INADL-2	PD	H	67	399	N
CIPP-3	PM	M	5	484	N	INADL-2	PD	H	67	390	N
CIPP-3	PM	M	5	485	N	INADL-2	PD	H	67	266	N
CIPP-3	PM	M	5	486	N	INADL-2	PD	H	67	745	N
CIPP-3	PM	M	5	487	N	INADL-2	PD	H	67	746	N
CIPP-3	PM	M	5	488	N	INADL-2	PD	H	67	707	N
CIPP-5	PM	M	6	489	N	INADL-2	PD	H	67	369	N
CIPP-5	PM	M	6	490	N	INADL-2	PD	H	67	747	N
CIPP-5	PM	M	6	491	N	INADL-2	PD	H	67	748	N
CIPP-5	PM	M	6	492	N	INADL-2	PD	H	67	749	N
CIPP-5	PM	M	6	493	N	INADL-2	PD	H	67	402	N
CIPP-5	PM	M	6	494	N	INADL-2	PD	H	67	750	N
CIPP-5	PM	M	6	495	N	INADL-2	PD	H	67	371	N
CIPP-5	PM	M	6	496	N	INADL-2	PD	H	67	751	N
CIPP-5	PM	M	6	497	N	INADL-2	PD	H	67	385	N
CIPP-5	PM	M	6	498	N	INADL-2	PD	H	67	425	N
CIPP-5	PM	M	6	499	N	INADL-2	PD	H	67	396	N
CIPP-8	PM	M	7	500	N	INADL-2	PD	H	67	752	N
CIPP-8	PM	M	7	501	N	DLG1-3	PD	H	68	174	N
CIPP-8	PM	M	7	0	N	DLG1-3	PD	H	68	728	N
CIPP-8	PM	M	7	83	N	DLG1-3	PD	H	68	401	N
CIPP-8	PM	M	7	472	N	DLG1-3	PD	H	68	753	N
CIPP-8	PM	M	7	19	N	DLG1-3	PD	H	68	380	N
CIPP-8	PM	M	7	502	N	DLG1-3	PD	H	68	402	N
CIPP-8	PM	M	7	503	N	DLG1-3	PD	H	68	754	N
CIPP-8	PM	M	7	445	N	DLG1-3	PD	H	68	368	N
CIPP-8	PM	M	7	48	N	DLG1-3	PD	H	68	170	N
CIPP-8	PM	M	7	504	N	DLG1-3	PD	H	68	755	N
CIPP-8	PM	M	7	446	N	DLG1-3	PD	H	68	383	N
CIPP-8	PM	M	7	449	N	DLG1-3	PD	H	68	369	N
CIPP-8	PM	M	7	8	N	DLG1-3	PD	H	68	39	N
CIPP-8	PM	M	7	505	N	DLG1-3	PD	H	68	756	N
CIPP-8	PM	M	7	27	N	DLG1-3	PD	H	68	396	N
CIPP-8	PM	M	7	506	N	DLG1-3	PD	H	68	404	N
CIPP-8	PM	M	7	6	N	DLG1-3	PD	H	68	757	N
CIPP-8	PM	M	7	507	N	DLG1-3	PD	H	68	382	N

CIPP-8	PM	M	7	508	N	DLG1-3	PD	H	68	758	N
CIPP-8	PM	M	7	509	N	DLG1-3	PD	H	68	759	N
CIPP-8	PM	M	7	510	N	DLG1-3	PD	H	68	760	N
CIPP-8	PM	M	7	67	N	DLG1-3	PD	H	68	378	N
CIPP-8	PM	M	7	511	N	DLG1-3	PD	H	68	415	N
CIPP-8	PM	M	7	68	N	DLG1-1	PD	H	69	761	N
CIPP-8	PM	M	7	512	N	DLG1-1	PD	H	69	407	N
CIPP-8	PM	M	7	13	N	DLG1-1	PD	H	69	762	N
CIPP-8	PM	M	7	4	N	DLG1-1	PD	H	69	369	N
CIPP-8	PM	M	7	52	N	DLG1-1	PD	H	69	763	N
CIPP-9	PM	M	8	446	N	DLG1-1	PD	H	69	764	N
CIPP-9	PM	M	8	513	N	DLG1-1	PD	H	69	403	N
CIPP-9	PM	M	8	514	N	DLG1-1	PD	H	69	404	N
CIPP-9	PM	M	8	515	N	DLG1-1	PD	H	69	765	N
CIPP-9	PM	M	8	45	N	DLG1-1	PD	H	69	402	N
CIPP-9	PM	M	8	53	N	DLG1-1	PD	H	69	371	N
CIPP-9	PM	M	8	23	N	DLG1-1	PD	H	69	766	N
CIPP-9	PM	M	8	516	N	DLG1-1	PD	H	69	397	N
CIPP-9	PM	M	8	5	N	DLG1-1	PD	H	69	399	N
CIPP-9	PM	M	8	517	N	DLG1-1	PD	H	69	756	N
CIPP-9	PM	M	8	18	N	DLG1-1	PD	H	69	767	N
CIPP-9	PM	M	8	0	N	DLG1-1	PD	H	69	385	N
CIPP-9	PM	M	8	83	N	DLG1-1	PD	H	69	768	N
CIPP-9	PM	M	8	447	N	DLG1-1	PD	H	69	170	N
CIPP-9	PM	M	8	17	N	DLG1-1	PD	H	69	380	N
CIPP-9	PM	M	8	32	N	DLG1-1	PD	H	69	697	N
CIPP-9	PM	M	8	445	N	LRRC7-1	PD	H	70	769	N
CIPP-9	PM	M	8	80	N	LRRC7-1	PD	H	70	94	N
CIPP-9	PM	M	8	34	N	LRRC7-1	PD	H	70	193	N
CIPP-9	PM	M	8	1	N	LRRC7-1	PD	H	70	298	N
CIPP-9	PM	M	8	51	N	LRRC7-1	PD	H	70	404	N
CIPP-9	PM	M	8	518	N	LRRC7-1	PD	H	70	371	N
CIPP-9	PM	M	8	20	N	LRRC7-1	PD	H	70	398	N
CIPP-9	PM	M	8	7	N	LRRC7-1	PD	H	70	375	N
CIPP-9	PM	M	8	469	N	LRRC7-1	PD	H	70	266	N
CIPP-9	PM	M	8	16	N	LRRC7-1	PD	H	70	427	N
CIPP-9	PM	M	8	62	N	LRRC7-1	PD	H	70	421	N
CIPP-9	PM	M	8	519	N	LRRC7-1	PD	H	70	385	N
CIPP-9	PM	M	8	78	N	LRRC7-1	PD	H	70	770	N
CIPP-9	PM	M	8	520	N	LRRC7-1	PD	H	70	114	N
CIPP-9	PM	M	8	43	N	LRRC7-1	PD	H	70	87	N
CIPP-9	PM	M	8	521	N	LRRC7-1	PD	H	70	397	N
CIPP-9	PM	M	8	67	N	LRRC7-1	PD	H	70	771	N
CIPP-9	PM	M	8	4	N	LRRC7-1	PD	H	70	407	N
CIPP-9	PM	M	8	21	N	LRRC7-1	PD	H	70	342	N
CIPP-9	PM	M	8	74	N	LRRC7-1	PD	H	70	405	N

CIPP-9	PM	M	8	32	N	LRRC7-1	PD	H	70	772	N
CIPP-9	PM	M	8	70	N	LRRC7-1	PD	H	70	773	N
CIPP-9	PM	M	8	508	N	LRRC7-1	PD	H	70	399	N
CIPP-9	PM	M	8	35	N	LRRC7-1	PD	H	70	369	N
CIPP-9	PM	M	8	6	N	LRRC7-1	PD	H	70	774	N
CIPP-9	PM	M	8	9	N	LRRC7-1	PD	H	70	368	N
CIPP-9	PM	M	8	15	N	LRRC7-1	PD	H	70	775	N
CIPP-9	PM	M	8	77	N	LRRC7-1	PD	H	70	411	N
CIPP-9	PM	M	8	514	N	LRRC7-1	PD	H	70	776	N
CIPP-9	PM	M	8	522	N	LRRC7-1	PD	H	70	378	N
CIPP-9	PM	M	8	50	N	LRRC7-1	PD	H	70	777	N
CIPP-9	PM	M	8	523	N	LRRC7-1	PD	H	70	103	N
CIPP-9	PM	M	8	2	N	LRRC7-1	PD	H	70	332	N
CIPP-9	PM	M	8	76	N	LRRC7-1	PD	H	70	170	N
CIPP-9	PM	M	8	524	N	LRRC7-1	PD	H	70	176	N
DVL1-1	PM	M	9	525	N	LRRC7-1	PD	H	70	778	N
DVL1-1	PM	M	9	526	N	MPP6-1	PD	H	71	176	N
DVL1-1	PM	M	9	527	N	MPP6-1	PD	H	71	779	N
DVL1-1	PM	M	9	528	N	MPP6-1	PD	H	71	371	N
DVL1-1	PM	M	9	482	N	MPP6-1	PD	H	71	780	N
DVL1-1	PM	M	9	529	N	MPP6-1	PD	H	71	415	N
DVL1-1	PM	M	9	530	N	MPP6-1	PD	H	71	378	N
DVL1-1	PM	M	9	531	N	MPP6-1	PD	H	71	781	N
DVL1-1	PM	M	9	456	N	MPP6-1	PD	H	71	782	N
DVL1-1	PM	M	9	532	N	MPP6-1	PD	H	71	380	N
DVL1-1	PM	M	9	62	N	MPP6-1	PD	H	71	783	N
DVL3-1	PM	M	10	45	N	MPP6-1	PD	H	71	138	N
DVL3-1	PM	M	10	473	N	MPP6-1	PD	H	71	430	N
DVL3-1	PM	M	10	470	N	MPP6-1	PD	H	71	369	N
DVL3-1	PM	M	10	475	N	MPP6-1	PD	H	71	784	N
DVL3-1	PM	M	10	23	N	MPP6-1	PD	H	71	388	N
DVL3-1	PM	M	10	454	N	MPP6-1	PD	H	71	785	N
DVL3-1	PM	M	10	15	N	MPP6-1	PD	H	71	428	N
DVL3-1	PM	M	10	57	N	MPP6-1	PD	H	71	263	N
DVL3-1	PM	M	10	463	N	MPP6-1	PD	H	71	342	N
DVL3-1	PM	M	10	35	N	MPP6-1	PD	H	71	375	N
DVL3-1	PM	M	10	65	N	MPP6-1	PD	H	71	382	N
DVL3-1	PM	M	10	466	N	MPP6-1	PD	H	71	417	N
DVL3-1	PM	M	10	3	N	MPP6-1	PD	H	71	786	N
DVL3-1	PM	M	10	467	N	MPP6-1	PD	H	71	787	N
DVL3-1	PM	M	10	476	N	MPP6-1	PD	H	71	788	N
DVL3-1	PM	M	10	41	N	PDZK1-1	PD	H	72	153	N
DVL3-1	PM	M	10	63	N	PDZK1-1	PD	H	72	381	N
DVL3-1	PM	M	10	16	N	PDZK1-1	PD	H	72	389	N
DVL3-1	PM	M	10	29	N	PDZK1-1	PD	H	72	275	N
DVL3-1	PM	M	10	468	N	PDZK1-1	PD	H	72	417	N

DVL3-1	PM	M	10	64	N	PDZK1-1	PD	H	72	216	N
DVL3-1	PM	M	10	465	N	PDZK1-1	PD	H	72	288	N
DVL3-1	PM	M	10	17	N	PDZK1-1	PD	H	72	789	N
DVL3-1	PM	M	10	472	N	PDZK1-1	PD	H	72	790	N
DVL3-1	PM	M	10	474	N	PDZK1-1	PD	H	72	388	N
DVL3-1	PM	M	10	73	N	PDZK1-1	PD	H	72	157	N
DVL3-1	PM	M	10	13	N	PDZK1-1	PD	H	72	791	N
DVL3-1	PM	M	10	22	N	PDZK1-1	PD	H	72	256	N
DVL3-1	PM	M	10	469	N	PDZK1-1	PD	H	72	430	N
ERBIN-1	PM	M	11	465	N	PDZK1-1	PD	H	72	380	N
ERBIN-1	PM	M	11	29	N	PDZK1-1	PD	H	72	371	N
ERBIN-1	PM	M	11	73	N	PDZK1-1	PD	H	72	765	N
ERBIN-1	PM	M	11	508	N	PDZK1-1	PD	H	72	407	N
ERBIN-1	PM	M	11	11	N	PDZK1-1	PD	H	72	177	N
ERBIN-1	PM	M	11	41	N	PDZK1-1	PD	H	72	403	N
ERBIN-1	PM	M	11	533	N	PDZK1-1	PD	H	72	401	N
ERBIN-1	PM	M	11	475	N	PDZK1-1	PD	H	72	399	N
ERBIN-1	PM	M	11	15	N	PDZK1-1	PD	H	72	412	N
ERBIN-1	PM	M	11	57	N	PDZK1-1	PD	H	72	402	N
ERBIN-1	PM	M	11	463	N	PDZK1-1	PD	H	72	792	N
ERBIN-1	PM	M	11	466	N	PDZK1-1	PD	H	72	194	N
ERBIN-1	PM	M	11	468	N	PDZK1-1	PD	H	72	369	N
ERBIN-1	PM	M	11	45	N	PDZK1-1	PD	H	72	404	N
ERBIN-1	PM	M	11	65	N	PDZK1-1	PD	H	72	793	N
ERBIN-1	PM	M	11	63	N	PDZK1-1	PD	H	72	794	N
ERBIN-1	PM	M	11	534	N	PDZK1-1	PD	H	72	374	N
ERBIN-1	PM	M	11	467	N	PDZK1-1	PD	H	72	795	N
ERBIN-1	PM	M	11	454	N	PDZK1-1	PD	H	72	796	N
ERBIN-1	PM	M	11	13	N	PDZK1-1	PD	H	72	382	N
ERBIN-1	PM	M	11	64	N	PDZK1-1	PD	H	72	385	N
ERBIN-1	PM	M	11	1	N	PDZK1-1	PD	H	72	396	N
ERBIN-1	PM	M	11	20	N	PDZK1-1	PD	H	72	248	N
ERBIN-1	PM	M	11	23	N	PDZK1-1	PD	H	72	96	N
ERBIN-1	PM	M	11	470	N	PDZK1-1	PD	H	72	797	N
ERBIN-1	PM	M	11	473	N	PDZK1-1	PD	H	72	292	N
ERBIN-1	PM	M	11	35	N	MAGI1-5	PD	H	73	381	N
ERBIN-1	PM	M	11	447	N	MAGI1-5	PD	H	73	390	N
ERBIN-1	PM	M	11	16	N	MAGI1-5	PD	H	73	302	N
ERBIN-1	PM	M	11	476	N	MAGI1-5	PD	H	73	798	N
ERBIN-1	PM	M	11	3	N	MAGI1-5	PD	H	73	174	N
ERBIN-1	PM	M	11	30	N	MAGI1-5	PD	H	73	799	N
ERBIN-1	PM	M	11	474	N	MAGI1-5	PD	H	73	734	N
ERBIN-1	PM	M	11	17	N	MAGI1-5	PD	H	73	421	N
ERBIN-1	PM	M	11	22	N	MAGI1-5	PD	H	73	406	N
ERBIN-1	PM	M	11	26	N	MAGI1-5	PD	H	73	428	N
ERBIN-1	PM	M	11	43	N	MAGI1-5	PD	H	73	800	N

ERBIN-1	PM	M	11	472	N	MAGI1-5	PD	H	73	801	N
ERBIN-1	PM	M	11	469	N	MAGI1-5	PD	H	73	352	N
GRIP1-6	PM	M	12	535	N	MAGI1-5	PD	H	73	802	N
GRIP1-6	PM	M	12	536	N	MAGI1-5	PD	H	73	417	N
GRIP1-6	PM	M	12	537	N	MAGI1-5	PD	H	73	803	N
GRIP1-6	PM	M	12	538	N	MAGI1-5	PD	H	73	804	N
GRIP1-6	PM	M	12	539	N	MAGI1-5	PD	H	73	416	N
GRIP1-6	PM	M	12	540	N	MAGI1-5	PD	H	73	430	N
GRIP1-6	PM	M	12	541	N	MAGI1-5	PD	H	73	415	N
GRIP1-6	PM	M	12	479	N	MAGI1-5	PD	H	73	731	N
GRIP1-6	PM	M	12	542	N	MAGI1-5	PD	H	73	805	N
GRIP1-6	PM	M	12	462	N	MAGI3-5	PD	H	74	806	N
GRIP1-6	PM	M	12	543	N	MAGI3-5	PD	H	74	807	N
HARMONIN-2	PM	M	13	474	N	MAGI3-5	PD	H	74	170	N
HARMONIN-2	PM	M	13	473	N	MAGI3-5	PD	H	74	422	N
HARMONIN-2	PM	M	13	475	N	MAGI3-5	PD	H	74	808	N
HARMONIN-2	PM	M	13	64	N	MAGI3-5	PD	H	74	809	N
HARMONIN-2	PM	M	13	41	N	MAGI3-5	PD	H	74	810	N
HARMONIN-2	PM	M	13	3	N	MAGI3-5	PD	H	74	431	N
HARMONIN-2	PM	M	13	15	N	MAGI3-5	PD	H	74	811	N
HARMONIN-2	PM	M	13	57	N	MAGI3-5	PD	H	74	717	N
HARMONIN-2	PM	M	13	463	N	MAGI3-5	PD	H	74	734	N
HARMONIN-2	PM	M	13	23	N	MAGI3-5	PD	H	74	812	N
HARMONIN-2	PM	M	13	73	N	MAGI3-5	PD	H	74	813	N
HARMONIN-2	PM	M	13	13	N	PSCDBP-1	PD	H	75	814	N
HARMONIN-2	PM	M	13	472	N	PSCDBP-1	PD	H	75	815	N
HARMONIN-2	PM	M	13	467	N	PSCDBP-1	PD	H	75	371	N
HARMONIN-2	PM	M	13	465	N	PSCDBP-1	PD	H	75	407	N
HARMONIN-2	PM	M	13	17	N	PSCDBP-1	PD	H	75	385	N
HARMONIN-2	PM	M	13	470	N	PSCDBP-1	PD	H	75	816	N
HARMONIN-2	PM	M	13	43	N	PSCDBP-1	PD	H	75	427	N
HARMONIN-2	PM	M	13	35	N	PSCDBP-1	PD	H	75	817	N
HARMONIN-2	PM	M	13	29	N	PSCDBP-1	PD	H	75	266	N
HARMONIN-2	PM	M	13	16	N	PSCDBP-1	PD	H	75	818	N
HARMONIN-2	PM	M	13	476	N	PSCDBP-1	PD	H	75	819	N
HARMONIN-2	PM	M	13	22	N	PSCDBP-1	PD	H	75	820	N
HARMONIN-2	PM	M	13	469	N	PSCDBP-1	PD	H	75	738	N
HARMONIN-2	PM	M	13	466	N	PSCDBP-1	PD	H	75	821	N
HARMONIN-2	PM	M	13	65	N	PSCDBP-1	PD	H	75	822	N
HARMONIN-2	PM	M	13	468	N	PSCDBP-1	PD	H	75	390	N
HARMONIN-2	PM	M	13	63	N	DVL2-1	PD	H	76	823	N
HARMONIN-2	PM	M	13	454	N	DVL2-1	PD	H	76	190	N
HARMONIN-2	PM	M	13	30	N	DVL2-1	PD	H	76	824	N
LARG-1	PM	M	14	33	N	DVL2-1	PD	H	76	825	N
LARG-1	PM	M	14	12	N	DVL2-1	PD	H	76	826	N
LIN-7C-1	PM	M	15	468	N	DVL2-1	PD	H	76	827	N

LIN-7C-1	PM	M	15	29	N	DVL2-1	PD	H	76	389	N
LIN-7C-1	PM	M	15	470	N	DVL2-1	PD	H	76	828	N
LIN-7C-1	PM	M	15	16	N	DVL2-1	PD	H	76	430	N
LIN-7C-1	PM	M	15	62	N	DVL2-1	PD	H	76	829	N
LIN-7C-1	PM	M	15	17	N	DVL2-1	PD	H	76	371	N
LIN-7C-1	PM	M	15	466	N	DVL2-1	PD	H	76	830	N
LIN-7C-1	PM	M	15	475	N	DVL2-1	PD	H	76	831	N
LIN-7C-1	PM	M	15	69	N	DVL2-1	PD	H	76	832	N
LIN-7C-1	PM	M	15	463	N	DLG2-3	PD	H	77	170	N
LIN-7C-1	PM	M	15	60	N	DLG2-3	PD	H	77	368	N
LIN-7C-1	PM	M	15	467	N	DLG2-3	PD	H	77	174	N
LIN-7C-1	PM	M	15	68	N	DLG2-3	PD	H	77	402	N
LIN-7C-1	PM	M	15	26	N	DLG2-3	PD	H	77	735	N
LIN-7C-1	PM	M	15	64	N	DLG2-3	PD	H	77	814	N
LIN-7C-1	PM	M	15	66	N	DLG2-3	PD	H	77	378	N
LIN-7C-1	PM	M	15	63	N	DLG2-3	PD	H	77	396	N
LIN-7C-1	PM	M	15	11	N	DLG2-3	PD	H	77	833	N
LIN-7C-1	PM	M	15	45	N	DLG2-3	PD	H	77	404	N
LIN-7C-1	PM	M	15	473	N	DLG2-3	PD	H	77	415	N
LIN-7C-1	PM	M	15	3	N	DLG2-3	PD	H	77	834	N
LIN-7C-1	PM	M	15	469	N	DLG2-3	PD	H	77	371	N
LIN-7C-1	PM	M	15	476	N	DLG2-3	PD	H	77	835	N
LIN-7C-1	PM	M	15	22	N	DLG2-3	PD	H	77	836	N
LIN-7C-1	PM	M	15	53	N	DLG2-3	PD	H	77	401	N
LIN-7C-1	PM	M	15	41	N	DLG2-3	PD	H	77	837	N
LIN-7C-1	PM	M	15	474	N	DLG2-3	PD	H	77	838	N
LIN-7C-1	PM	M	15	57	N	DLG2-3	PD	H	77	382	N
LIN-7C-1	PM	M	15	472	N	DLG2-3	PD	H	77	839	N
LIN-7C-1	PM	M	15	465	N	DLG2-3	PD	H	77	384	N
LIN-7C-1	PM	M	15	544	N	DLG2-3	PD	H	77	369	N
LIN-7C-1	PM	M	15	73	N	DLG2-3	PD	H	77	377	N
LIN-7C-1	PM	M	15	17	N	DLG2-3	PD	H	77	713	N
LIN-7C-1	PM	M	15	30	N	MPDZ-3	PD	H	78	430	N
LIN-7C-1	PM	M	15	65	N	MPDZ-3	PD	H	78	840	N
LIN-7C-1	PM	M	15	52	N	MPDZ-3	PD	H	78	835	N
LIN-7C-1	PM	M	15	454	N	MPDZ-3	PD	H	78	841	N
LIN-7C-1	PM	M	15	35	N	MPDZ-3	PD	H	78	248	N
LIN-7C-1	PM	M	15	43	N	MPDZ-3	PD	H	78	388	N
LIN-7C-1	PM	M	15	23	N	MPDZ-3	PD	H	78	207	N
LIN-7C-1	PM	M	15	70	N	MPDZ-3	PD	H	78	842	N
LRRC7-1	PM	M	16	473	N	MPDZ-3	PD	H	78	294	N
LRRC7-1	PM	M	16	545	N	MPDZ-3	PD	H	78	268	N
LRRC7-1	PM	M	16	59	N	MPDZ-3	PD	H	78	843	N
LRRC7-1	PM	M	16	471	N	MPDZ-3	PD	H	78	786	N
LRRC7-1	PM	M	16	488	N	MPDZ-3	PD	H	78	193	N
LRRC7-1	PM	M	16	546	N	MPDZ-3	PD	H	78	390	N

LRRC7-1	PM	M	16	4	N	MPDZ-3	PD	H	78	844	N
LRRC7-1	PM	M	16	533	N	MPDZ-3	PD	H	78	845	N
LRRC7-1	PM	M	16	466	N	MPDZ-3	PD	H	78	846	N
LRRC7-1	PM	M	16	72	N	MPDZ-3	PD	H	78	231	N
LRRC7-1	PM	M	16	464	N	MPDZ-3	PD	H	78	371	N
LRRC7-1	PM	M	16	547	N	MPDZ-3	PD	H	78	234	N
LRRC7-1	PM	M	16	548	N	MPDZ-3	PD	H	78	847	N
LRRC7-1	PM	M	16	436	N	MPDZ-3	PD	H	78	200	N
LRRC7-1	PM	M	16	508	N	PDLIM4-1	PD	H	79	848	N
LRRC7-1	PM	M	16	549	N	PDLIM4-1	PD	H	79	773	N
LRRC7-1	PM	M	16	550	N	PDLIM4-1	PD	H	79	144	N
LRRC7-1	PM	M	16	551	N	PDLIM4-1	PD	H	79	701	N
LRRC7-1	PM	M	16	552	N	PDLIM4-1	PD	H	79	849	N
LRRC7-1	PM	M	16	534	N	PDLIM4-1	PD	H	79	369	N
LRRC7-1	PM	M	16	462	N	PDLIM4-1	PD	H	79	850	N
LRRC7-1	PM	M	16	452	N	PDLIM4-1	PD	H	79	229	N
LRRC7-1	PM	M	16	553	N	PDLIM4-1	PD	H	79	176	N
LRRC7-1	PM	M	16	465	N	PDLIM4-1	PD	H	79	398	N
LRRC7-1	PM	M	16	63	N	PDLIM4-1	PD	H	79	851	N
MAGI-1-6	PM	M	17	554	N	PDLIM4-1	PD	H	79	852	N
MAGI-1-6	PM	M	17	555	N	PDLIM4-1	PD	H	79	430	N
MAGI-1-6	PM	M	17	51	N	PDLIM4-1	PD	H	79	853	N
MAGI-1-6	PM	M	17	556	N	PDLIM4-1	PD	H	79	232	N
MAGI-1-6	PM	M	17	534	N	PDLIM4-1	PD	H	79	817	N
MAGI-1-6	PM	M	17	557	N	PDLIM4-1	PD	H	79	388	N
MAGI-1-6	PM	M	17	54	N	PDLIM4-1	PD	H	79	778	N
MAGI-2-2	PM	M	18	63	N	PDLIM4-1	PD	H	79	112	N
MAGI-2-2	PM	M	18	446	N	PDLIM4-1	PD	H	79	184	N
MAGI-2-2	PM	M	18	68	N	SLC9A3R2-2	PD	H	80	854	N
MAGI-2-2	PM	M	18	502	N	SLC9A3R2-2	PD	H	80	91	N
MAGI-2-2	PM	M	18	67	N	SLC9A3R2-2	PD	H	80	407	N
MAGI-2-2	PM	M	18	26	N	SLC9A3R2-2	PD	H	80	855	N
MAGI-2-2	PM	M	18	448	N	SLC9A3R2-2	PD	H	80	856	N
MAGI-2-2	PM	M	18	27	N	SLC9A3R2-2	PD	H	80	371	N
MAGI-2-2	PM	M	18	23	N	SLC9A3R2-2	PD	H	80	294	N
MAGI-2-2	PM	M	18	19	N	SLC9A3R2-2	PD	H	80	389	N
MAGI-2-2	PM	M	18	508	N	SLC9A3R2-2	PD	H	80	369	N
MAGI-2-2	PM	M	18	454	N	SLC9A3R2-2	PD	H	80	97	N
MAGI-2-5	PM	M	19	447	N	SLC9A3R2-2	PD	H	80	857	N
MAGI-2-5	PM	M	19	558	N	SLC9A3R2-2	PD	H	80	858	N
MAGI-2-5	PM	M	19	448	N	SLC9A3R2-2	PD	H	80	177	N
MAGI-2-5	PM	M	19	436	N	SLC9A3R2-2	PD	H	80	114	N
MAGI-2-6	PM	M	20	39	N	SLC9A3R2-2	PD	H	80	748	N
MAGI-2-6	PM	M	20	50	N	SLC9A3R2-2	PD	H	80	300	N
MAGI-2-6	PM	M	20	21	N	SLC9A3R2-2	PD	H	80	859	N
MAGI-2-6	PM	M	20	23	N	SLC9A3R2-2	PD	H	80	860	N

MAGI-2-6	PM	M	20	8	N	SLC9A3R2-2	PD	H	80	368	N
MAGI-2-6	PM	M	20	559	N	SLC9A3R2-2	PD	H	80	193	N
MAGI-2-6	PM	M	20	555	N	SLC9A3R2-2	PD	H	80	861	N
MAGI-2-6	PM	M	20	2	N	SLC9A3R2-2	PD	H	80	862	N
MAGI-2-6	PM	M	20	67	N	SNTA1-1	PD	H	81	863	N
MAGI-2-6	PM	M	20	68	N	SNTA1-1	PD	H	81	294	N
MAGI-2-6	PM	M	20	34	N	SNTA1-1	PD	H	81	864	N
MAGI-2-6	PM	M	20	554	N	SNTA1-1	PD	H	81	865	N
MAGI-2-6	PM	M	20	6	N	SNTA1-1	PD	H	81	866	N
MAGI-2-6	PM	M	20	514	N	SNTA1-1	PD	H	81	867	N
MAGI-2-6	PM	M	20	445	N	SNTA1-1	PD	H	81	398	N
MAGI-2-6	PM	M	20	54	N	SNTA1-1	PD	H	81	415	N
MAGI-2-6	PM	M	20	560	N	SNTA1-1	PD	H	81	868	N
MAGI-2-6	PM	M	20	561	N	SNTA1-1	PD	H	81	869	N
MAGI-2-6	PM	M	20	65	N	SNTA1-1	PD	H	81	369	N
MAGI-2-6	PM	M	20	7	N	SNTA1-1	PD	H	81	378	N
MAGI-2-6	PM	M	20	446	N	SNTA1-1	PD	H	81	247	N
MAGI-2-6	PM	M	20	449	N	SNTA1-1	PD	H	81	374	N
MAGI-2-6	PM	M	20	25	N	SNTA1-1	PD	H	81	870	N
MAGI-2-6	PM	M	20	19	N	SNTA1-1	PD	H	81	835	N
MAGI-2-6	PM	M	20	13	N	SNTA1-1	PD	H	81	380	N
MAGI-2-6	PM	M	20	22	N	SNTA1-1	PD	H	81	99	N
MAGI-2-6	PM	M	20	562	N	SNTA1-1	PD	H	81	871	N
MAGI-3-1	PM	M	21	563	N						

Table S1.b PDZ Domain sequences (Domain ID, Sequence in FASTA format)

Domain ID	PDZ Domain Sequence
0	GGLGISIKGGRENKMPILISKIFKGLAADQTEALFVGDAILSVNGEDLSSATHDEAVQALKKT GKEVVLEVKYMK
1	GGLGISIKGGKENKMPILISKIFKGLAADQTQALYVGDAILSVNGADLRDATHDEAVQALKR AGKEVLLEVKYMR
2	KGLGFSIAGGVGDQHIPGDNSIYVTKIIDGGAAQKDGRLQVGDRLLMVNNYSLEEVTHEEA VAILKNTSDVVYLKVGKPT
3	TGLGFNIVGGEDGEGIFVSFILAGGPADLSGELQRGDQILSVNGIDLRGASHEQAAAALKGA GQTVTIIAQYQP
4	DALGISIAGGKGSPLGDIPFIAMIQANGVAARTQKLKVGDRIVSINGQPLDGLSHTDAVNLL KNAFGRILLQVVADT
5	QSLGIRIVGYVGT AHPGEASGIYVKSIIIPGSAAYHNGQIQVNDKIVAVDGVNIQGFANQDVV EVLNRNAGQVVHLLVRRK
6	KGLGFSILDYQDPLDPTRSVIVIRSLVADGVAERSGELLPGDRLVSVNEFSLDNATLAEAVEV LKAVPPGVVHLGICKPL
7	SGLGISVGGKDTPLDAIUIHEVYEEGAAARDGRLWAGDQILEVNGVDLRSSSHEEAITALR QTPQKVRLVVYRDE
8	RGLGLSIVGKRSGVVFISDIVKGGAADLDGRLIRGDQILSVNGEDMRHASQETVATILKCV QGLVQLEIGRLR
9	HFLGISIVGQSNDRGDGGIYIGSIMKGGAVAADGRIEPPGDMLLQVNDVNFENMSNDDAVRV

	LREIVSQTGPISLTVAK
10	NFLGISIVGQSNERGDGGIYIGSIMKGGAVAADGRIEPGDMLLQVNEINFENMSNDDAVRVL REIVHKPGPITLTVAKCW
11	PELGFSISGGVGGRGNPFRPDDDGIFVTRVQPEGPASKLLQPGDKIIQANGYSFINIEHGQAVS LLKTFHNAVDLIIVREV
12	GPLGITISGTEEPDPIISSLTKGGLAERTGAIHIGDRILAINSSSLKGGKPLSEAIHLLQMAGETV TLKIKKQT
13	RGLGCSISSGPIQKPGIFVSHVKPGSLSAEVGLTGDQIVEVNGIDFTNLDHKEAVNVLKSSRS LTISIVAGA
14	NGFGLTVSGDNPVQSVKEDGAAMRAGVQTGDRIIKVNGTLVTHSNHLEVVKLIRSGSYV ALTVQGRP
15	EGLGFNIMGGKEQNSPIYISRIIPGGIADRHGGLKRGDQLLSVNGVSVEGEHHEKAVELLKA AQGKVKLVVRYTP
16	PGLGFSISGGISGQGNPFKPSDKGIFVTRVQPDGPASNLLQPGDKILQANGHSFVHMEHEKA VLLLKSFQNTVDLVIQREL
17	KGFGFSLRGGREYNMDLYVLRLAEDGPAERCGKMRIGDEILEINGETTKNMKHSRAIELIKN GGRRVRLFLRRGD
18	MGFGFTIIGGDEPDEFLQVKSVIPDGPAAQDGKMETGDVIVYINEVCVLGHTHADVVKLFQS VPIGQSVNLVLCRGY
19	EGFGFVISSLNRPESGATITVPHKIGRIIDGSPADRCALKVGDRI LAVNGQSIINMPHADIVK LIKDAGLSVTLRIIPQE
20	KGFGFSIRGGREYKMDLYVLRLAEDGPAIRNGRMRVGDQIIEINGESTRDMTHARAIELIKS GGRRVRLLLKRGD
21	MGFGFTIIGGDRPDEFLQVKNVLKDGPAAQDGKIAPGDVIVDINGNCVLGHTHADVVQMFQ LVPVNQYVNLTLCRGY
22	KGFGFAIADSPTGQKVKMILDSQWCQGLQKGDIIKEIYHQNVQNLTHLQVVEVLKQFPVGA DVPLLLIRGG
23	RGFGFSLRGGKEYNMGLFILRLAEDGPAIKDGRIHVGDQIVEINGEPTQGITHTRAIELIQAGG NKVLLLLRPGT
24	EGLGFNIMGGKEQNSPIYISRVIPGGVADRHGGLKRGDQLLSVNGVSVEGEHHEKAVELLK AAQGSVKLVVRYTP
25	EPLGATIKKDEQTGAITVARIMRGGAAADRSLIHVGDDELREVNIPVEDKRPEEIIKILSQSKG AITFKIIPST
26	GGLGFSVVGLRSENREGELGIFVQEIQEGSVAHRDGRLKETDQILAINGQVLDQTITHQQAISI LQKAKDTVQLVIARGS
27	TGLGLSIVGGSDTLLGAIHIEVYEEGAACKDGRLWAGDQILEVNGIDLKATHDEAINVLR QTPQRVRLTYRDE
28	KGLGLSIVGKRNDTG VVSDIVKGGIADADGRLMQGDQILMVNGEDVRHATQEAVAALLK CSLGAVTLEVGRVK
29	DSLGLSIAGGVGSPLGDVPIFIAMMHPNGVAAQTQKLRVGDRIVTICGTSTDGMTHTQAVN LMKNASGSIEVQVVAGG
30	DGLGFSIVGGYGSPPHGLPIYVKT VFAKGAAEDGRLKRGDQIIAVNGQSLEGVTHEEAVAI LKRTKGTVTLMVLS
31	RGLGFSILDYQDPIDPANTVIVIRSLVPGGIAEKDGRLFPGDRLMFVNDINLENSTLEEAVEAL KGAPSGMVRIGVAKPL
32	QYGFNLHSDKSRPGQYIRSVDPGSPASHSGLRAQDRLIEVNGQNVGLRHAEVVARIKAQ EDEARLLVVDPE
33	GGLGFLVKERVSKPPVIISDLIRGGAAEQSGLIQAGDIILAVNDRPLVDLSYDSALEVLRGIAS ETHVVLLIRGP
34	SGLGFNIVGGTDQQYVSNDSGIYVSRIKEDGAAAQDGRLQEGDKILSVNGQDLKNLLHQDA VDLFRNAGCAVSLRVQHRL
35	KPLGFYIRDGSSVRVTPHGLEKVP GIFISRLVPGGLAQSTGLLAVNDEVLEVNGIEVSGKSLD QVTDMMIANSRNLITVRPAN
36	QNYGFFLRIEKD TDGHLIRVIEEGSPA EKAGLLDGDRVLRINGVVFVDKEEHAQVVELVRKSG NSVTLLVLDGD
37	NGYGFYLRAGPEQKQGIKIDIEPGSPA EAGLKNNDLVAVNGKSVEALDHDG VVEMIRKG GDQTLLVLDKE
38	AQLGFNIRGGKASQLGIFISKVIPDS DAHRAGLQEGDQVLAVNDVDFQDIEHSKAVEILKTA REISMRVRRFFP
39	KGLGFSIAGGVGNQHIPGDNSIYVTKIIEGGAAHKDGRLQIGDKILAVNSVGLIEDVMHEDAV

	AALKNTYDVVYLKVAKPS
40	TGLGFNIVGGEDGEGIFISFILAGGPADLSGELRKGDQILSVNGVDLRNASHEQAAIALKNAG QTVTIIAQYKP
41	GSLGISVTGGVNTSVRHGGIYVKAIIPKGAESDGRHKGDRVLA VNGVSLEGATHKQAVET LRNTGQVVHLLLEKGO
42	KGLGFSIAGGIGNQHIPGDNSIYITKIIEGGAAQKDGRLQIGDRLLAVNNTNLQDVRHEEAVA SLKNTSDMVYLKVAKPG
43	TGLGFNIVGGEDGEGIFVSFILAGGPADLSGELRRGDRILSVNGVNLRNATHEQAAAALKRA GQSVTIVAQYRP
44	SGLGFSIAGGTDNPHIGDDSSIFITKIITGGAAAQDGRLRVNDCILRVNEADV RDVTHSKAVE ALKEAGSIVRLYVKRRK
45	KGLGFSIAGGVGNQHIPGDNSIYVTKIIEGGAAHKDGKLGKQIGDKLLAVNSVCLEEVTHEEAV TALKNTSDFVYLKVAKPT
46	GGLGFSIAGGKGSTPYKGDDEGIFISRVSEEGPAARAGVRVGDKLELVNGVALQDAEHHEA VEALRGAGAAVQMRVWRER
47	KGLGFSIAGGKGSTPYRAGDGGIFISRIAEGGAAHRAGTLQVGDRVLSINGVDMTEARHDH AVSLLTAASPTISLLERET
48	GPLGLSIVGGSDHSSHPFGVQDPGVFISKVLPRGLAARCGLRVGDRILAVNGQDVREATHQE AVSALLRPCLELCLLVRRDP
49	GSLGFNIIGRPCVDNQGDSSEGIFVSKIVDSGPAAKEGGLQIHDRIIEVNGKDLSTRATHDQ AVEAFKTAKEPIVVQVLRRT
50	EGFGFVLRGAKAQTPIEEFTPTPAFPALQYLESVDEGGVAWRAGLRMGDFLIEVNGQNVVK VGHRQVVNMIRQGGNTLMVKVVMVTRHPD
51	EGFGFVLRGAKAETPIEFTPTPAFPALQYLESVDVEGVAWRAGLRTGDFLIEVNGVNVVK VGHKQVVGLIRQGGNRLVMKVVSVT
52	APWGF TLKGLERGEPLIISKIEGGKADS VSSGLQAGDEVIHINEVALSSPREAVSLVKGS YKTLRLVVRDV
53	APWGFRISSGRDFHTPIIVTKVTERGKAEAADLRPGDIIVAINGQSAENMLHAEAQSKIRQSA SPLRLQLDRSQ
54	FGFGIAISSGRDNPHFQSGETSIVISDVLKGGPAEGQLQENDRVAMVNGVSMDNVEHAFV QQLRKSGKNAKITIRKK
55	RGFGIAVSSGRDNPHFENGETSIVISDVLPGGPADGLLQENDRVVMVNGTPMEDVLHSFAV QQLRKSGKIAAIVVKRPR
56	RGFGIAVSSGHDRAAGSVVSDVVPGGPAEGLRRTGDHIVMVNGVSVENVTSAFAIQILKT CTKTANVTVKRPR
57	LVQFQKNTDEPMGITLKMNELNHCIVARIMHGGMIHRQGT LHVGD EIREINGISVANQTVEQ LQKMLREMRGSITFKI
58	EVNLLKGP KGLGFSIAGGIGNQHIPGDNSIYITKIIEGGAAQKDGRLQIGDRLLAVNNTNLQD VRHEEAVASLKNTSDMVYLKV
59	RVRVEKDP ELGFSISGGVGGRGNPFRPDDDGIFVTRVQPEGPASKLLQPGDKIIQANGYSFINI EHGQAVSLLKTFQNTVELII
60	VFELLKPPSGGLGFSVVGRLSENREGELGIFVQEIQEGSVAHRDGR LKETDQILAINGQALDQT ITHQQAISILQKAKDTVQLVI
61	TIEISKGR TGLGLSIVGGSDTLGAIHIEVYEEGAACKDGRLWAGDQILEVNGIDLKATHD EAINVLRQTPQRVRLTL
62	TVEMKKGPTDSLGISIAGGVGSPLGDVPIFIAMMHPTGVAAQTQKLRVGDRIVTICGTSTEG MTHTQAVNLLKNASGSIEMQV
63	TLTILRQTGGLGISIAGGKGSTPYKGDDEGIFISRVSEEGPAARAGVRVGDKLELVNGVALQ GAEHHEAVEALRGAGTAVQMRV
64	EIKLIKGP KGLGFSIAGGVGNQHIPGDNSIYVTKIIEGGAAHKDGKLGKQIGDKLLAVNNVCLEE VTHEEAVTALKNTSDFVYLKV
65	RIVIHGSTGLGFNIVGGEDGEGIFISFILAGGPADLSGELRKGDQILSVNGVDLRNASHEQAA IALKNAGQTVTIIA
66	VACLARSERGLGFSIAGGKGSTPYRAGDAGIFVSRIAEGGAAHRAGTLQVGDRVLSINGVD VTEARHDHAVSLLTAASPTIALLL
67	EVELINDG SGLGFGIVGGKTSGVVVRTIVPGLADRDRGRLQTDHILKIGGTNVQGMTSEQV AQVLRNCGNSVRMLV
68	KVVLRHGSTGLGFNIVGGEDGEGIFISFILAGGPADLSGELRKGDRIISVNSVDLRAASHEQA AAALKNAGQAVTIVA
69	EITLERGNSGLGFSIAGGTDNPHIGDDSSIFITKIITGGAAAQDGRLRVNDCILRVNEVDVRDV

	THSKAVEALKEAGSIVRLYV
70	CVRIEKNPGLGFSISGGISGQGNPFKPSDKGIFVTRVQPDGPASNLLQPGDKILQANGHSFVH MEHEKAVLLKSFQNTVDLVI
71	ILGIHKRAGEPLGVTRVENNDLVIARILHGGMIDRQGLLHVGDIIKEVNGHEVGNPKELQ ELLKNISGSVTLKI
72	ECKLSKQEGQNYGFFLRIEKDTEGHLVVRVVEKCSPAEKAGLQDGRVLRINGVFVDKEEHM QVVDLVRKSGNSVTLLV
73	DVEIRGENEGFGFVIVSSVSREAGTTFAGNACVAMPHKIGRIIEGSPADRCGKLVGDRIL AVNGCSITNKSHSDIVNLIKEAGNTVTLRI
74	DVFLRKQESGFGFRVLGGDGPQSIYIGAIHPLGAAEKDGRRLRAADELMCIDGIPVKGKSHK QVLDLMTTAARNGHVLLTV
75	LVTVEKQDNETFGFEIQSYRPNQACSEMFTLICKIQEDSPAHCAGLQAGDVLANINGVS TEGFTYKQVVDLIRSSGNLLTIET
76	TVTLNMEKYNFLGISIVGQSNERGDGGIYIGSIMKGGAVAADGRIEPPGDMLLQVNDMNFEN MSNDDAVRVLRDIVHKPGPIVLTV
77	KVVLHKGSTGLGFNIVGGEDGEGIFVSFILAGGPADLSGELQRGDQILSVNGIDLRGASHEQ AAAALKGAGQTVTIIA
78	DVELTKNVQGLGITIAGYIGDKKLEPSGIFVKSITKSSAVEHDGRIQIGDQIIAVDGTNLQGF NQQAVEVLRHTGQTVLLTL
79	SVTLRGPSPWGFRLVGGRRDFSAPLTISR VHAGSKAALAALCPGDLIQAINGESTELMTHLEA QNRKIGCHDHLTSLV
80	LCHLRKGPQGYGFNLHSDKSRPGQYIRSVDPGSPAARSLRAQDRLIEVNGQNVEGLRHA E VVASIKAREDEARLLV
81	RVTVRKADAGGLGISIKGGRENKMPILISKIFKGLAADQTEALFVGDAILSVNGEDLSSATHD EAVQVLKKTGKEVVLEV

Table S1.c Peptide sequences (Peptide ID, Peptide sequence in FASTA format)

Peptide ID	Peptide Sequence	Peptide ID	Peptide Sequence	Peptide ID	Peptide Sequence
0	KETAL	301	KNTSV	602	CTSLM
1	KQTSV	302	RQTSL	603	YCQFF
2	RETTV	303	RTTRV	604	NVVFT
3	RETDL	304	WETDV	605	YDILR
4	RESIV	305	WETMV	606	IKGLF
5	LESEV	306	FETLV	607	YEAVL
6	GETTV	307	YETLV	608	YVGDL
7	DETSI	308	RETWV	609	CCTCV
8	LETSL	309	WSTDV	610	YYMYF
9	IETHV	310	GDTWV	611	SWTTC
10	DETNL	311	FETWI	612	FIHYM
11	VETDV	312	VETWV	613	CTTPA
12	SETQV	313	LESWL	614	DHSVV
13	QETRL	314	RETWL	615	FCKYE
14	PETSV	315	PETWV	616	YFSWQ
15	KESLV	316	ESDWL	617	KFVYL
16	RESEI	317	LETWI	618	FCVEP
17	IESDV	318	WETWV	619	KDSAW
18	IFTDV	319	VETWL	620	IVVEF
19	LESMV	320	KEWFL	621	MTSHN

20	MVTEV	321	VEYFL	622	LMTEC
21	RTPPV	322	HEWFL	623	NDLEL
22	MLTEV	323	DEYFL	624	IIGRC
23	LQSAV	324	REYYL	625	FSSFV
24	KESSI	325	REYWL	626	ARSSL
25	RISSV	326	REWFL	627	KIDNC
26	IIAWV	327	REYFL	628	LERLI
27	FLTWL	328	QEYFL	629	FNVML
28	KEWLI	329	LEYFL	630	RQGEL
29	TGIQV	330	QEWFL	631	CKGWK
30	KEYFF	331	KEWFI	632	WEPEP
31	KEYFI	332	IEYFL	633	ITIYS
32	KEYYV	333	REWFI	634	WWTSN
33	LVSIC	334	GEWFL	635	IIDAI
34	RISNV	335	WETYL	636	PISSW
35	KVDSV	336	WSTWL	637	YVKEI
36	KISSL	337	RSTLL	638	LPSIL
37	QSVEV	338	SSTYL	639	MESQM
38	LGAYV	339	YSTFL	640	FAIFE
39	HWFDV	340	YSSWL	641	FVIQY
40	GSVEV	341	FSTWL	642	LDVCN
41	KSQYV	342	YSTRM	643	QEGWA
42	LPVQV	343	FSTYL	644	LSTRW
43	RKDYV	344	WSTFL	645	TIWIQ
44	GHFNF	345	WSSRM	646	HENYW
45	LNDYV	346	KSTRL	647	NLTTK
46	KESSL	347	KQTWL	648	SVHTV
47	EESSV	348	WSTYL	649	EEFYA
48	EDSDV	349	HQTWL	650	RTYSC
49	CSDSL	350	FSSRL	651	NLVAD
50	VDTRV	351	WSTLL	652	HWMSP
51	STTRV	352	KSTFL	653	RIFSS
52	GDTSL	353	FSTWM	654	QVTEE
53	GAAAV	354	FETFL	655	AATTF
54	LLTDV	355	FETLL	656	NVEEG
55	YVSNL	356	RSTYL	657	WSSYP
56	RVSAL	357	FSTRL	658	RFLWE
57	RDSVV	358	LSTWL	659	HSFRH
58	VTTRL	359	YSSRL	660	SPCLL
59	EDSFL	360	RGTWL	661	MGTWG
60	NESKV	361	LSTYL	662	CAKCL
61	HGTSI	362	ESTWL	663	DADYL
62	QQSNV	363	HSTFL	664	FYPRN
63	RGTSI	364	KSTWL	665	TDIYF
64	AQTRL	365	WWLDV	666	FEGGD
65	IQTQI	366	WWMDV	667	ISVGN

66	DHTRL	367	WFLDV	668	DDAPL
67	NATRL	368	WWYDA	669	EESRR
68	LPTRL	369	TYSDW	670	ESDGV
69	KETVA	370	WFIDV	671	TELRI
70	SSSTL	371	RVADA	672	SQTVT
71	GATGL	372	WFFDA	673	PAKLR
72	TTSSL	373	WWFDA	674	TCSNK
73	AREYV	374	WfyDA	675	YVWRF
74	KYDYV	375	WYLDV	676	QSSWR
75	KKNYV	376	WWFDV	677	KDYRS
76	ASNYV	377	WSFWI	678	TGSFP
77	SKEYV	378	TSGWF	679	GGPRT
78	GKDYV	379	HSFWV	680	NVSVC
79	KRDYV	380	LDFWF	681	LSGTV
80	KSAHV	381	SSGWF	682	YSEYC
81	TKNYV	382	FKLWF	683	HHKGC
82	LTGYV	383	LLGFF	684	VWPSD
83	KNAYV	384	LLGIF	685	ANNIK
84	TFFDV	385	YFGGL	686	HGPYL
85	RFFDV	386	FFGFF	687	AIVAA
86	VFFDV	387	LETRV	688	FHMHG
87	RYFDI	388	LCTRV	689	ALNTV
88	QFFDV	389	WTLRV	690	ADVIK
89	KYFDV	390	KVTSI	691	FVPWP
90	SFFDV	391	KCTRV	692	FCAIL
91	LYFDV	392	NETSV	693	PCMWL
92	RYFDV	393	KVTRV	694	TKACF
93	FYFDV	394	MTTRV	695	CIWEF
94	IFFDV	395	LETSV	696	NYDEY
95	TYFDV	396	WTFL	697	CHTDT
96	FFFDV	397	FSYYL	698	KLNVK
97	QFFNV	398	ILGIF	699	KMRSV
98	MYFDV	399	LFFRL	700	LSHSV
99	HFFDV	400	FYFYL	701	ENTDQ
100	VYFDV	401	TLFHL	702	NYPDV
101	WFFDV	402	IYFYL	703	SDCGV
102	TWFDV	403	FLGLF	704	GEFTV
103	VYFYV	404	FSFFF	705	KERDR
104	RQTDV	405	WDFHL	706	ICLLV
105	RWTTV	406	TLGHF	707	YCCFV
106	KSTTV	407	NFWRI	708	QARRV
107	TSTDV	408	ESPGL	709	FAHDH
108	RETRV	409	ESAWL	710	FEERK
109	KWSDV	410	ESPWL	711	RTREV
110	IWTDV	411	ESPWM	712	PKTRV
111	YSTDV	412	ETDWL	713	DGAHV

112	IWSDV	413	ESEWL	714	GAHWG
113	RMTDV	414	ESGWL	715	FYWHL
114	FWSDV	415	ESDWM	716	CDFWI
115	KETRV	416	EPPWL	717	FRYVV
116	RETDV	417	CDTKF	718	DKRAV
117	KETLV	418	FDTRF	719	RQSML
118	KNTWV	419	GSSWL	720	KFSRS
119	VWTDV	420	CSTFL	721	SASRW
120	RWTSV	421	GSTYF	722	PVPLV
121	RSTIV	422	FDTRL	723	LKPEV
122	KWTDV	423	CDTYL	724	SETRF
123	RETVV	424	FTTWL	725	HGNIV
124	RETLV	425	LDTYL	726	YNYQV
125	KSTVV	426	WSSWL	727	CGTPE
126	TWTDV	427	CTTRL	728	TWTQD
127	RHTDV	428	NNTWF	729	SGGLV
128	RSTVV	429	RETEL	730	RSEKV
129	KSTDV	430	RDTRP	731	KGENV
130	RETQV	431	RETRS	732	RGSPW
131	THTLV	432	RSTRL	733	KVSCV
132	FDSWV	433	RSTSL	734	IWCMV
133	TDTWV	434	KCDEV	735	VRTWS
134	NDTWV	435	TKSEV	736	CFTSH
135	FETWV	436	GDEPV	737	VEK GK
136	RDTWV	437	AEEDF	738	RMIQV
137	FETWL	438	GGTVV	739	KMIPG
138	FDDWV	439	EEGEE	740	ECTPT
139	YDTWV	440	QRTWP	741	AEDCI
140	MDTWV	441	QEPAL	742	TEKRR
141	FQTWV	442	KEPTF	743	PEHLI
142	RDSWV	443	FWHED	744	GDPIV
143	IDTWV	444	TIIFL	745	QEVNA
144	WDTFV	445	VLSSV	746	RARMF
145	SDTWV	446	KVELV	747	VEMPT
146	WDSWV	447	GQYWV	748	QPIWQ
147	LATWV	448	KAMAI	749	ESVWA
148	YDDWV	449	TSDQL	750	NLEEV
149	WDTWV	450	LFQPQ	751	TNIQF
150	ADTWV	451	AKHYI	752	CFWWG
151	FDTWL	452	IPKGQ	753	QFIGV
152	LETWL	453	NRFWA	754	SCIMV
153	YDEWV	454	APRSV	755	ALTED
154	VDTWV	455	AGILQ	756	SGTFQ
155	HDSWV	456	RVGQF	757	PNISI
156	LDTWV	457	PERSK	758	ASTMH
157	FESWV	458	VGLWW	759	PATAR

158	DDTWV	459	FCLPC	760	RQFSH
159	PDTWV	460	MPKRV	761	VESWQ
160	LDEWV	461	GIQCD	762	KKTCL
161	IETWL	462	TERNG	763	VWIAV
162	YDTFV	463	VTDLS	764	LPTVG
163	FDTWV	464	PAVAE	765	KMTVE
164	FHTWV	465	QEDGA	766	LATRH
165	NSFWV	466	APPVP	767	APTLP
166	FLLWL	467	VLRCE	768	WWLGV
167	FILWL	468	RESKC	769	IALWA
168	RSTWV	469	RGMSI	770	IKDWW
169	FRLWL	470	RDQSI	771	LDDHQ
170	FRLFL	471	PAILE	772	KITWW
171	FLGWV	472	LVTSV	773	FPSWG
172	FRFWV	473	EFIGA	774	MVSWK
173	RSFWV	474	TAEMF	775	MEVWT
174	FTWWL	475	ANVHA	776	TEINV
175	TSFWV	476	ANPEI	777	MANWD
176	FLGKV	477	QFGIP	778	VEDHA
177	ILGWV	478	KATNE	779	IEQHY
178	RRSRV	479	NNVTQ	780	VAIWL
179	RVSDV	480	KVWTC	781	EELAK
180	RISDV	481	TIAAN	782	FEKWW
181	RRSDV	482	ITDVK	783	LYIFL
182	RITRV	483	GGEPL	784	SEKIM
183	RKSDV	484	KVSQL	785	QEFWS
184	RISRV	485	DRIRV	786	NEAGD
185	KRSDV	486	SEPPV	787	CEQCC
186	RCSRV	487	AFTDG	788	TEVGN
187	KISDV	488	ESRSE	789	YQRRM
188	RCSDV	489	WWGIH	790	YAVEL
189	RITDV	490	QDHWC	791	TGLQL
190	RVSRV	491	LPSHP	792	EGARL
191	RQSDV	492	SRSFR	793	NSSNC
192	RHSDV	493	SEdle	794	WMVAL
193	KISRV	494	KEEHQ	795	ISTPV
194	WWTDV	495	SSITI	796	WSRWE
195	FSTWV	496	FQKFS	797	YSQRY
196	FWTWV	497	HDAII	798	DPLDT
197	WHTWV	498	CAGFP	799	CSIEA
198	WWTWV	499	WEYQI	800	YVCDL
199	WATWV	500	YDDFT	801	GWFQA
200	MGTWV	501	LILIG	802	QHTNV
201	WFTWV	502	NYQFC	803	RRIPQ
202	WSTWV	503	KQTAL	804	ELPDE
203	FGTWV	504	PAIEV	805	WSFPL

204	WYTWV	505	MYDHL	806	HYSQI
205	RETRL	506	RWKFC	807	STLPV
206	LETDL	507	VQLEA	808	GSDDH
207	RETSM	508	GPVPV	809	HSGAV
208	RETSL	509	LYIYC	810	VKPDD
209	FETDL	510	FTLFK	811	VSTQY
210	METHL	511	MVSRA	812	RSCLK
211	CETSL	512	VITSH	813	VSCKA
212	CETDL	513	PHSSC	814	IVTWR
213	YETDL	514	IYYKV	815	YHCWR
214	KETHL	515	DSQTT	816	YDRKV
215	FETRL	516	KAVPV	817	RETPD
216	RETDI	517	RMVPV	818	YMIWS
217	SETDL	518	RRSSV	819	RLNPF
218	FETHL	519	DLSVV	820	ADKSV
219	RETHL	520	SSFLV	821	RLLNV
220	HETDL	521	KGFHV	822	AESPG
221	RETSI	522	KEFYA	823	CEKDD
222	NETHL	523	PFYSV	824	MNCMF
223	FETSL	524	IHQNS	825	PEQQS
224	SETFL	525	PNGLQ	826	PPKGT
225	LETHL	526	MWPLM	827	LHGAA
226	NETDL	527	PFSFY	828	RLDFH
227	LETNL	528	RTISD	829	NEILS
228	QWTDV	529	ATTMH	830	QSQVV
229	RQTLV	530	FVRLI	831	FLRDM
230	RQTWV	531	LSMFR	832	KLRCK
231	RQSWV	532	AIFHD	833	RLSRY
232	KETAV	533	VTSQL	834	CSRTV
233	KHTEV	534	ESVKI	835	NLTNA
234	KSTIV	535	IDVDD	836	KTERY
235	KHTWV	536	GCTSW	837	LECSN
236	RETLI	537	FVTMQ	838	TDLSI
237	RQTRV	538	QNVFI	839	EYRNV
238	YETWV	539	EIDRT	840	ILSTT
239	RSTDV	540	FAWRL	841	VIFGN
240	RSTFV	541	LDRIV	842	PDRQR
241	KETSV	542	FDRGK	843	ASVLI
242	YNTWV	543	SVKIF	844	DLTGI
243	HETLV	544	SESKV	845	FQQHT
244	RSTLV	545	TKGES	846	PNYLF
245	KHTQV	546	TAEAA	847	TTIAH
246	RNTWV	547	GAEVA	848	CRTIL
247	KTSWV	548	VHEDA	849	SRHWI
248	RNTYV	549	ETGST	850	QSTGG
249	RETIV	550	APRSA	851	EFKHL

250	RETLI	551	ADSKQ	852	EEGIQ
251	RWTDV	552	LTEHE	853	EHPSD
252	KTTLV	553	ASKTD	854	TSSLR
253	RTTWV	554	CPSES	855	AQHVL
254	VWSDV	555	MLTDV	856	EARTL
255	HETWV	556	VGIPI	857	PPDEL
256	RSSDV	557	HPPDT	858	GVNIL
257	RHTIV	558	NPRGT	859	LHVCL
258	FETRV	559	IFGAS	860	EKTES
259	RWTLL	560	VTTDC	861	WITRC
260	YSTWV	561	LKTDC	862	GPLGL
261	RETSV	562	ISAEV	863	MSTNM
262	RDTPV	563	FSPRC	864	RNRPY
263	IHTWV	564	HKQVV	865	VEYRY
264	RTTDV	565	PYFLF	866	RPHPV
265	RNIWV	566	QSTFN	867	RLQDQ
266	RWTTL	567	YGTTP	868	RELVV
267	RNTLV	568	TTLWY	869	GFTLE
268	IETLV	569	FSDVL	870	LSKRL
269	KQTRV	570	VKRYF	871	PEWDL
270	RETRI	571	IAGVV		
271	KSTRV	572	EDTDT		
272	SETRV	573	KGFYV		
273	KTTRV	574	RTTLV		
274	RHTSV	575	IEKLM		
275	KTTRI	576	HLSVL		
276	KSTSV	577	EIAYK		
277	RSTRV	578	PIDFS		
278	LETPL	579	PIPAP		
279	SETRL	580	CSTYR		
280	HDTWV	581	LCCIF		
281	LETWV	582	REWLF		
282	LETDV	583	FHIRI		
283	KDTWV	584	PMTTS		
284	IETWV	585	GNTIK		
285	DETWV	586	SENEL		
286	PIYWV	587	LMVRV		
287	VEYFF	588	DSSNC		
288	REYFF	589	SWIWM		
289	TEWV	590	PSWYF		
290	REWV	591	NEVPR		
291	HEWV	592	NKQHF		
292	KIFWV	593	CSCFL		
293	RIWV	594	TTGAP		
294	EIWV	595	FVGNI		
295	RIFWV	596	NAYYE		

296	TEWFF	597	DDKFF
297	RSTSV	598	NQGQG
298	KQTSL	599	NTMGC
299	YETSV	600	GMVPV
300	RESSV	601	LFCNL

Table S2 Class data of PDZ domains (PDZ domain name, Organism(M = mouse, H = human), Class Label(Class I,Class II or Class I-II))

PDZ domain name	Organism	Class Label
A1-SYNTROPHIN-1	M	Class I
CHAPSYN-110-2	M	Class I-II
CHAPSYN-110-3	M	Class I-II
CIPP-10	M	Class II
CIPP-3	M	Class II
CIPP-5	M	Class II
CIPP-8	M	Class II
CIPP-9	M	Class I-II
DVL1-1	M	Class II
DVL3-1	M	Class II
ERBIN-1	M	Class II
GRIP1-6	M	Class II
HARMONIN-2	M	Class II
LARG-1	M	Class I
LIN-7C-1	M	Class I
LRRC7-1	M	Class I
MAGI-1-6	M	Class II
MAGI-2-6	M	Class II
MAGI-3-1	M	Class II
MAGI-3-2	M	Class II
MAGI-3-5	M	Class II
MALS2-1	M	Class I
MUPP1-1	M	Class II
MUPP1-10	M	Class II
MUPP1-11	M	Class II
MUPP1-12	M	Class II
MUPP1-13	M	Class II
MUPP1-5	M	Class II
NHERF-2-2	M	Class I-II
NNOS-1	M	Class II

OMP25-1	M	Class I-II
PSD95-2	M	Class I-II
PSD95-3	M	Class I-II
PTP-BL-2	M	Class II
SAP102-2	M	Class I
SAP102-3	M	Class I
SAP97-1	M	Class I-II
SAP97-2	M	Class I-II
SAP97-3	M	Class I-II
ZO-1-1	M	Class I
ZO-2-1	M	Class I-II
ZO-3-1	M	Class II
CASK-1	H	Class II
DLG3-2	H	Class I-II
ERBB2IP-1	H	Class I-II
MPDZ-1	H	Class I-II
MPDZ-10	H	Class I-II
MPDZ-12	H	Class I-II
SCRIB-1	H	Class I-II
DLG1-2	H	Class II
DLG4-3	H	Class I-II
SCRIB-2	H	Class I-II
INADL-2	H	Class II
DLG1-3	H	Class I-II
DLG1-1	H	Class I-II
LRRC7-1	H	Class I-II
MPP6-1	H	Class I-II
PDZK1-1	H	Class I
MAGI1-5	H	Class II
MAGI3-5	H	Class I
PSCDBP-1	H	Class I-II
DVL2-1	H	Class II
DLG2-3	H	Class I
MPDZ-3	H	Class I-II
PDLIM4-1	H	Class I
SLC9A3R2-2	H	Class I-II
SNTA1-1	H	Class I-II

Table S3 Data table of 218 PDZ Domains used to scan human proteome(In total, 61 X-ray and nine NMR structures were retrieved from the PDB and 148 homology models were created by SWISS-MODEL. Model quality is estimated using template sequence ID (percentage of the identical residues between target and template sequences) and QMEAN score (a scoring function that measures multiple geometrical aspects of protein structure, ranging from 0 to 1 with higher values indicating more reliable models))

Uniprot	Uniprot Id	Start Index	End Index	Experiment	PDB ID	Template PDB ID	Template Seq ID	QMEAN Score
AHNAK2-1	Q8IVF2	122	195	SWISS-MODEL		3SHW A	0,39	0,603
APBA1-1	Q02410	660	741	SWISS-MODEL		1U3B A	1,00	0,810
APBA1-2	Q02410	755	821	SWISS-MODEL		1U3B A	1,00	0,581
APBA2-1	Q99767	571	653	SWISS-MODEL		1U3B A	0,85	0,792
APBA2-2	Q99767	666	733	SWISS-MODEL		1U3B A	0,93	0,514
APBA3-1	O96018	396	479	SWISS-MODEL		2YT7 A	1,00	0,806
APBA3-2	O96018	491	559	XRAY	2YT8			
ARHGAP2 1-1	Q5T5U3	49	159	NMR	2YUY			
ARHGAP2 3-1	Q9P227	52	156	SWISS-MODEL		2YUY A	0,81	0,609
ARHGEF1 1-1	O15085	51	118	SWISS-MODEL		2DLS A	1,00	0,921
ARHGEF1 2-1	Q9NZN5	77	147	SWISS-MODEL		2OMJ A	1,00	0,847
CAR14-1	Q9BXL6	570	659	SWISS-MODEL		1Z87 A	0,30	0,442
CASK-1	O14936	489	573	XRAY	1KWA			
CNKR1-1	Q969H4	198	286	SWISS-MODEL		2DKR A	0,22	0,458
CNKS2-1	Q8WXI2	225	293	SWISS-MODEL		2E7K A	0,29	0,643
CNKS3-1	Q6P9H4	219	288	SWISS-MODEL		2E7K A	0,29	0,688
CYTIP-1	O60759	76	163	XRAY	2Z17			
DEPTOR-1	Q8TB45	330	408	SWISS-MODEL		2D90 A	0,31	0,879
DLG1-1	Q12959	221	312	SWISS-MODEL		1ZOK A	0,99	0,603
DLG1-2	Q12959	316	406	XRAY	2G2L			
DLG1-3	Q12959	463	544	SWISS-MODEL		1PDR A	1,00	0,938
DLG2-1	Q15700	100	183	SWISS-MODEL		2WL7 A	0,98	0,997
DLG2-2	Q15700	196	278	SWISS-MODEL		2BYG A	1,00	0,953
DLG2-3	Q15700	418	518	XRAY	2HE2			
DLG3-1	Q92796	134	216	XRAY	2I1N			
DLG3-2	Q92796	223	315	XRAY	2FE5			

DLG3-3	Q92796	389	464	XRAY	1UM7			
DLG4-1	P78352	67	151	SWISS-MODEL		3GSL B	1,00	0,966
DLG4-2	P78352	163	245	SWISS-MODEL		3GSL A	1,00	0,991
DLG4-3	P78352	301	416	XRAY	1TP3			
DLG5-3	Q8TDM6	1353	1426	XRAY	1UIT			
DLG5-4	Q8TDM6	1509	1580	SWISS-MODEL		2QG1 A	0,32	0,594
DVL1-1	O14640	254	337	SWISS-MODEL		1MC7 A	1,00	0,624
DVL1L1-1	P54792	260	340	SWISS-MODEL		2KAW A	0,99	0,629
DVL2-1	O14641	270	353	XRAY	2REY			
DVL3-1	Q92997	252	335	SWISS-MODEL		1L6O A	0,96	0,977
ERBB2IP-1	Q96RT1	1321	1413	XRAY	1MFL			
FRMPD1-1	Q5SYB0	67	133	SWISS-MODEL		2FNE C	0,33	0,791
FRMPD2-2	Q68DX3	950	1036	SWISS-MODEL		1VJ6 A	0,61	0,910
FRMPD2-3	Q68DX3	1080	1168	SWISS-MODEL		1B8Q A	0,38	0,518
FRMPD3-1	Q5JV73	62	132	SWISS-MODEL		1WHD A	0,34	0,819
FRMPD4-1	Q14CM0	79	156	SWISS-MODEL		2EDV A	0,36	0,837
GIPC1-1	O14908	136	211	SWISS-MODEL		3GGE A	0,65	0,852
GIPC2-1	Q8TF65	125	200	XRAY	3GGE			
GIPC3-1	Q8TF64	120	195	SWISS-MODEL		3GGE A	0,63	0,698
GOPC-1	Q9HD26	293	369	XRAY	2DC2			
GORASP2-1	Q9H8Y8	5	76	SWISS-MODEL		3RLE A	1,00	0,857
GRD2I-1	A4D2P6	10	85	SWISS-MODEL		2EDV A	0,36	0,509
GRD2I-2	A4D2P6	279	357	SWISS-MODEL		2KV8 A	0,36	0,686
GRIP1-1	Q9Y3R0	56	135	SWISS-MODEL		2QT5 A	1,00	0,866
GRIP1-2	Q9Y3R0	154	237	XRAY	2JIL			
GRIP1-3	Q9Y3R0	261	335	SWISS-MODEL		1V62 A	0,64	0,804
GRIP1-4	Q9Y3R0	472	562	SWISS-MODEL		1P1D A	0,99	0,624
GRIP1-5	Q9Y3R0	577	657	SWISS-MODEL		1P1D A	0,98	0,804
GRIP1-6	Q9Y3R0	676	753	SWISS-MODEL		1N7E A	1,00	0,953
GRIP1-7	Q9Y3R0	1008	1084	SWISS-MODEL		1M5Z A	0,99	0,902
GRIP2-1	Q9C0E4	52	130	SWISS-MODEL		2QT5 A	0,79	0,889
GRIP2-2	Q9C0E4	151	227	SWISS-MODEL		2QT5 A	0,70	0,962

GRIP2-3	Q9C0E4	254	331	XRAY	1V62			
GRIP2-4	Q9C0E4	466	543	SWISS-MODEL		1X5R A	1,00	0,766
GRIP2-5	Q9C0E4	561	640	SWISS-MODEL		1P1D A	0,88	0,704
GRIP2-6	Q9C0E4	659	736	SWISS-MODEL		1N7E A	0,90	1,000
GRIP2-7	Q9C0E4	944	1021	SWISS-MODEL		1M5Z A	0,70	
HTRA1-1	Q92743	370	468	NMR	2YTW			
HTRA2-1	O43464	359	442	SWISS-MODEL		2PZD B	1,00	0,838
HTRA3-1	P83110	350	441	XRAY	2P3W			
IL16-1	Q14005	221	301	SWISS-MODEL		2ENO A	0,49	0,778
IL16-3	Q14005	111	1189	SWISS-MODEL		1X6D A	1,00	0,866
INADL-1	Q8NI35	138	219	SWISS-MODEL		2DB5 A	1,00	0,792
INADL-2	Q8NI35	231	342	NMR	2DLU			
INADL-3	Q8NI35	369	451	SWISS-MODEL		2DMZ A	0,99	0,845
INADL-5	Q8NI35	692	769	XRAY	2D92			
INADL-6	Q8NI35	107	1155	XRAY	2EHR			
INADL-7	Q8NI35	124	1319	XRAY	2DAZ			
INADL-8	Q8NI35	144	1518	XRAY	2DM8			
INADL-9	Q8NI35	153	1613	SWISS-MODEL		2QG1 A	0,75	1,000
INADL-10	Q8NI35	168	1760	SWISS-MODEL		2IWP B	0,66	0,973
LDB3-1	O75112	11	83	XRAY	1RGW			
LIMK1-1	P53667	168	256	SWISS-MODEL		2YUB A	0,40	0,583
LIMK2-1	P53671	155	238	SWISS-MODEL		2YUB A	0,95	0,622
LIN7A-1	O14910	111	188	SWISS-MODEL		2DKR A	0,92	0,793
LIN7B-1	Q9HAP6	96	172	XRAY	2DKR			
LIN7C-1	Q9NUP9	96	173	SWISS-MODEL		2DKR A	0,94	0,827
LMO7-1	Q8WWI	104	1129	XRAY	2EAQ			
LRRC7-1	Q96NW7	145	1535	SWISS-MODEL		2H3L B	0,75	0,856
MAGI1-2	Q96QZ7	478	544	XRAY	2KPK			
MAGI1-3	Q96QZ7	646	722	SWISS-MODEL		3BPU A	0,95	0,756
MAGI1-4	Q96QZ7	849	923	SWISS-MODEL		2Q9V A	0,97	0,949
MAGI1-5	Q96QZ7	100	1092	SWISS-MODEL		1UEW A	0,67	0,752
MAGI1-6	Q96QZ7	115	1230	SWISS-MODEL		2R4H A	0,96	0,901
MAGI2-1	Q86UL8	26	98	SWISS-MODEL		2HE4 A	0,35	0,535

MAGI2-2	Q86UL8	429	497	XRAY	1UEQ			
MAGI2-3	Q86UL8	605	684	SWISS-MODEL		1UJV A	1,00	0,824
MAGI2-4	Q86UL8	783	860	XRAY	1UEW			
MAGI2-5	Q86UL8	923	1008	SWISS-MODEL		1UEW A	1,00	0,708
MAGI2-6	Q86UL8	115	1227	XRAY	1WFV			
		0						
MAGI3-2	Q5TCQ9	440	504	SWISS-MODEL		1UEQ A	0,74	0,725
MAGI3-3	Q5TCQ9	603	680	SWISS-MODEL		3SOE A	1,00	0,924
MAGI3-4	Q5TCQ9	757	833	SWISS-MODEL		1UEP A	0,63	0,750
MAGI3-5	Q5TCQ9	879	961	SWISS-MODEL		1UEW A	0,63	0,754
MAGI3-6	Q5TCQ9	104	1126	SWISS-MODEL		1WFV A	0,65	1,000
		9						
MAST1-1	Q9Y2H9	974	1052	XRAY	3PS4			
MAST2-1	Q6P0Q8	110	1193	SWISS-MODEL		2KQF A	1,00	0,710
		4						
MAST3-1	O60307	950	1039	SWISS-MODEL		3KHF B	1,00	0,875
MLLT4-1	P55196	101	1091	SWISS-MODEL		1XZ9 A	1,00	0,530
		4						
MPDZ-1	O75970	136	228	SWISS-MODEL		2O2T A	0,98	0,855
MPDZ-2	O75970	258	334	SWISS-MODEL		2DLU A	0,68	0,758
MPDZ-3	O75970	373	464	SWISS-MODEL		2IWN A	0,95	0,955
MPDZ-4	O75970	562	630	SWISS-MODEL		2DAZ A	0,38	0,850
MPDZ-5	O75970	703	784	SWISS-MODEL		2D92 A	0,63	0,836
MPDZ-6	O75970	101	1077	SWISS-MODEL		3B76 B	0,39	0,601
		1						
MPDZ-7	O75970	115	1240	XRAY	2IWQ			
		1						
MPDZ-8	O75970	135	1429	SWISS-MODEL		2DAZ A	0,76	0,785
		3						
MPDZ-9	O75970	148	1562	SWISS-MODEL		2DKR A	0,39	0,732
		7						
MPDZ-10	O75970	162	1717	XRAY	2OPG			
		3						
MPDZ-11	O75970	172	1805	XRAY	2QG1			
		8						
MPDZ-12	O75970	186	1945	SWISS-MODEL		2IWP B	1,00	0,887
		2						
MPDZ-13	O75970	199	2070	XRAY	2FNE			
		0						
MPP1-1	Q00013	74	150	XRAY	2EV8			
MPP3-1	Q13368	141	216	SWISS-MODEL		3O46 A	0,80	0,853
MPP4-1	Q96JB8	161	233	SWISS-MODEL		3O46 A	0,59	0,912
MPP5-1	Q8N3R9	260	333	XRAY	1VA8			
MPP6-1	Q9NZW	129	207	SWISS-MODEL		2E7K A	0,75	0,771
	5							

MYO18A-1	Q92614	225	310	SWISS-MODEL		1G9O A	0,29	0,631
NOS1-1	P29475	20	96	XRAY	1QAV			
PARD3-1	Q8TEW0	282	349	SWISS-MODEL		2DB5 A	0,29	0,587
PARD3-3	Q8TEW0	597	667	SWISS-MODEL		2K1Z A	0,97	0,630
PARD3B-1	Q8TEW8	211	292	SWISS-MODEL		2O2T A	0,30	0,716
PARD3B-2	Q8TEW8	391	471	SWISS-MODEL		2KOJ A	0,61	0,842
PARD3B-3	Q8TEW8	507	593	SWISS-MODEL		1WG6 A	0,99	0,533
PARD6A-1	Q9NPB6	160	248	SWISS-MODEL		1RZX A	0,84	0,779
PARD6B-1	Q9BYG5	162	240	XRAY	1NF3			
PARD6G-1	Q9BYG4	163	241	SWISS-MODEL		1NF3 D	0,90	0,682
PDLIM1-1	O00151	7	83	XRAY	2PKT			
PDLIM2-1	Q96JY6	1	85	XRAY	2PA1			
PDLIM3-1	Q53GG5	11	85	SWISS-MODEL		1V5L A	0,96	0,706
PDLIM4-1	P50479	1	90	XRAY	2V1W			
PDLIM5-1	Q96HC4	12	84	XRAY	2UZC			
PDLIM7-1	Q9NR12	10	82	XRAY	2Q3G			
PDZD11-1	Q5EBL8	50	126	SWISS-MODEL		1WI2 A	1,00	0,835
PDZD2-2	O15018	342	417	SWISS-MODEL		2DM8 A	0,47	0,812
PDZD2-3	O15018	592	665	SWISS-MODEL		2ENO A	0,44	0,968
PDZD2-4	O15018	728	814	SWISS-MODEL		2JRE A	0,35	0,533
PDZD2-5	O15018	262 6	2694	SWISS-MODEL		1X6D A	0,52	0,846
PDZD3-1	Q86UT5	121	194	SWISS-MODEL		1G9O A	0,41	0,821
PDZD3-2	Q86UT5	231	298	SWISS-MODEL		2OCS A	0,39	0,866
PDZD3-3	Q86UT5	333	410	SWISS-MODEL		2V9O E	1,00	1,000
PDZD4-1	Q76G19	130	215	SWISS-MODEL		1WH1 A	0,75	0,710
PDZD7-1	Q9H5P4	86	169	NMR	2EEH			
PDZK1-1	Q5T2W1	1	108	SWISS-MODEL		2EDZ A	0,89	0,813
PDZK1-2	Q5T2W1	142	210	NMR	2EEI			
PDZK1-3	Q5T2W1	247	321	SWISS-MODEL		2D9O A	0,88	0,855
PDZK1-4	Q5T2W1	384	456	SWISS-MODEL		2VSP D	1,00	0,932
PDZRN3-1	Q9UPQ7	257	340	NMR	1UHP			
PDZRN3-2	Q9UPQ7	429	505	SWISS-MODEL		1WH1 A	1,00	0,730
PDZRN4-1	Q6ZMN 7	232	315	SWISS-MODEL		1UHP A	0,70	0,839
PDZRN4-2	Q6ZMN	412	488	SWISS-		1WH1 A	0,79	0,782

	7			MODEL				
PICK1-1	Q9NRD5	25	101	XRAY	2GZV			
PPP1R9A-1	Q9ULJ8	509	590	SWISS-MODEL		3HVQ C	1,00	0,933
PPP1R9B-1	Q96SB3	498	578	XRAY	3EGG			
PTPN13-1	Q12923	109	1176	SWISS-MODEL		2DKR A	0,49	0,788
PTPN13-2	Q12923	137	1445	SWISS-MODEL		1Q7X A	0,99	0,355
PTPN13-3	Q12923	150	1584	SWISS-MODEL		2OGP A	0,39	0,688
PTPN13-4	Q12923	179	1866	SWISS-MODEL		2DKR A	0,35	0,616
PTPN13-5	Q12923	189	1955	SWISS-MODEL		1UEZ A	0,39	0,772
PTPN3-1	P26045	513	596	SWISS-MODEL		2VPH A	0,71	0,830
PTPN4-1	P29074	520	603	XRAY	2CS5			
RADIL-1	Q96JH8	976	1062	NMR	1UM1			
RAPGEF6-1	Q8TEU7	538	610	SWISS-MODEL		1UF1 A	0,51	0,821
RGS12-1	O14924	26	97	XRAY	2KV8			
RGS3-1	P49796	302	374	XRAY	2F5Y			
RHPN1-1	Q8TCX5	542	611	SWISS-MODEL		1VAE A	0,43	0,662
RHPN2-1	Q8IUC4	524	592	XRAY	2VSV			
RIMS1-1	Q86UR5	608	689	SWISS-MODEL		2CSS A	1,00	0,734
SCRIB-1	Q14160	725	816	XRAY	2W4F			
SCRIB-2	Q14160	853	958	NMR	1WHA			
SCRIB-3	Q14160	100	1091	SWISS-MODEL		3GSL A	0,44	0,745
SCRIB-4	Q14160	110	1190	XRAY	1UJU			
SDCBP-1	O00560	117	193	XRAY	1YBO			
SDCBP-2	O00560	198	274	SWISS-MODEL		1NFE A	1,00	0,865
SDCBP2-1	Q9H190	111	186	SWISS-MODEL		1W9E B	0,69	0,872
SDCBP2-2	Q9H190	195	265	SWISS-MODEL		1NFE A	0,70	0,869
SHANK2-1	Q9UPX8	250	339	SWISS-MODEL		1Q3O A	0,90	0,832
SHANK3-1	Q9BYB0	565	668	SWISS-MODEL		1Q3O A	0,86	0,719
SHROOM3-1	Q8TF72	36	111	SWISS-MODEL		2EDP A	0,63	0,745
SHROOM4-1	Q9ULL8	19	93	NMR	2EDP			
SIPA1-1	Q96FS4	690	759	SWISS-MODEL		2EEH A	0,32	0,723
SIPA1L1-1	O43166	957	1026	SWISS-MODEL		2YT8 A	0,31	0,684
SIPA1L2-1	Q9P2F8	959	1026	SWISS-MODEL		1G9O A	0,33	0,804
SIPA1L3-1	O60292	975	1042	SWISS-MODEL		2YT8 A	0,34	0,671

SLC9A3R1-1	O14745	20	92	XRAY	1G9O			
SLC9A3R1-2	O14745	159	232	SWISS-MODEL		2KRG A	1,00	0,824
SLC9A3R2-2	Q15599	147	229	XRAY	2HE4			
SNTA1-1	Q13424	83	171	SWISS-MODEL		1QAV A	0,99	0,804
SNTB1-1	Q13884	117	193	SWISS-MODEL		2VRF A	0,86	0,993
SNTB2-1	Q13425	118	196	XRAY	2VRF			
SNTG1-1	Q9NSN8	60	137	SWISS-MODEL		1Z87 A	0,45	0,769
SNTG2-1	Q9NY99	76	155	SWISS-MODEL		1Z87 A	0,54	0,639
SYNJ2BP-1	P57105	16	99	SWISS-MODEL		2JIK A	1,00	0,977
SYNPO2-1	Q9UMS6	7	89	SWISS-MODEL		1WF7 A	0,38	0,696
SYNPO2L-1	Q9H987	7	89	SWISS-MODEL		2EDP A	0,43	0,644
TIAM1-1	Q13009	856	920	XRAY	2D8I			
TIAM2-1	Q8IVF5	891	977	SWISS-MODEL		1KY9 B	0,36	0,588
TJP1-1	Q07157	26	108	XRAY	2H2C			
TJP1-2	Q07157	189	263	XRAY	2RCZ			
TJP1-3	Q07157	429	499	SWISS-MODEL		1UF1 A	0,40	0,783
TJP2-1	Q9UDY2	35	118	XRAY	1CSJ			
TJP2-2	Q9UDY2	307	386	XRAY	3E17			
TJP2-3	Q9UDY2	518	581	SWISS-MODEL		1UF1 A	0,38	0,783
TJP3-1	O95049	16	90	SWISS-MODEL		2H2B A	0,56	0,966
TJP3-2	O95049	195	272	SWISS-MODEL		2OSG A	0,58	0,594
TJP3-3	O95049	394	461	SWISS-MODEL		1UM7 A	0,43	0,792
USH1C-1	Q9Y6N9	91	166	SWISS-MODEL		3K1R A	0,99	1,000
USH1C-2	Q9Y6N9	220	289	SWISS-MODEL		2KBS A	1,00	0,932
USH1C-3	Q9Y6N9	460	527	SWISS-MODEL		1V6B A	0,96	0,837
WHRN-1	Q9P202	144	217	XRAY	1UEZ			
WHRN-2	Q9P202	288	358	XRAY	1UF1			
WHRN-3	Q9P202	820	888	SWISS-MODEL		1UFX A	1,00	1,000

BIBLIOGRAPHY

1. Kuriyan J, Cowburn D (1997) Modular peptide recognition domains in eukaryotic signaling. *Annu Rev Biophys Biomol Struct* 26: 259–288.
2. Facciuto F., Cavatorta A.L., Valdano M.B., Marziali F., Gardiol D. (2012) Differential expression of PDZ domain-containing proteins in human diseases – challenging topics and novel issues , *FEBS Journal Volume 279, Issue 19*, pages 3538-3548
3. Madsen K.L. , Buming T., Niv M.Y., Chang C., Dev K., Weinstein H., Gether U. (2005) Molecular Determinants for the Complex Binding Specificity of the PDZ Domain in PICK1*, *JBC Papers in Press*, DOI 10.1074/jbc.M500577200
4. Songyang, Z., Fanning, A. S., Fu, C., Xu, J., Marfatia, S. M., Chishti, A. H., Crompton, A., Chan, A. C., Anderson, J. M., and Cantley, L. C. (1997), Recognition of Unique Carboxyl-Terminal Motifs by Distinct PDZ Domains, *Science* 275, 73–77
5. Stricker, N. L., Christopherson, K. S., Yi, B. A., Schatz, P. J., Raab, R. W., Dawes, G., Bassett, D. E., Jr., and Li, M. (1997) PDZ domain of neuronal nitric oxide synthase recognizes novel C-terminal peptide sequences, *Nat. Struct. Biol.* 4, 336–342
6. Velthuis AJW, Sakalis PA, Fowler DA, Bagowski CP (2011) Genome-Wide Analysis of PDZ Domain Binding Reveals Inherent Functional Overlap within the PDZ Interaction Network, *PLoS ONE* 6(1): e16047. doi:10.1371/journal.pone.0016047
7. Tonikian R, Zhang Y, Sazinsky SL, Currell B, Yeh JH, Reva B, Held HA, Appleton BA, Evangelista M, Wu Y, et al: A specificity map for the PDZ domain family. *PLoS Biol* 2008, 6:e239.
8. Stiffler MA, Chen JR, Grantcharova VP, Lei Y, Fuchs D, Allen JE, Zaslavskaja LA, MacBeath G: PDZ domain binding selectivity is optimized across the mouse proteome. *Science* 2007, 317:364–369.
9. Chen JR, Chang BH, Allen JE, Stiffler MA, MacBeath G: Predicting PDZ domain-peptide interactions from primary sequences. *Nat Biotechnol* 2008, 26:1041–1045.
10. Hui S, Bader GD: Proteome scanning to predict PDZ domain interactions using support vector machines. *BMC Bioinformatics* 2010, 11:507.
11. Kalyoncu S, Keskin O, Gursoy A: Interaction prediction and classification of PDZ domains *BMC Bioinformatics* 2010, 11:357
12. Hui et al.: Predicting PDZ domain mediated protein interactions from structure. *BMC Bioinformatics* 2013 14:27
13. Berman HM, Westbrook J, Feng Z, Gilliland G, Bhat TN, Weissig H, Shindyalov IN, Bourne PE: The Protein Data Bank. *Nucleic Acids Res* 2000, 28:235–242
14. Arnold K, Bordoli L, Kopp J, Schwede T: The SWISS-MODEL workspace: a web-based environment for protein structure homology modelling. *Bioinformatics* 2006, 22:195–201.
15. Marsh AJ, Teichmann AS: Relative Solvent Accessible Surface Area Predicts Protein Conformational Changes upon Binding. *Structure* 2011, 19(6): 859-867
16. Hubbard SJ, Thornton JM: NACCESS 1993. (Department Biochemistry and Molecular Biology, U. C., Ed.)

17. Steinkellner G, Rader R, Thallinger GG, Kratky C, Gruber K: VASCo: computation and visualization of annotated protein surface contacts. *BMC Bioinformatics* 2009, 10:32.
18. Li X, Foley EA, Kawashima SA, Molloy KR, Li Y, Chait BT, Kapoor TM: Examining post-translational modification-mediated protein–protein interactions using a chemical proteomics approach. *The Protein Society* 2012, DOI: 10.1002/pro.2210
19. Lee HJ, Zheng JJ: PDZ domains and their binding partners: structure, specificity, and modification, *Cell Communication and Signaling* 2010, 8:8 doi:10.1186/1478-811X-8-8
20. Vapnik VN: Adaptive and learning systems for signal processing, communications, and control. , 1998, *Statistical Learning Theory*. Wiley, New York
21. Chang C-C, Lin C-J: LIBSVM: a library for support vector machines. *ACM Transactions on Intelligent Systems and Technology* 2011, 2:27:21–27:27.
22. Garcia V, Sanchez JS, Mollineda RA, Alejo R, Sotoca JM: The class imbalance problem in pattern classification and learning, *II Congreso Español de Informática*
23. Ivarsson Y, Arnold R, McLaughlin M, Nim S, Joshi R, Ray D, Liu B, Teyra J, Pawson T, Moffat J, Li SSC, Sidhu SS, Kim PM: Large-scale interaction profiling of PDZ domains through proteomic peptide-phage display using human and viral phage peptidomes. *PNAS* 2014, vol. 111 no. 7
24. Murciano-Calles J, Marin-Argany M, Cobos ES, Villegas S, Martinez JC : The Impact of Extra-Domain Structures and Post-Translational Modifications in the Folding/Misfolding Behaviour of the Third PDZ Domain of MAGUK Neuronal Protein PSD-95. *PLoS ONE* 2014, 9(5): e98124. doi:10.1371/journal.pone.0098124
25. Turner B, Razick S, Turinsky AL, Vlasblom J, Crowdy EK, Cho E, Morrison K, Donaldson IM, Wodak SJ: iRefWeb: interactive analysis of consolidated protein interaction data and their supporting evidence. *Database (Oxford)* 2010, 2010:baq023.
26. Stark C, Breitkreutz BJ, Chatr-Aryamontri A, Boucher L, Oughtred R, Livstone MS, Nixon J, Van Auken K, Wang X, Shi X, et al: The BioGRID Interaction Database: 2011 update. *Nucleic Acids Res* 2011, 39:D698–704.
27. Bader GD, Betel D, Hogue CW: BIND: the Biomolecular Interaction Network Database. *Nucleic Acids Res* 2003, 31:248–250.
28. Aranda B, Achuthan P, Alam-Faruque Y, Armean I, Bridge A, Derow C, Feuermann M, Ghanbarian AT, Kerrien S, Khadake J, et al: The IntAct molecular interaction database in 2010. *Nucleic Acids Res* 2010, 38:D525–531.
29. Ruepp A, Waegele B, Lechner M, Brauner B, Dunger-Kaltenbach I, Fobo G, Frishman G, Montrone C, Mewes HW: CORUM: the comprehensive resource of mammalian protein complexes–2009. *Nucleic Acids Res* 2010, 38:D497–501.
30. Salwinski L, Miller CS, Smith AJ, Pettit FK, Bowie JU, Eisenberg D: The Database of Interacting Proteins: 2004 update. *Nucleic Acids Res* 2004, 32:D449–451.
31. Mishra GR, Suresh M, Kumaran K, Kannabiran N, Suresh S, Bala P, Shivakumar K, Anuradha N, Reddy R, Raghavan TM, et al: Human protein reference database–2006 update. *Nucleic Acids Res* 2006, 34:D411–414.
32. Ceol A, Chatr Aryamontri A, Licata L, Peluso D, Briganti L, Perfetto L, Castagnoli L, Cesareni G: MINT, the molecular interaction database: 2009 update. *Nucleic Acids Res* 2010, 38:D532–D539.

33. Cho, K.O., Hunt, C.A. and Kennedy, M.B. : The rat brain postsynaptic density fraction contains a homolog of the *Drosophila* discs-large tumor suppressor protein. 1992, *Neuron* 9, 929–942.
34. Woods, D.F. and Bryant, P.J. : ZO-1, DlgA and PSD-95/SAP90: homologous proteins in tight, septate and synaptic cell junctions. 1993, *Mech. Dev.* 44, 85–89.
35. Kim, E., Niethammer, M., Rothschild, A., Jan, Y.N. and Sheng, M.: Clustering of Shaker-type K⁺ channels by interaction with a family of membrane-associated guanylate kinases. 1995, *Nature* 378, 85–88.
36. McGee, A. W. & Brecht, D. S. : Assembly and plasticity of the glutamatergic postsynaptic specialization. *Curr. Opin.* 2003, *Neurobiol.* 13, 111–118.
37. Hu, L. A. et al. : β 1-adrenergic receptor association with PSD-95. Inhibition of receptor internalization and facilitation of β 1-adrenergic receptor interaction with N-methyl-D-aspartate receptors. 2000, *J. Biol. Chem.* 275, 38659–38666.
38. Irie, M. et al. : Binding of neuroligins to PSD-95. 1997, *Science* 277, 1511–1515.
39. Gardoni, F. et al. : The NMDA receptor complex is altered in an animal model of human cerebral heterotopia. , 2003, *J. Neuropathol. Exp. Neurol.* 62, 662–675.
40. Beuming T., Skrabanek L., Niv M.Y., Mukherjee P. and Weinstein H. : PDZBase: A protein-protein interaction database for PDZ-domains. , 2005, *Bioinformatics.* 21(6):827-8.
41. Furey T., Cristianini N., Duffy N., Bednarski D., Schummer M., Haussler D.: Support vector machine classification and validation of cancer tissue samples using microarray expression data. ,2000, *Bioinformatics,* 16, 906–914.
42. Cristianini,N. and Shawe-Taylor,J.: *An Introduction to Support Vector Machines.*, 2000, Cambridge University Press, MA.
43. Zien,A., Rätsch,G., Mika,S., Schölkopf,B., Lengauer,T. And Müller,K.-R.: Engineering support vector machine kernels that recognize translation initiation sites., 2000, *Bioinformatics,* 16, 799–807
44. Liao,L. and Noble,W.S.: Combining pairwise sequence similarity and support vector machines for remote protein homology detection.,2002, *Proceedings of the Sixth Annual International Conference on Computational Molecular Biology,* pp. 225-332.
45. Ding,C. and Dubchak,I: Multiclass protein fold recognition using support vector machines and neural networks.,2001, *Bioinformatics,* 17, 349–358.
46. Vert,J.-P. and Kanehisa,M: Graph-driven features extraction from microarray data using diffusion kernels and kernel CCA. In Becker,S., Thrun,S. and Obermayer,K. (eds), 2003, *Advances in Neural Information Processing Systems 15.* MIT Press, Cambridge, MA.
47. Bock,J.R. and Gough,D.A: Predicting protein-protein interactions from primary structure.,2001 ,*Bioinformatics,* 17, 455-460.